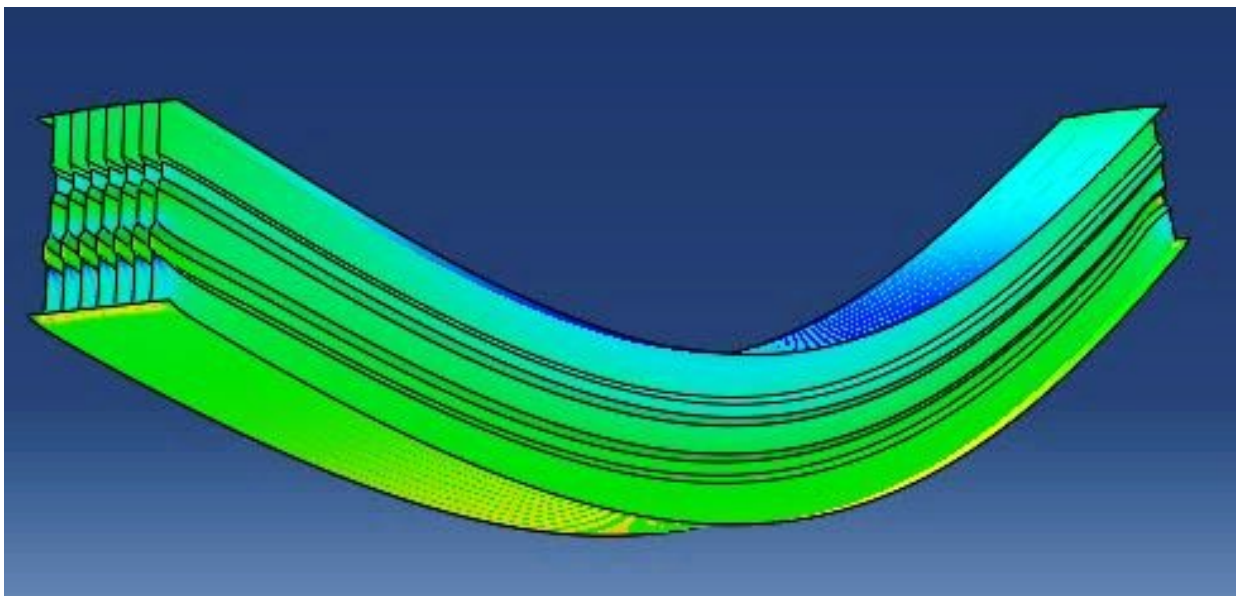




CHALMERS
UNIVERSITY OF TECHNOLOGY



Conceptual design and manufacture of ecoduct using fibre reinforced polymer composite materials

HANNA GEIGER

OLENA SHKUNDALOVA

Department of Architecture and Civil Engineering

Division of Structural Engineering

Research Group: Lightweight Structures

CHALMERS UNIVERSITY OF TECHNOLOGY

Master's Thesis ACEX30-19-96

Gothenburg, Sweden 2019

Conceptual design and manufacture of ecoduct using fibre reinforced polymer composite materials

Master's thesis in structural engineering and building technology

OLENA SHKUNDALOVA

HANNA GEIGER

Department of Architecture and Civil Engineering

Division of Structural Engineering

Research group: Lightweight Structures

CHALMERS UNIVERSITY OF TECHNOLOGY

Gothenburg, Sweden 2019

Conceptual design and manufacture of ecoduct using fibre reinforced polymer composite materials

Master's thesis in structural engineering and building technology

OLENA SHKUNDALOVA

HANNA GEIGER

© Olena Shkundalova & Hanna Geiger, 2019

Examensarbete ACEX30-19-96

Institutionen för arkitektur och samhällsbyggnadsteknik

Chalmers tekniska högskola, 2019

Department of Architecture and Civil Engineering

Division of Structural Engineering

Research group: Lightweight Structurers

Chalmers University of Technology

SE-412 96 Göteborg

Sweden

Telephone: + 46 (0)31-772 1000

Cover:

Deformed cross-section of ecoduct with stresses in main direction.

Department of Architecture and Civil Engineering

Gothenburg, Sweden, 2019

Conceptual design and manufacture of ecoduct using fibre reinforced polymer composite materials

Master's thesis in structural engineering and building technology

OLENA SHKUNDALOVA

HANNA GEIGER

Department of Architecture and Civil Engineering

Division of Structural Engineering

Research Group: Lightweight Structures

Chalmers University of Technology

ABSTRACT

The growth of transport infrastructure has led to the fragmentation of the natural habitat of many animal species in Sweden. Ecoducts, large bridges with a layer of soil and vegetation on top of it, provide a safe crossing of highways for animals. In this thesis, the design of an ecoduct made of fibre reinforced polymer composites (FRP) was developed. The aim was to develop a typical solution for the ecoduct that could be further used in the design of ecoducts made of FRP composites in Sweden. Initially, the conditions and requirements for ecoducts in Sweden were studied by literature review and interview with an expert in the field. It was concluded that motorways and highways contribute most to the fragmentation effect. A minimum width for ecoducts of 30 m and a recommendation of tree vegetation on the edges of the ecoduct was identified. The possibilities and advantages of FRP as a building material for ecoducts were investigated. 19 preliminary design solutions were developed in order to determine the most suitable ecoduct structural system with an emphasis on the bearing capacity of the structural elements of different cross-sections. The types and performance of FRP composites under static load were evaluated to select the most efficient composite materials for the design of ecoducts. Existing production possibilities were considered for the further prospects of manufacturing of the bridge elements. The final proposed design includes a detailed design of the bridge members and provides several possible solutions for the structural joints. Finite element analyses were performed to optimize the final design decision. The deflection under the static load, maximum allowable stresses and buckling behavior of the bridge sections were investigated. Humidity, temperature and creep effects on the FRP material were taken into consideration. The proposed design is an effective solution in terms of the carrying capacity of the developed section and the material use.

Key words: FRP, design, ecoduct, eco-bridge, composite, polymer, carbon fibre, glass fibre, mechanical properties, FE analysis, deck, beam, connection, joint.

Konceptuelltdesign och produktion av ekodukt av fiber armerad polymer-kompositer

Examensarbete inom konstruktionsteknik

OLENA SHKUNDALOVA

HANNA GEIGER

Institutionen för arkitektur och samhällsbyggnadsteknik

Avdelningen för Structural Engineering

Forskargrupsnamn: Lightweight Structures

Chalmers tekniska högskola

SAMMANFATTNING

Transportinfrastrukturer i vårt samhälle växer. Detta leder till en ökad fragmentering av det naturliga habitatet för många arter i Sverige. Ekodukter, stora beväxta broar, ger djur möjlighet att korsa stora barriärer som motorvägar. I detta arbete presenteras en konceptuell design för en ecoduct av FRP. Målet var att utveckla en lösning som kan anses som typiskt för svenska förhållanden. För att kunna definiera ett relevant fall på ekodukter i en svensk miljö studerades regler och rekommendationer i en litteraturstudie. En intervju med en expert inom området genomfördes också. Slutsatsen som drogs var att motorvägar och stora landsvägar bidrar mest till fragmenteringseffekten. Minimalbredden av 30 m och rekommendation angående trädvegetation på kanterna blev identifierad. Materialet FRP blev undersökt angående för att avgöra lämpligheten och identifiera möjliga lösningar. 19 preliminära designlösningar utvecklades och undersöktes med tyngdpunkt på deformation och produktion. Fukt, temperatur och krypning blev beaktade. Det slutgiltiga lösningsförslaget inkluderar en optimerad geometri med hänsyn till spänningar, deformationer, instabilitet och förslag för skarvar.

Nyckelord: FRP, design, ekodukt, vildbro, komposit, polymer, kolfiber, glasfiber, FE analys.

Contents

1	Introduction.....	1
1.1	Aim.....	2
1.2	Method	2
1.3	Limitations	3
1.4	Outline of the thesis.....	4
2	Infrastructure and fauna	5
2.1	Barriers	7
2.2	Ecoducts – Requirements and recommendations.....	9
2.3	Requirements on ecoducts.....	13
3	FRP composite material properties.....	16
3.1	FRP and conventional building materials	16
3.2	Resin.....	18
3.3	Fibres.....	20
3.3.1	Glass fibre	22
3.3.2	Carbon fibre	22
3.3.3	Aramid fibre.....	23
3.3.4	FRP composites	23
3.4	Physical properties	24
3.4.1	Temperature and density.....	25
3.4.2	Mechanical properties	26
3.5	Sustainability.....	27
3.6	Durability	28
3.7	Production Methods	30
3.8	Connections.....	32
3.8.1	Structural joints for FRP elements.....	32
3.8.2	Failure modes of structural joints of FRP elements.....	34
3.8.3	Choice of configurations of structural joints	36
3.9	Guidelines and codes.....	37
4	Case study	38
4.1	Bridge geometry and loading conditions	38
4.1.1	Load combinations.....	42
4.1.2	Design requirements	44
4.1.3	Joint design requirements for FRP ecoduct members.....	46
4.2	Discussion: the case study.....	47
5	Preliminary design	49

5.1	FRP composite material properties used for the preliminary design	49
5.1.1	Preliminary design proposals	49
5.1.2	First evaluation.....	56
5.1.3	Detailed description and evaluation of 3 chosen concepts	59
5.1.4	Second evaluation	64
5.2	Discussion of preliminary design.....	65
6	Final design.....	66
6.1	Material properties of FRP laminate	66
6.1.1	Relevant conversion factors	66
6.1.2	Partial safety factors.....	68
6.1.3	Glass and carbon fibres material properties	69
6.1.4	Resin material properties	69
6.2	Relevant material properties of the FRP laminate	70
6.3	Handcalculations: optimization of the section and verification of deflections 72	
6.4	Modeling in Abaqus	76
6.4.1	Material properties	76
6.4.2	Material orientations	76
6.4.3	Loads.....	76
6.4.4	Boundary conditions	77
6.4.5	Geometries	79
6.5	Results	81
6.5.1	Static analysis.....	81
6.5.2	Buckling analysis	89
6.6	Discussion of the final design	92
7	Discussion.....	96
8	Conclusion	97
	References.....	99
	Appendix A – Interview questions	103
	Appendix B – Permeability of Swedish barriers.....	104
	Appendix C – Barriers effects.....	106
	Appendix D – Road width	108
	Appendix E – Load combination	110
	Appendix F – Preliminary design	116
	Appendix G – Hand calculations, final design	123

List of Figures

Figure 1. Streams of animals trying to cross a road. Figure after A. Seiler, Olsson, & Lindqvist, (2015).....	5
Figure 2. Total permeability of a barrier as a function of total number of passages and their effectiveness.	6
Figure 3. Suggestion for ecoduct at E14 Timmervägen after Norwegian model. Drawings from Trafikverket/Sundsvall municipality (Sundsvall Komun, 2018).....	11
Figure 4. Motorway transverse section used in this thesis.....	14
Figure 5. Highway transverse section used in this thesis.....	14
Figure 6. Young's modulus comparison.	17
Figure 7. Stress-strain diagram, FRP & steel.....	17
Figure 8. Strength-temperature dependence curves for different building materials. .	18
Figure 9. Irreversible bonding chains between the molecules of the thermoset resin (ACMA, 2016).....	19
Figure 10. Reversible bonding between the molecules of the thermoplastic resin (ACMA, 2016).....	19
Figure 11. Fibre orientation in FRP composite.....	21
Figure 12. Stress-strain diagram for different fibre types.	22
Figure 13. Basic failure modes in bolted laminate connection.	34
Figure 14. Loading modes of the bonded connection.....	35
Figure 15. Typical joint configurations (The European structural polymeric composites group, 1996).....	36
Figure 16. Service vehicle.....	38
Figure 17. Distribution of load from vehicle.	39
Figure 18. Half-section of proposed soil thickness on ecoduct.	40
Figure 19. Loads on section of bridge. Height of the loads in the figure gives an approximate impression of the relative value of the loads compared to each other. The position of the service vehicle can be at any place between the edge section.	41
Figure 20. Deflections according to Eurocomp.	44
Figure 21. Failure modes of the ecoduct section in bending and shear.	45
Figure 22. Loading types of bolted connection.	47

Figure 23. Principal construction of beam-deck structural system.	50
Figure 24. Principal construction of beam solution.	54
Figure 25. Pultruded bridge section design solution.	59
Figure 26. Whole sandwich section connected with bolts.	60
Figure 27. Design 19. Bridge is shown in black color, the soil level – in green.	60
Figure 28. Adhesive connection possibilities for bearing deck structural system.	61
Figure 29. Mechanical connections for bearing deck system.	62
Figure 30. Mechanical connections for bearing deck system.	62
Figure 31. Mechanical connection of the beam to the deck of an ecoduct.	62
Figure 32. Different possibilities for manufacturing design 19.	63
Figure 33. Laminate layers for flanges and webs in the deck section.	71
Figure 34. Possible configurations of web thickness and spacing as a function of height (middle section). The index numbers give the spacing oh the webs.	73
Figure 35. Possible configurations of web thickness and spacing as a function of height (edge section).	73
Figure 36. Height of cross-section as a function of flange thickness.	74
Figure 37. Height of crossection as a function of flange thickness (edge section).	74
Figure 38. Web spacing as a function of web thickness in edge section.	75
Figure 39. Coordinate systems used for Abaqus model.	76
Figure 40. Load distribution on model in Abaqus.	77
Figure 41. Boundary conditions for the 1 m width bridge deck section.	77
Figure 42. Lateral deflection of webs over the support for BC1 and BC2.	78
Figure 43. Conditions for BC1.	78
Figure 44. Crossection of the final ecoduct design.	79
Figure 45. Maximum stresses, normal stresses S_{xx} in the bottom flange. Characteristic load combination.	82
Figure 46. Maximal vertical deflections of the bridge deck in characteristic load combination.	83
Figure 47. Minimum lateral deflection of web, characteristic load combination.	83

Figure 48. Maximum lateral deflection of web, characteristic load combination.	84
Figure 49. Lateral deflection, U_y , along web stiffeners. Geometry G8 and characteristic load case.....	85
Figure 50. Lateral deflection, design G8. The deflection in y direction ranges from +/- 11 mm. The deflection is most pronounced along the two web stiffeners. The exact form of the deformation along the stiffeners is presented in figure 49.	86
Figure 51. Vertical deflection, geometry G8.	86
Figure 52. Stresses S_{xx} , geometry G8.	87
Figure 53. Stresses S_{xy} , geometry G8.	87
Figure 54. Stresses S_{xy} , geometry G8.	88
Figure 55. Lateral deflection U_2 , geometry with the straight webs.....	88
Figure 56. Positive eigenvalues for the first 10 buckling modes for different geometries.	90
Figure 57. Eigenvalues for first buckling mode for different geometries.....	90
Figure 58. First buckling mode of the edge section (blue arrow in the figure indicate the vertical direction in the global coordinate system).	92
Figure 59. Internal moment in stiffener. Increased a) or e) increases lateral deformation of stiffener.	93
Figure 60. Section of typical motorway in Sweden.	109

List of Tables

Table 1. Casualties on different road types in Sonderjylland County Denmark. The species recorded are Roe deer, fox badger, hare and hedgehog (A Seiler & Folkesson, 2003). Survey during 20 months (November 1995 – August 1997).....	8
Table 2. Barrier effect in Swedish road and railway system. This table is a simplified version of the data from Seiler et al., 2015 presented in Appendix B.	9
Table 3. Type of barrier and associated span in Sweden. The span is taken as the minimal required span for newbuild roads. The calculations are presented in appendix D. The length of barriers the length along the roads and railways that are not near to a crossing.	14
Table 4. FRP & Conventional materials comparison.	16
Table 5. Thermal expansion coefficient for different configurations of fibres (Friberg & Olsson, 2014).	25
Table 6. Range of density for FRP with both normal and more extreme values (Friberg & Olsson, 2014).	25
Table 7. Influence of the fibre orientation in FRP composite material (Friberg & Olsson, 2014).	26
Table 8. Shear strength and shear modulus for different composite configurations with unidirectional fibre orientations (Friberg & Olsson, 2014).	27
Table 9. Characteristics of joint categories.	33
Table 10. Characteristic snow load for some combinations of snow zone and elevation above sea-level.	40
Table 11. Combination factors for variable loads.	42
Table 12. Partial safety factors.	42
Table 13. Maximum shear and bending moment values.	43
Table 14. Load on an ecoduct in different states.	43
Table 15. Cross-sectional constants calculation from Eurocomp and PNG Design.	44
Table 16. Material parameters used in preliminary design.	49
Table 17. Material need for the different conceptual designs.	50
Table 18. Production methods for different design solutions.	52
Table 19. Material need and production method for different beam solutions.	55

Table 20. Evaluation criteria. For the first evaluation only the criteria's marked with blue were used.....	56
Table 21. Weighting of evaluation criteria for first evaluation.	57
Table 22. Results from first evaluation.....	58
Table 23. Evaluation criteria for second evaluation.	64
Table 24. Second evaluation.	65
Table 25. Conversion factors to be taken into account.	67
Table 26. Total conversion factors.....	68
Table 27. Comparison of safety factors from Eurocomp and PNG Design recommendations.	68
Table 28. Typical values of fibre properties.	69
Table 29. Polyester resin material properties.....	70
Table 30. Material properties of FRP for flange and web sections of the bridge deck.	72
Table 31. Design requirements with corresponding design and geometry parameters.	72
Table 32. Final geometry according to hand calculations. Pre-cambering = 30mm. ..	75
Table 33. Deflections and deflection requirements for handcalculations.....	75
Table 34. Geometry of crossection.	80
Table 35. Static analysis results (Abaqus), deflections in Y and Z directions are presented, normal stresses in X direction, shear stresses in XY plane with regard to the material orientation in the webs are also presented.	82
Table 36. Results geometry nr. G8, different load cases.	84
Table 37. Results geometry nr G8, edge section.	85
Table 38. Results straight webs, characteristic load combination.	85
Table 39. Results of the buckling analysis for different geometries of the bridge deck section.	89
Table 40. The 1st buckling modes for the different deck section geometries. The red, green and blue arrows in the pictures are showing the X, Y and Z directions respectively.	91
Table 41. Five first eigenvalues for the edge section.....	92

Table 42. Utilization ratios for stresses in ultimate limit stat and quasi permanent limit state.	94
Table 43. Calculation of loads and load combinations for different load cases.	110

Preface

The design of an ecoduct made of fibre reinforced polymeric (FRP) materials was developed. The project was started in February and ended in June 2019. The work was done at ÅF Consult company, Gothenburg, Sweden.

The work was done under the supervision of Valbona Mara, PhD in Structural Engineering (ÅF Infrastructure), and Professor Reza Haghani Dogaheh as examiner (Chalmers University of Technology).

Gothenburg, June 2019

Hanna Geiger and Olena Shkundalova

Notations

Roman upper-case letters

A_{shear}	Shear area of cross-section
E_{creep}	Young's modulus for long term load situation (creep taken into account)
E_{f1}	Elastic modulus in direction 1 (x)
E_{f2}	Elastic modulus in direction 2 (y)
E_{instant}	Young's modulus for instant load situation
E_r	Young's modulus for resin
G_{creep}	Shear modulus of long term load situation (creep taken into account)
G_{ed}	Design shear modulus of the FRP laminate
G_f	Shear modulus for the fibre
G_{instant}	Shear modulus for instant load situation
G_r	Shear modulus for the resin
G_t	Glass transition temperature
I	Moment of inertia for bending in main direction (around Y axis)
L	Length of one bridge span
M_{ed}	Maximum design bending moment
M_{uls}	Maximum bending moment on a bridge in ultimate load combination.
Q_1	Load from service vehicle, axis 1 in SLS
Q_2	Load from service vehicle, axis 2 in SLS
Q_{1uls}	Load from service vehicle, axis 1 in ULS
Q_{2uls}	Load from service vehicle, axis 2 in ULS
S_{xy}	Shear stresses in XY direction
S_{xx}	Normal stresses in X direction
$U_{z \text{ hand}}$	Deformations in vertical Z direction, hand calculation
U_z, U_y	Deflection in Z and Y directions respectively
$U_{z \text{ nr } 8}$	Deformations in vertical Z direction, geometry G8
$U_{z \text{ straight}}$	Deformation in Z direction from abaqus with straight webs
W	Total width of ecodeck
V_{ed}	Maximum shear force
V_{uls}	Ultimate shear force acting on a bridge

Roman lower-case letters

b	Spacing of webs
f_{ed}	Design strength of the laminate
f_{dt}	Design tensile strength of the laminate
$f_{d\tau}$	Design and design shear strength of the laminate
f_{kt}	Characteristic tensile strength of the laminate
$f_{k\tau}$	Characteristic shear strength of the laminate
g	Self-weight of bridge
h	Height of cross-section
h_{edge}	Height of soil in edge section of the bridge
h_{middle}	Height of soil in middle section of the ecodeck
q_{fk}	Distributed variable load for pedestrian bridge
$q_{\text{edge soil}}$	Load from soil in the edge section of the ecodeck
q_{soil}	Load from soil in the middle section of the ecodeck

s_k	Characteristic snow load
t_v	Accumulated load duration (hours)
t_f	Flange thickness
t_w	Web thickness

Greek lower-case letters

α	Angle of stiffener
δ_0	Initial deformation before loads are applied also called precambering
δ_1	Instantaneous deflection of the deck section under the permanent loads
δ_2	Variation of the deflection of the beam, due to the variable loading plus any time dependent deformations due to permanent loading
δ_{creep}	Deformations in Z direction from creep part of permanent load
δ_{max}	Sagging in the final state relative to the straight line joining the supports
$\gamma_{G,j}$	Partial safety factor for permanent load number j
γ_M	Partial safety factor for material properties
γ_{M2uls}	Partial safety factor accounting for the lamina production process
$\gamma_{Q,j}$	Partial coefficient for the variable load number j
$\gamma_{Qf,j}$	Partial coefficient for the variable load number j
ϵ_{f1}	Strain in direction 1 (x)
ϵ_{f2}	Strain in direction 2 (y)
η_c	Conversion factor accounting for the long-term influence of temperature, humidity, creep on laminate
η_{cf}	Conversion factor for the fatigue effects.
η_{cm}	Conversion factor for humidity effects;
η_{ct}	Conversion factor for temperature effects;
η_{cv}	Conversion factor for creep effects;
η_{vc20}	Conversion factor to account for creep effects for the reference period of 20 years.
λ	Eigenvalue for buckling
ν_f	Poisson's ratio
ξ	Reduction factor for permanent loads
ρ_r	Density of the resin
ρ_f	Density of the fibre
ρ_{soil}	Density of soil
σ_{xx}	Normal stresses in X direction
σ_{xy}	shear stresses in XY direction
τ_{ed}	Shear stress
ψ_0	Factor for combination of variable load
ψ_1	Factor for frequent value of variable load
ψ_2	Factor for quasi permanent value of variable load

ESPEC – organization, measuring the level of F-gases (fluorinated greenhouse gases), aiming to reduce the environmental deplete with the use of low Global Warming Potential (GWP) refrigerants.

Swedish government agencies

“Trafikverket” is a Swedish state agency responsible for a long-term planning of the transport infrastructure at the national level. Responsibilities - construction and maintenance of large parts of the transport infrastructure. The predecessors were Vägverket (roads) and Banverket (railway). Since some of the recommendations about ecoducts are based on the old recommendations, both will be referred to in this thesis. The term “Swedish transport administration” will be used to refer to Trafikverket, and “old Swedish transport administrations” to Banverket and Vägverket.

1 Introduction

The increasing amount of transportation infrastructure has a negative effect on wildlife. Some of these effects can be coupled to the fragmentation of the natural habitats for different animal species. Sometimes, populations are cut off from each other, which usually results in a limited gene-pool or extinction (A Seiler & Folkesson, 2003).

In 2014, 47200 accidents with large wild animals were reported in Sweden. Since then, the number of accidents has been increasing every year and at 2018 about 63700 accidents were reported (Nationella Viltolycksrådet, 2017). Between 2003 and 2012 there were in average 5 deadly accidents each year. Economic damage from wildlife accidents is estimated at an average of 2,600 million SEK per year ("Viltolyckor mot ny rekordnivå - Nyheter (Ekot) | Sveriges Radio," 2016).

This has resulted in an increasing interest in construction of ecoducts. After the collapse of the scaffolding and following demolition of the ecoduct Sandsjöbacka in 2017, research of an alternative approach to the construction was begun (Trafikverket, 2018). The hope is that an approach with the use of fibre reinforced polymer (FRP) materials in construction of superstructures will lead to a design that can compete in economic terms with traditional methods and that is superior with regard to construction time and disturbance for society and environment. A master thesis at Chalmers in 2018 proved that the use of FRP composites can result in 50% reduction in construction cost of ecoducts with minimum possible disturbance on traffic (Sandahl & Hällerstål, 2018).

At the moment, ecoducts in Sweden are mainly made of reinforced concrete. This conventional material has a number of advantages, such as high compressive strength, durability and ability to withstand high temperatures. However, its weight is relatively high compared to its strength. In an alternative replacement for concrete and steel, lightweight FRP materials can be used for construction of prefabricated FRP ecoducts. Due to its high strength and durability, low weight and flexibility in the choice of forms, fibre reinforced composite materials can become a profitable alternative to steel and concrete (Naqvi et al., 2018). One of the advantages of using FRP in bridge construction is the ability to have hybrid solutions and to successfully combine them with elements made of concrete and steel (Wan, 2014), having the mechanical properties of the FRP composites close to that of steel and the weight close to that of plastic (Bhatt & Goe, 2017).

An advantage of the use of FRP composites is that it does not rust as steel does (Wan, 2014). High stiffness and strength to weight ratio and high fatigue resistance are the factors making the use of FRP materials profitable and rational in the bridge construction (Mara, Haghani, & Harryson, 2014). New techniques, methods of fabrication and production opportunities which have developed during the last decades have reduced the production and construction cost (Niket M. Telang, 2006), (Wan, 2014). Construction of the ecoduct made of FRP offers great production opportunities since the composite structural members can be prefabricated and assembled on site during the erection process.

FRP composite materials do not require painting, do not rot and have high resistance to aggressive media. FRP is also usually dimensionally stable in Swedish conditions, but fire protection should be given special attention.

Even though FRP seems to be suitable material for the construction of ecoducts, very little investigation has been done on this specific issue. There was a study on how the ecoduct at Sandsjöbacka could be built in FRP (Sandahl & Hällerstål, 2018). However, the general situation in Sweden was not investigated. It was, therefore, important to investigate which specific conditions and demands there exist for ecoducts in Sweden.

There exists a wide range of practice for how ecoducts are defined and designed. Different countries apply different methods with a large scatter of results with a difference mainly in the width of the superstructure and the level of vegetation. Those different cases give each a distinct load situation, and the involved loads should be taken into consideration to be able to design a material- and cost- efficient ecoduct. One of the main loads on an ecoduct is mostly the soil load.

This, in combination with a fairly constant case of large roads as barriers, invites for a design that can be applied in a wide range of specific projects.

By doing a thorough analysis of the structural requirements on an ecoduct, an effective design with FRP materials can be made. Since the goal is to develop a design which could lead to a lower bridge cost compared to conventional methods, the problem is to optimize the material use.

1.1 Aim

The aim of this thesis was to develop a competitive concept for a fibre reinforced polymer ecoduct design, which can be considered as a typical design solution for Swedish conditions. To this end, the mechanical characteristics of composite materials and the possibility of their use in the design of ecoduct were studied.

1.2 Method

Literature review on FRP applicable in bridge construction

The project starts with a review over the existing literature concerning FRP in connection with bridge construction. A previous master thesis from Chalmers was chosen as a background for this study (Friberg & Olsson, 2014). There has been done much effort to compile information of interest in designing FRP bridges. To be able to mainly focus on design, this work was taken advantage of.

Literature review on ecoducts in Sweden

To gather information about the relevant typical context in Sweden, literature on existing ecoducts was reviewed. The requirements on ecoduct design from the Swedish Transport Administration (Trafikverket) and bridge design requirement from Eurocodes were considered. Places and conditions with the largest theoretical need for placement of ecoducts were identified.

Interview

An interview with an expert in ecoducts was conducted via Skype. The questions are presented in Appendix A. The interview was used as a starting point in order to identify the main issues of ecoduct design that should be given priority attention.

Preliminary design

Preliminary design of several proposals for ecoducts was done, including a variety in both material and structural solutions. 19 concepts were developed and analyzed in terms of manufacturability and ease of construction. The preliminary design was focused on the requirements on the deflection limits during the lifetime of the bridge as this is the governing criterion.

The goal was to distinguish and consider the effects of various parameters on the resulting behavior of the superstructure. Estimation of the deflection under the influence of environmental degradation factors such as temperature and humidity, as well as long-term

loading, taking into account the effect of creep, was the main criterion determining the design efficiency. Various structural systems were analyzed and a study of various geometries of structural members was performed in order to establish the most efficient design.

Of the 19 concepts, 5 were chosen for further, more precise investigation. Focusing on the production opportunities and considering various types of connections for structural elements, the final design was chosen.

Final design

The final design of the ecoduct was based on the study of preliminary designs. Finite element analysis was used to investigate buckling behavior and stresses. The analysis aimed at optimizing the geometry of the preliminary design. The results of the study were confirmed with hand-calculations checks to ensure the design requirements on allowable deflections and sectional utilization ratio with regard to material strength (Carattere, 2017; The European structural polymeric composites group, 1996).

1.3 Limitations

In order to make an ecoduct design more specific and fitting the Swedish conditions, the following limitations were imposed. The project includes several initial designs, based on which the final design was developed.

The preliminary designs include:

- The maximum deflection limit of the bridge span concerning different environmental degradation factors and long-term loading effects;
- Choice of the type and calculation of the amount of FRP composite materials required for the designed superstructure;
- Consideration over the existing manufacturing possibilities allowing fast and cost-efficient production of FRP bridge parts;
- Prediction of the possibility of quick and easy erection of the bridge.

The preliminary designs exclude:

- Checks on material strength;
- Consideration of the buckling behavior of the ecoduct.

To select the final design, a simplified analysis of the design efficiency, cost of production and materials, ease of manufacture and assembly of the structural elements, as well as other design criteria was carried out. The focus was on the production and material cost, possibility to ease manufacture and assemble the structural elements.

The final design includes:

- Analyses of buckling behavior of the proposed sections in ultimate load state;
- Checks on the material strength requirements with maximum allowable stresses in sections for the short term and long-term loading conditions.
- Checks on the deflections under the short and long-term load.

The analysis was conducted with existing models and guidelines for FRP construction. The focus was on European guidelines.

1.4 Outline of the thesis

Chapter 2: Infrastructure and fauna

Requirements and recommendations on ecoduct design are investigated in this chapter. First, the general description of the problem that transport infrastructure causes for the movement of animals is presented. Thereon, various types of barriers typical for Sweden are described. The issues described are both general investigations into the design of ecoducts and official recommendations and regulations. Finally, a set of requirements on ecoducts in Sweden is formulated.

Chapter 3: FRP composite material properties

Since knowledge about FRP as a building material is not widespread, this chapter discuss the FRP composite material features. The resins and fibres types are described separately. This is followed by a section on the physical properties of the final laminate. The influence of the temperature, moisture, development of creep and mechanical properties of FRP are described. Specific production methods, connections and the existing guidelines for the design with FRP are also described.

Chapter 4: Case study

Based on the investigation described in chapter “Infrastructure and fauna”, a case study is formulated. This includes the definition of the span and width of the bridge, as well as the loading conditions.

Chapter 5: Preliminary design

In this chapter several design solutions are suggested. The designs are based on deflection requirements and productions possibilities. The chapter concludes with a two-step evaluation, and a final design is chosen for further optimization.

Chapter 6: Final design

Here, one design chosen from the preliminary designs is optimized. First, an optimization of height and thickness of the structural members is done based on analytical calculations. Then, a finite element analysis is conducted to optimize the geometry with regard to buckling behavior of developed section. Buckling and stresses are investigated.

2 Infrastructure and fauna

Many kinds of animals move substantially during their lifetime. The infrastructure network, used for transportation, divides the natural habitat for many animals into small areas. By this, an individual animal can be hindered from free movement and, thus, have obstacles to its procreation or feeding habits. That effect can limit the size of the gene pool or the amount of food available. That hindering in movement is called barrier effect and incorporates several parts, see Figure 1 (A Seiler & Folkeson, 2003; Andreas Seiler, Olsson, & Lindqvist, 2015):

- Hindrance - the animals cannot get over the barrier for physical reasons.
- Killed - animals try to cross the road but are killed in the attempt. In case of larger mammals this can represent a considerable risk for the vehicle involved.
- Scared - animals approach a potential crossing but choose not to try to cross and return.
- Survival - a (usually small) portion of animals succeeded to cross the barrier.

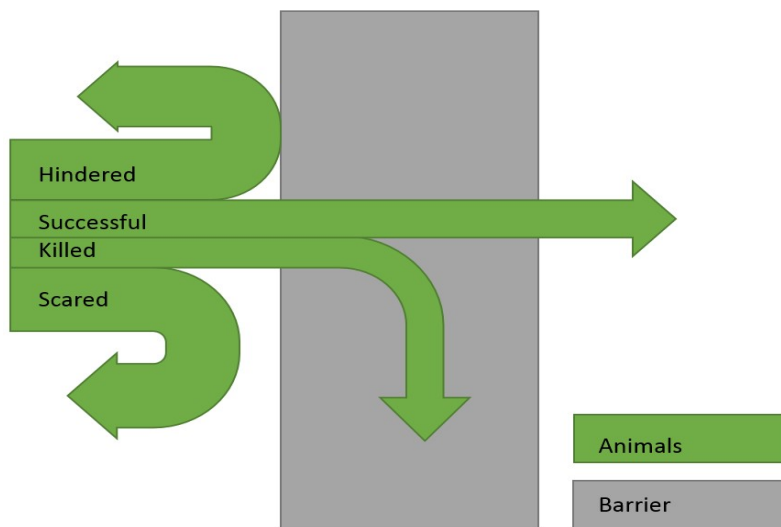


Figure 1. Streams of animals trying to cross a road. Figure after A. Seiler, Olsson, & Lindqvist, (2015).

Permeability is a term describing potential passages for animals. The term describes common opportunities for animals to overcome the barrier. Good permeability is created by a sufficient number of fauna passages. It can be both special transitions, and already existing bridges. Special passages, such as ecoducts, are much more effective in comparison with existing road bridges or tunnels. Together, the total number of passes and their effectiveness give the overall permeability of the barrier, as shown in Figure 2 (Andreas Seiler et al., 2015). The effectiveness of a passage is measured by comparing the number of animals approaching the passage with the number of successful crossings. It can also be calculated as a function of the width, length and height of a passage.

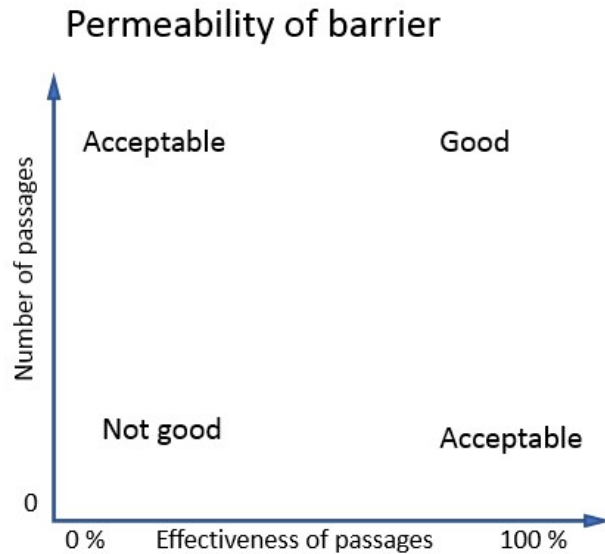


Figure 2. Total permeability of a barrier as a function of total number of passages and their effectiveness.

Since the barrier effect and permeability of the road are very different for different animals and cannot be analyzed for each species, a simplification is made. Usually that simplification is to use one species to indicate the demands. Ungulates and especially moose are used for that purpose in Sweden. Moose has high demands on permeability. Moose is also very demanding on the quality of the passage, therefore, a passage that is used by moose is properly used by other species as well (Andreas Seiler et al., 2015). This is a simplification, especially in the design of details more species should be considered. The described approach, however, is useful if a large-scale area is analyzed.

The road barrier effect can be reduced in several ways. The collective term for a measure against a barrier effect is called faunapassage and may work in different ways (A Seiler & Folkesson, 2003; Andreas Seiler et al., 2015). A faunapassage can be a way for a specific animal with specific need to cross the road. An example is a moose that needs to travel from pasture to pasture. Faunapassages can also work as a general measure to ensure a variation in the genepool of a species. The terms for faunapassages can vary widely from country to country or even person to person. Definitions may also vary; some sources state that ecoducts should not be used by anyone other than animals. Other sources point out the usefulness for hikers, riders or farmers. For the purposes of this thesis the following terms and definitions will be used:

- Ecoducts are bridges for animals, they mimic nature and should be experienced as continuation of the environment. Animals are the main users, other users may be hikers, forest industry and farmers. Use by other users must be assessed on a case-by-case basis and regulated.
- Faunabridges are the bridges that are built specially for animals. They are narrower than ecoducts, covered with a thin layer of soil and there might be low vegetation. In some cases, a small road might be on one side of the faunabridge.
- Viaducts, in Sweden called “Landskapsbro” are high bridges with a large area of the natural environment below.
- Tunnels can work for some animals, but ungulates often shy away from low and dark places.

These definitions and descriptions are taken according to the Swedish literature and recommendations. Recommendations for exact configuration of the ecoducts can be found in Swedish Transport administrations guidelines (Calluna AB, 2012; Vägverket & Banverket, 2005).

Road or pedestrian bridges can be used by some animals depending on the exact configuration. Long and narrow bridges are often avoided by most animals.

2.1 Barriers

As mentioned earlier, different animals are affected in different ways by different barriers. The European overview has attempted to classify how different species are affected by various barriers generating the fragmentation effect caused by transport infrastructure (A Seiler & Folkeson, 2003). The result can be found in appendix C. This can be paraphrased as follows:

- Small species such as beetles, spiders, amphibians, reptiles, and small mammals such as mice are strongly affected by the barriers. The barrier effect is full and strong even for small roads. There is some correlation between size of animal, road size and barrier effect. Also, railways can present total or strong barriers for those animals.
- Flying species are affected by traffic. Turbulence may lead to fatal injuries.
- Butterflies experience barrier effect from roads surfaces due to microclimate effects. Because of maneuvering difficulties, they may have troubles navigating fences.
- Mammals of mid and larger sizes can cross roads and railways. The barrier effects depend on the size of the animals, the width of the road and the traffic intensity. The barrier effect can range from:
 - total for fenced motorways, high intensity traffic railways and highspeed trains (HSR & TGV);
 - partly for bigger roads or fenced roads with passages;
 - very low for small roads and railways with little traffic.

It should also be mentioned that the barrier effect of trains has been less well studied but seems to depend on the traffic intensity.

Swedish Transport Administration has general recommendations/guidelines on how to approach the transport infrastructure in terms of a landscape/nature. They state that there must be passages for ungulates for every 4th km on newly build large roads (Trafikverket, 2016).

The same European review of the fragmentation due to transport infrastructure, as mentioned earlier in this section, gave numbers from a Danish study. The study claims that motorways have a much higher animal casualty rate per kilometer than other roads. The total animal casualties (from the entire motorway network) are however lower than for secondary roads. This is presented in Table 1.

Table 1. Casualties on different road types in Sonderjylland County Denmark. The species recorded are roe deer, fox badger, hare and hedgehog (A Seiler & Folkesson, 2003). Survey for 20 months (November 1995 – August 1997).

	Motorway	Highway	Secondary road	All roads
Casualties per km of road	2,3	1,9	1,7	1,8
Casualties across network	2960	3017	3449	8827

In a study of ungulate collisions in Sweden the findings were that there is a correlation between roads with a speed limit of 90 km/h and ungulate collisions. The statistic suggests that ungulates experience such roads as barriers even without fences (Andreas Seiler, 2004). On the other hand, collision densities were inversely correlated to highways and roads with speed limit 70km/h. It seems that ungulates experience minor roads (speed limit under 70 km /h) as a lesser barrier. Highways on the other hand are nearly always fenced, which means that animals are stopped in their attempt to cross before they reach the roadway.

P. Björkman, an expert in the design of ecoducts mentioned in a skype interview the high demands of ecoducts over motorways. There was also a discussion about the differences between the northern and southern parts of Sweden. Even if there are more barriers in the south, there is more wildlife in the north. Björkman mentioned also the fact that moose's in the southern part of Sweden never get old enough to learn new tracks.

In a study done for the Swedish transport administration the barrier effect of Swedish roads for ungulates were assessed. The following structures were considered most likely to act as barriers (Andreas Seiler et al., 2015):

- Roads with average daily use over a year (ÅDT) of more than 400 vehicles;
- Roads with capacity for more than 2000 average daily use over a year;
- Roads with speed limit of more than 100 km/h;
- Railway with more than 80 trains / day;
- Major railways (Stambana) with more than 50 trains/day;
- Railway with a speed limit of more than 150 km /h;
- Structures close to each other or to a town.

Apart from assessing the roads, the fauna passages along those roads were also analyzed in this study. This was used to assess the total permeability of the barriers in Sweden. A simplified result is presented in Table 2. The term “barrier” here is the distance along the road that is more than a certain distance from the nearest passage. That distance can be no more than 2 km and is less if the effectiveness of the fauna passage is limited (Andreas Seiler et al., 2015). The distance of 2 km was chosen, because an adult moose can move about 4 km in one day and, thus, theoretically can cross the road in that time.

Table 2. Barrier effect in Swedish road and railway system. This table is a simplified version of the data from Seiler et al., 2015 presented in Appendix B.

Barriertype	Barrier [km]	Total [km]	% barrier
Motorway	5393	7646	70
Higway (Riksväg)	4412	9307	47
Other roads	2999	84975	3,5
High barrier Railway	5581	6038	90
Low barrier Railway	293	5450	5

2.2 Ecoducts – Requirements and recommendations

Ecoducts are one of the most expensive ways to meet the needs of animals. This suggests that the needs of animals, as well as the intended services for animals, must be investigated very carefully.

In Sweden, there are very few official rules regarding the design of ecoducts. Some of them are presented below:

The regulations for road design (VGU) gives the minimal width of 30 m (Vägars och gators utformning, 2015).

The Swedish transport administration gives essentially two recommendations (Calluna AB, 2012):

- The ecoduct should be at least 30 m wide.
- The ratio between width and length should be at least 0.8.

The old Swedish transport administration (Vägverket & Banverket, 2005) guideline provides the following recommendations:

- The ecoduct should be at least 40 m wide.
- The ratio between width and length should be at least 0.8.
- The width can be reduced to 20 m if the objective is to create a corridor for moving species that are insensitive to traffic or where the topography is channeling.
- The thickness of the soil filling above the ecoduct should be:
 - 0.3 m - for grass and herbs,
 - 0.6 m - for bushes,
 - 1 m - for trees.
- Service life should be 50-100 years.

“Width” is defined here as the distance between the fences or screens. “Length” is defined as the length of the bridge from the animal’s perspective. Since such parameter is difficult to define, the total length is used here. “Span” is the span of the bridge from a structural perspective i. e. the length between supports.

Plants generate an acidic soil environment. In Sweden about 90 % of soil in the first 50 cm has a pH of more than 4. The pH is usually lower with increasing depth (“SLU,” 2019).

There are further principals given in the recommendations provided by old Swedish transport administration. They are meant to create a passage that animals do not experience as a barrier:

- Screen noise and light from traffic Most animals shy away from noise and light, which should be dampened/screened of as much as possible. If the ecoduct is very wide, a row of trees can be planted. Otherwise screens made of concrete or timber can be used. On the other hand, animals avoid tunnel-like environments. A high and solid screen might give that impression (Andreas Seiler et al., 2015). Also, different animals might need different height in screens.
- Continues landscape - to create the least barrier-effect the ecoduct should be experienced as a natural continuation of the surrounding landscape. Continuity with regard to slopes, sightlines and vegetation should be achieved.
- The whole ecoduct should be visible from each side. Some animals will not go into a potential threatening situation. Therefore, the whole ecoduct should be well visible from both sides of the road.
- It is necessary to create hiding spaces. Especially smaller animals need hiding spaces like grass, bushes or stones to be comfortable.

It should be pointed out that all the principals mentioned above should be studied for each specific case. The local landscape, vegetation, fauna and traffic must be analyzed in detail to be able to design the most efficient ecoduct.

Vegetation requirements

In an interview P. Björkman noted that it is important that vegetation fits into the surrounding. In his opinion, vegetation screens seem more natural than solid screens, animals can shy away from the passage with a large screen, in case they create a tunnel-like environment. Vegetation should be similar to the surrounding. This might not always be feasible. High Spruce and Pine are two dominating tree species in Sweden. Their root systems make them however unsuitable for plantation on bridges. An alternative might be bushes and trees such as rowan. In that case, a soil layer of 1-2 m on the ecoduct is needed. The most important issue with the soil layer, besides its thickness, is that the soil layer should be too dense. That might result in a lack of oxygen for the plants.

Special care should be put to those principals at the entries/exits of the passage. Even if the ecoduct itself is ideally designed, animals can refuse to use it if the environment is perceived as dangerous or unattractive.

P. Björkman mentioned the need for fencing along the edges. He emphasized the importance of planning the fencing early in the process. The actual fastening of the fences on the structure should be considered, as well as the connection to the fences along the road.

A suggestion for an ecoduct at E14 Timmervägen is shown in Figure 3. The project was mentioned by P. Björkman as a very good design. The flanges of the bridge create a natural barrier against the traffic and provide an open and well visible surrounding. Since the trees are at some distance to the edge, there is a small risk for trees falling on the road below.

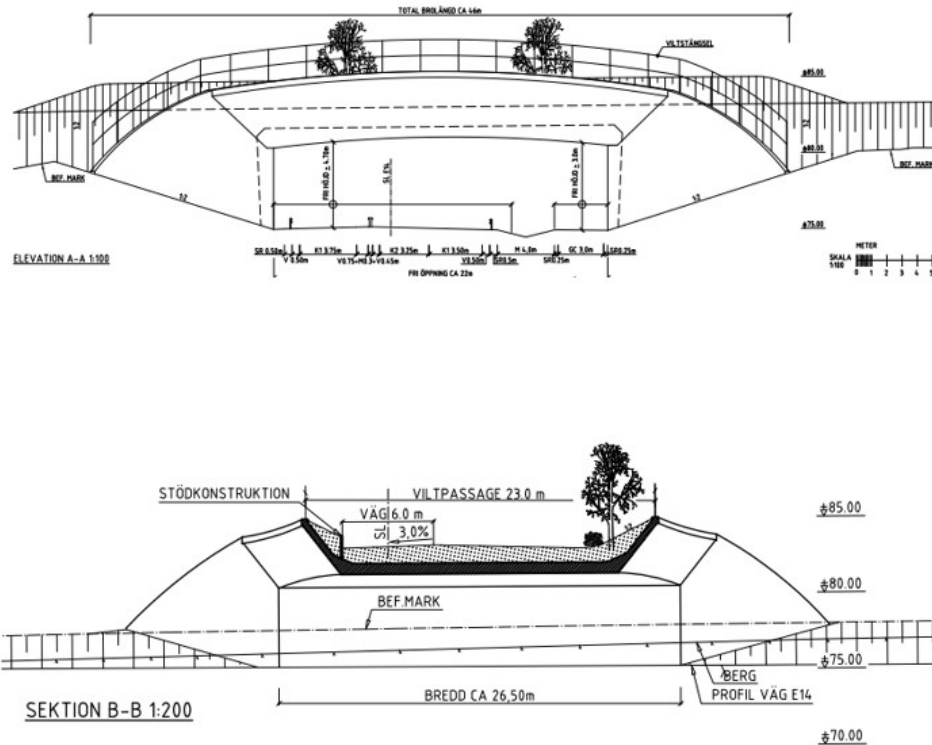


Figure 3. Suggestion for ecoduct at E14 Timmervägen after Norwegian model. Drawings from Trafikverket/Sundsvall municipality (Sundsvall Komun, 2018).

Users of ecoducts

The economic situation and financing are often the main determining factors influencing the choice of the type and design of the bridge. It is often a usual practice to combine several types of passages so that people also can use the ecoduct, if necessary. P. Björkman mentioned a benefit of an additional use of the ecoduct by hikers or horse riders. An interesting option is the idea to allow farmers or the forest industry the use the ecoduct. The logic behind that proposal is the frequency of use. Depending on the local situation, the forest industry might need access to an area every 20th year, or a farmer that needs access to one field might go there every 3d month. Such use can be justified, because it gives an economic benefit without disturbing the animals too much.

Shape of ecoducts

To maximize the effect of the ecoduct a channeling effect should be achieved. Apart from the importance of the placement in the specific topology, the design of the ecoduct is important. The bridge itself can be formed with parabola shaped sides. The slope to the ecoduct should not be too steep and the connection to the fencing along the roads should be well designed (Calluna AB, 2012). Parabola formed ecoducts have been used quite widely but there seems to be no studies on the effectiveness of this measure (Jondelius, 2011).

A further measure that can be taken according to P. Björkman is to allocate ecoducts in the vicinity of the places of main attraction for animals, where they are more likely gathered, such as forests and water bodies.

Existing ecoducts

How the above-mentioned principles and recommendations are applied can vary quite significantly. One of the easiest parameters to compare is the width of the ecoduct. In Europe, the width varies from 80 m (there exist one ecoduct with $W = 800$ m, but that's considered more like a tunnel) to about 8 m, which by many would be classified as a fauna bridge rather than ecoduct.

The width of 20 to 80 m is more common for ecoducts. This range of width is used widely in Austria, Germany, Switzerland, the Netherlands and Luxembourg. There are some narrower overpasses in France and Spain, those are about 8-20 m wide (A Seiler & Folkeson, 2003).

Ecoducts and different animal species

A German examined the behavior of animals both before the roads/bridges were built and after some years of use (Georgii et al., 2011). The study included capture-recapture of smaller species, flight pattern observation of butterflies and birds and video material and tracking for larger animals. For the smallest species the finding of the study was that the bridges were used fairly much. As an example, ground beetles adapted to open habitats dominated over those adapted to the forest environments. This also applies to thick scrubber bridges that should have been attractive to woodland dwelling species. The authors concluded that a corridor along which the animals could move was important.

A similar pattern was observed with grasshoppers. Before the construction of the road, grasshoppers were found in the whole area. After the road and the bridge were built, not a single one was found in the immediate vicinity. The surrounding near the bridge had changed quite dramatically and was no longer suited for this type of grasshoppers. Georgii et al., 2011 came to the conclusion that the changed habitat prevented animals from moving 300 m from their new habitat to the bridge. This meant that the ecoduct had zero practical efficiency for this species.

Flying species seemed also to prefer the ecoducts. Butterflies were observed to prefer the bridge. There was also a high mortality observed by butterflies crossing the bridge over the road. It was also observed that bats seemed to prefer the bridges with straight plantations of trees compared with scattered plantations. The authors noted that some bat species are known to navigate with the help of treetops. Some bird species were observed to prefer the ecoducts. Forest dwelling species used the bridge more than the open habitat species.

Mammals also used the ecoducts. Georgii et al., 2011 showed that mammals prefer ecoducts or viaducts over other passages, including faunapassages adjusted to ungulates. It should be noted that predators seemed to be less sensitive to what kind of faunapassage they used. The use of each individual bridge was varied and ranged from 2 to 50 animals per night. The study analyzed various attributes of the bridge and made the following conclusions (Georgii et al., 2011):

Width and length

The use of the bridge increased with increasing width. There was some negative influence with increasing length.

Age

The use of the bridges increased with increasing age of the ecoduct. A denser vegetation counteracted that development in several cases.

Position

The bridges at forest edges were used most. Bridges in the forest were used more than in an open landscape.

Vegetation

Mammals preferred the open parts of the ecoducts.

Traffic noise

There seems to be some difference in the use of ecoducts depending on how well the traffic noise is damped.

Human presence

Georgii et al. reported a negative influence on the use of ecoducts with human presence. This included the presence of people as well as a developed infrastructure, such as roads.

2.3 Requirements on ecoducts

According to the material presented in Sections 2.1 and 2.2, requirements on ecoducts can be summarized. According to these requirements a specific case was formulated in this thesis. It should be noted that these formulations are written with respect to the structural system that will be designed for the ecoduct.

Span

The span for the design depends mainly on which type of road should be crossed. The main types of barriers are motorway, highway and railways. In VGU (the Swedish requirements for the design of roads) the widths for different roads are given. The spans used here were derived from motorways/highways in rural area. Following assumptions have been done:

- Safety railings are assumed on both sides.
- The width of the mid-verge is taken 5 m. This is made to accommodate mid-supports. 1 m on each side must be kept free for the use of the safety railing.
- The verges for tunnels are used. Even if ecoducts technically are bridges, the driving experience, especially with a small span, is like a tunnel.

In Table 3 the spans derived are shown, the calculations are presented in Appendix D. The first number represents the minimum span. In that case the bridge foundations are very close to the road (1 m from the safety railings). Usually that should be avoided. A common practice is to create a slope of 1:2 outside that area. The second span given is for the case when the bridge goes up 2/3 of the maximum free height of the bridge with a slope of 1:2. The road sections for motorway and highway used here are presented in Figure 4 and Figure 5. In Table 3 the total length of each barrier type is presented together with its span.

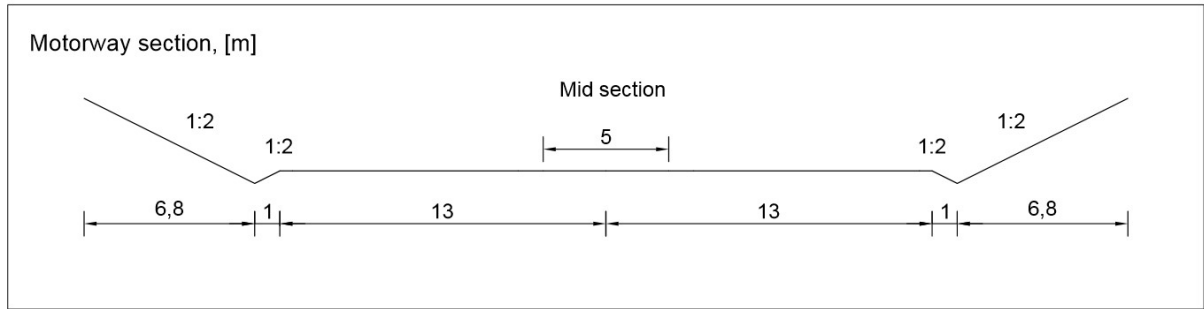


Figure 4. Motorway transverse section used in this thesis.

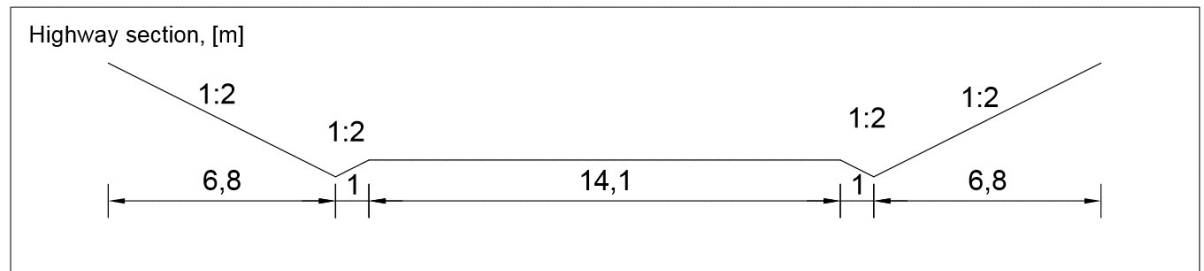


Figure 5. Highway transverse section used in this thesis.

The span of railway bridges is coupled to the sightlines along the bridge (Trafikverket, 2015). Those are in turn dependent on the curve radius, the maximum allowed speed on the line and the width of the tracks. Therefore it is difficult to arrive at a specific span for a general case.

Table 3. Type of barrier and associated span in Sweden. The span is taken as the minimal required span for newbuild roads. The calculations are presented in appendix D. The length of barriers the length along the roads and railways that are not near to a crossing.

Barrier type	Length of barrier [km]	Span over the road [m]
Motorway, (Europaväg)	5393	28,0 – 40,6
Highway, (Riksväg)	4412	16,1 – 29,7
Railway	5581	Varies

Width

The ecoduct must be at least 30 m wide (Trafikverket, 2015). This gives the length to width ratio (equation 1):

$$\frac{Width}{Length} = \frac{30}{16,1} = 1,9 \quad (1)$$

This ratio is more than the recommended 0,8 (Calluna AB, 2012).

Service Life

A service life of 100 years should be achieved (Vägverket & Banverket, 2005). The vegetation on the bridge should be designed so that a long-term pH does not get lower than 4.

Connection to surrounding

The bridge must be able to connect to the surrounding without any visible markings. The visibility of the foundation structure should be minimized.

A parabola shape of the bridge might increase the channeling effect. However, this assumption has not been investigated.

Fencing & Screens

There must be possibilities to install fences or screens at the edge of the bridge. The screens might be up to 2 m height ("Älg - Svenska Jägareförbundet," 2019). For Reindeer herding the fencing should be placed at some distance from the edge. The fencing and screens must be connected to the existing game fences along the road.

Vegetation

It should be possible to plant trees at least in some parts of the bridge. The edges are the most important parts in this case. This requires a layer of soil of at least 1 m height.

There should be a possibility to plant bushes on the bridge. This requires 0,6 m of soil.

There must be a possibility to grow grass and herbs on the entire bridge. This requires 0,3 m soil.

There should be a possibility to make earth mounds at the edges of the bridge.

It must be possible lay out larger boulders as hindrances for vehicles. If the fences are designed in a good way, this might be done outside the structural span of the bridge.

It should be possible to lay out a bunch of small boulders as a habitat for some species.

There would be additional value in the possibility to lead a small stream over the bridge.

Vehicles

There would be additional value if the bridge could allow access to vehicles such as tractors and forest machinery.

Inclination

The bridge span should have a small inclination so that at least a roe deer could look over the entire bridge. The argumentation behind this is that there isn't any smaller animal that has the need to be able to see the whole surface of the bridge. Predators are less sensible to details like this and hares are too small. Roe deer is about 70-75 cm in shoulder height. Wild boar is about 1 m in Sweden. "The bridge" includes here the bridge from the perspective of the animal. This makes the exact calculation more difficult since the exact distance at which the animals stand is not known. If an eye height of 0.9 m is assumed, this gives an indication about the maximum height difference of the bridge.

3 FRP composite material properties

This chapter aims at giving a general introduction to FRP in civil engineering. There will be a brief comparison between FRP and conventional building materials. Different types of resins and fibres will be described followed by a description of the physical and mechanical properties of FRP composites. Production methods, sustainability, durability and fire resistance will be discussed in this section. Existing codes and guidelines used in design will be also described.

The composite material consists, basically, of the resin matrixes and the fibre (U. Berardi & Dembsey, 2015) with recognizable interfaces between them (Niket M. Telang, 2006). The resulting mechanical properties of the final material are higher than that of the raw materials separately (Keck & Fulland, 2019). The resin should provide resistance of the material to the environmental and chemical factors, while the main purpose of fibre is to provide strength, stiffness and thermal stability to the composite (Sonnenschein, Gajdosova, & Holly, 2016). FRP composites are materials more resistant to the electromechanical corrosion in comparison with steel reinforcement (Sonnenschein et al., 2016).

The main influence on mechanical properties is exerted by the type, filling volume and arrangement of the fibres, type of the matrix, fibre orientation in the polymeric material, quality of the production (Sonnenschein et al., 2016). The conditions of bonding, called interphase, which includes perfect bonding and de-bonding of fibre with a surrounding polymeric material, causes significant influence on physical properties of the composite (Wenkai, 2015).

3.1 FRP and conventional building materials

In order to justify the choice of FRP composite materials to be used in design, a comparison of performance of different building materials was made, which can be seen in Table 4 (Akkad, 2011), (Anping Mengke Wire Mesh Manufacture Co., 2015), (U. Berardi & Dembsey, 2015).

Table 4. FRP & Conventional materials comparison.

	FRP (GFRP, CFRP)	Steel	Concrete	Timber
Production and construction				
Density (kg/m³)	1550	7500	2200	200-1400
Strength to weight ratio	highest	medium	high	low
Thickness of the members	very thin	thin	thick	thick
Length of the elements	unlimited	limited	limited	limited
Material cost	high	normal	normal	low
Life cycle cost	low	normal	normal	high
Maintenance	low	high	medium	high
Installation complexity	very easy	difficult	very	easy
Installation time	very short	long	very long	short
Mechanical properties				
Tensile strength (MPa)	170-240	450	2-5	low
Flexural strength (MPa)	205-240	450	3-5	80
Thermal conductivity (W/m* °C)	0.57	46.55	0.8	0.15-0.04
Thermal expansion (10⁻⁶ m/m* °C)	20	12	14.5	3

Performance under the environmental factors				
Corrosion resistance	high	low	medium	no
Fire resistance	high	low	medium	low
Impact resistance	high	medium	high	medium
Fatigue resistance	high	medium	medium	low

A comparison of Young's modulus of different building materials and the stress-strain relations in tension can be seen in Figure 6 and Figure 7 (J.G. Teng, 2001).

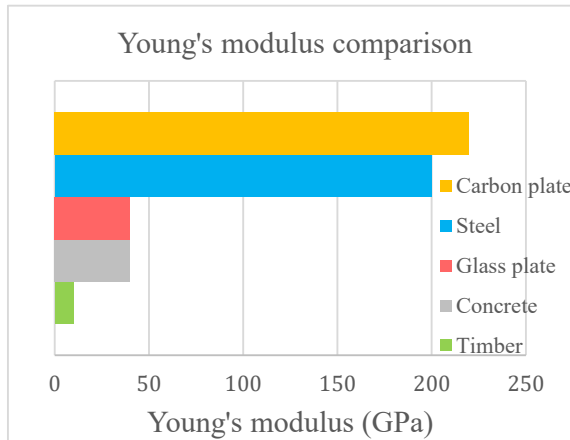


Figure 6. Young's modulus comparison.

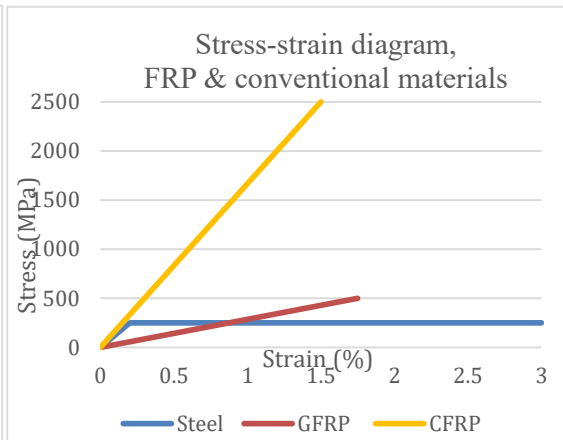


Figure 7. Stress-strain diagram, FRP & steel.

Observing the diagrams shown in Figure 6 and 7 together with Table 4 it can be concluded, that the mechanical properties of the FRP composite materials can compete with traditional building materials. However, the fibre volume fraction in the composite material should be considered.

FRP offers a wide range of design possibilities due to high dimensional stability and the ability to adopt the mechanical properties of the FRP composite material in accordance with the design needs and application requirements. It can be done by selecting the type of resin and fibre, fibre length, volume fraction, directions and number of the fibre layers in laminate, etc. The parameters, influencing the mechanical properties of the FRP composites are further described in the following sections (Sections 3.2 - 3.4, 3.7, 6.1, 6.2).

Temperature impact

The dependence of strength on temperature influence for different building materials can be seen in Figure 8 (Kodur, Bisby, Green, & Chowdhury, 2005).

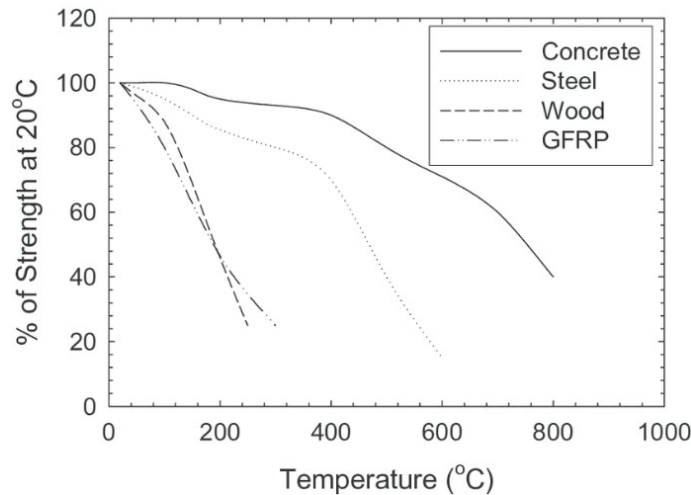


Figure 8. Strength-temperature dependence curves for different building materials.

From Figure 8 it can be concluded, that the strength of GFRP material is the lowest compared to other building materials which means that FRP structures need additional covers and protection against fire.

3.2 Resin

Resins in the composite material are responsible for the transfer of stresses between the reinforcing fibres, gluing them together and protecting fibres from mechanical damage and environmental influences.

There are two common types of resin: thermoplastics (Figure 9) and thermosetting materials (Figure 10) that are used in FRP production (ACMA, 2016), (WPL, 2013).

Thermosets

Thermosets are mostly used for the production of composites. The process of polymerization converts the resin from the liquid to the solid form, which is an irreversible act. Examples of thermosets include polyester, vinyl ether, epoxy, and polyurethane.

Polyester

Unsaturated polyester resins (UPR) constitute approximately 75% of the total resin used in the production of composites. Polyesters are easy to modify and adapt when building polymer chains. These resins can be modified according to the needs of the customer and are manufactured with specified mechanical properties.

Epoxy

The main advantages of epoxy resins are their mechanical properties, such as resistance to corrosion, environmental effects and elevated temperatures, excellent adhesion with other materials. They have a lower shrinkage in comparison with polyester resins. Due to the increased viscosity of the epoxy resin, there is a need to add additional hardeners due to the increased heat capacity, which can substantially affect the mechanical properties of the final product.

Vinyl ester

Vinyl esters successfully combine the advantages of epoxy resins and unsaturated polyester resins. They cure faster and are more convenient to handle. Vinyl esters can provide higher stiffness and corrosion resistance to the composite material.

Phenol

Phenols are a type of phenol-based carbolic acid resin. It can be produced in red, black and brown colors, and the production process itself is accompanied by the release of condensates. The advantages of composites whose polymer matrixes are based on phenol are high sound insulation and noise absorbing properties, corrosion and fire resistance.

Polyurethanes

Polyurethanes are widely used in everyday life. They can be used as a coating, glue, foam, and many other forms. This type of resin is quickly cured, wearproof durable and elastic material resistant to chemical damage. Polyurethane adhesives are widely used in construction as a binder between various composite elements or concrete (ACMA, 2016).

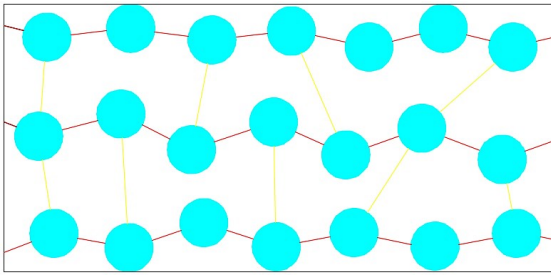


Figure 9. Irreversible bonding chains between the molecules of the thermoset resin (ACMA, 2016).

Indicative values of thermoset resins properties can be found in “Prospect for New Guidance in the Design of FRP Structures”.

Thermoplastics

Due to the fact that thermoplastic resins are not crosslinked, the main advantage of their use is their ability to be processed repeatedly. Thermoplastics can be re-melted and reused, which is the result of the reversible bonding between the molecules of the polymeric chains (see Figure 10). The most prominent examples of thermoplastic resins are ABS, polyethylene, polystyrene and polycarbonate. Thermoplastics have usually lower strength and are not generally used for the production of bearing structural components.

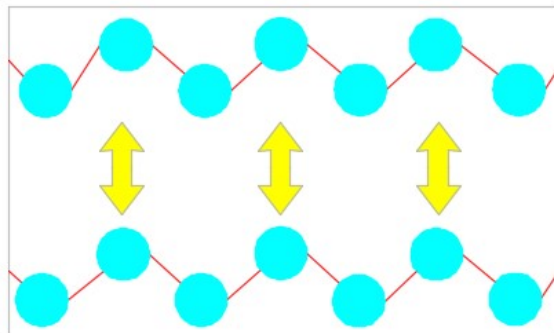


Figure 10. Reversible bonding between the molecules of the thermoplastic resin (ACMA, 2016).

3.3 Fibres

There are three main types of fibre used in the manufacture of composite materials in the construction industry: glass fibre, carbon fibre, aramid. Fibres can be produced of different length, which gives a significant influence to the mechanical performance of the composite material (Bhagwat, Ramachandran, & Raichurkar, 2017). Fibres provide strength in the direction of the length of the fibre, so their orientation in the material is of great importance for the bearing capacity of the structural element.

The most influencing factors to the mechanical properties of composite material with regard to fibre are:

1. Volume of the filling

Fibres make 30% to 70% of the volume of the composite and up to 50% of its weight (Sonnenschein et al., 2016). Various types of reinforcement may be used, such as continuous fibres, chopped fibres or particles (Keck & Fulland, 2019). Tests on the effect of filling volume on mechanical properties showed that the maximum load increased with an increase in the volume fraction of the fibre in the composite material.

2. Fibre length

The fibres used in FRP composite can be of different length:

- short fibres;
- chopped fibres;
- long fibres;
- woven fibres.

Based on the length of the fibre, the following categories of the composite materials can be described with the fibre as reinforcement:

- short/long fibres – fibrous composites;
- particles – particulate composites;
- flake flakes – flake composites;
- fillers – filler composites.

The length of the continuous and discontinuous fibres, its size, shape and concentration in the laminate strongly affects the material strength of the final product. This provides a wide range of options for various applications of the FRP composites.

A very small diameter of the fibres (few to 100 microns) has the following advantages:

- The reduced possibility for inherent flaws results in increase of the ultimate strength of the thin fibre compared to the thicker fibres;
- The thin fibres are better bonded into the polymer matrix;
- Thinner fibres are more flexible and more susceptible to bending without breaking the fibre.

3. Bond properties

The maximum bond strength of glass and carbon fibre reinforced polymers are similar and its material properties are highly dependent on the manufacturing technique (Farooq & Banthia, 2018a).

4. Fibre orientation

The fibre orientation in FRP composites has a significant influence on the mechanical properties of the final product. The fibre orientations can be seen in Figure 11.

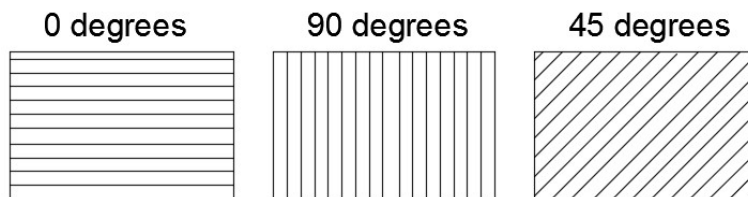


Figure 11. Fibre orientation in FRP composite.

0° - The most commonly used orientation of the fibre, in which the fibres are placed in the direction of the load, thereby ensuring maximum strength and rigidity in this direction. Also, this type of reinforcement arrangement contributes to an increase in flexural strength and bending stiffness. To increase the torsional strength, it is recommended to add layers with a direction of 90 degrees (Composites, 2018).

90° - To apply this direction of reinforcement will be cost-effective when it is necessary to ensure bending in two directions, for example when the material is squeezed or oscillated under load preventing the premature deformation (Composites, 2018). The maximum loading can be achieved with a 90 degree fibre orientation (Keck & Fulland, 2019).

45° - The most suitable reinforcement direction if the aim is to create a quasi-isotropic layer, usually used in combination with 0 and 90 degrees layers. In combination with layers with 0 and 90-degree directions, it differs from bidirectionally reinforced materials in that the quasi-isotropic properties are the same in all directions. This direction of reinforcement is effective if the material is intended to twist and bend (Composites, 2018). This direction is most efficient for taking up shear forces.

The difference on mechanical properties of composites with different fibre directions is further explained in Section 3.4.2.

Crack pattern

It should be specified that there are two possible failure modes of the fibre reinforced polymeric layer: the break-out of the fibre itself, and the failure in the matrix of the composite element.

The direction of the crack propagation mainly depends on the fibre orientation in the layer. The cracks under the compact tension (static loading) propagates in the direction of fibre (Keck & Fulland, 2019).

There also exist a correlation between the volume fraction of the fibre and the development of the crack path. For the composite materials with a low volume fraction of reinforcement, the crack path is not significantly dependent on the direction of the fibre. With a higher volume fractions of reinforcement, the crack initially grows along the initial plane of the crack, then bends in the direction of the fibres, finally continuing his grow in the direction of the fibre (Keck & Fulland, 2019).

Comparison of different fibre types

The mechanical properties of fibres differ, and the comparison is shown in Figure 12 .

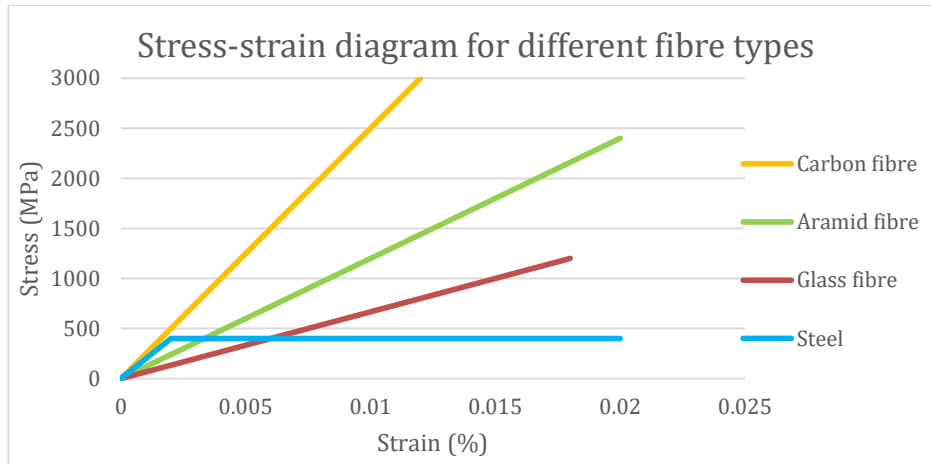


Figure 12. Stress-strain diagram for different fibre types.

From Figure 12 it can be seen, that the fibres have different mechanical capacity and the fibre type for the FRP material can be selected depending on the application needed.

3.3.1 Glass fibre

Glass fibre (GF) is a material made from the fine fibres of glass. The advantages of glass fibres are bulk strength and light weight, but one of the biggest disadvantages is the inability to withstand high temperatures. Glass fibre has a lower modulus of elasticity, low shear modulus and Poisson's ratio in comparison with a carbon fibre (Bhagwat et al., 2017).

Glass fibre can be made of B_2O_3 , SiO_2 , l_2O_3 , MgO , or CaO in powdered form (Bhagwat et al., 2017) and there can be four different types of the fibre glass which has different material properties:

A-glass - its composition is close to window glass and is mainly used for process equipment production;

C-glass - has higher resistance to the impact of aggressive environment;

E-glass - has high thermal insulation properties;

AE-glass - has high alkali resistance.

Fibreglass has the highest properties immediately after production. If scratches and damages appear on the surface during processing and handling (GFRP), the strength and ductility of the fibre decreases. Humidity is the main factor impairing the mechanical properties of the fibre, since moisture is easily adsorbed by the material and can cause the appearance of microscopic cracks and defects (Kiron 2013).

3.3.2 Carbon fibre

Carbon fibres (CF) are commonly used as reinforcement in high performance composites (CFRP) using thermosets or thermoplastic resins as a polymeric matrix (Naqvi et al., 2018). This composite type is much more expensive than the GFRP composites. The orientation of the fibre plays a decisive role in the mechanical properties of the material (Bhagwat et al., 2017).

Carbon fibre have a good strength and low elongation, can be produced from organic precursors, including PAN (polyacrylonitrile), rayon, and pitches. Typically the consist of more than 99% carbon in the composition.

This type of fibre is resistant to high temperatures. The main disadvantage of the fibres is their high cost of the final product, due to the high cost of the material and the energy intensity of the production process. Carbon fibre composites are less ductile than these based on glass or aramid fibre.

Carbon fibre-based composites can corrode in contact with metals. This is a cathodic reaction. If the composite is placed in a solution in a contact with the metallic parts of the structure (in case of the hybrid structures) there will be a difference between the galvanic potentials of the composite and metal and hydroxide ions will be generated. In that case the fibres become open to a solution and the composite corrodes. To prevent corrosion in contact with metal, the composite material is recommended to be protected with protective coatings.

There are few groups of the carbon fibre material in accordance with its properties:

- Ultra-high-modulus, type UHM (modulus >450 GPa)
- High-modulus, type HM (modulus between 350-450 GPa)
- Intermediate-modulus, type IM (modulus between 200-350 GPa)
- Low modulus and high-tensile, type HT (modulus < 100Gpa, tensile strength > 3.0 GPa)
- Super high-tensile, type SHT (tensile strength > 4.5 GPa) (Bhatt & Goe, 2017).

3.3.3 Aramid fibre

Aramid is an artificial material, the fibres have a low density and high impact resistance and higher tensile strength under fatigue loading compared to glass and carbon fibres. This type of fibres have high electrical and thermal insulation properties, and high resistance to chemical damage and environmental influences. Kevlar fibre is the most used of the aramid fibre.

Aramid fibres have about five times higher strength than steel with the same weight. The material is able to withstand temperatures of more than 500 degrees Celsius without damage (Fibremax Ltd, n.d.). These mechanical properties result in a relatively high price of the material (H.M. Yang, 2000).

One of the biggest disadvantages of the aramid based composite is the lack of adhesion to the matrix, which results in a low transverse tensile strength, compressive strength in a longitudinal direction of the fibre and lower interlayer shear strength. Similar to a carbon fibre, aramid fibres also have a negative coefficient of thermal expansion which means that these materials contract upon heating (H.M. Yang, 2000).

3.3.4 FRP composites

Configuration of composite

Based on the reinforcement type, the FRP composite materials can be classified as follows:

1. Fibre reinforced composites;
2. Laminar composites;
3. Particulate reinforced composites.

FRP composites can be produced of different volume and fraction of fibre in the composite material. In this way the material strength can be adopted to the conditions in which the laminate is predicted to be used to meet the exact application needs.

The combination of composites

Since the use of glass fibre and carbon fibrebased composites has its advantages and disadvantages, in recent years an increasing number of studies have been directed towards the search for hybrid solutions for the efficient use of both types of fibre in the design simultaneously.

The major advantage of carbon fibre is a higher modulus of elasticity, this type of the reinforcement provides stiffness and the main characteristics of the carrying capacity. Carbon fibre is able to withstand high temperatures much better in comparison with glass fibre (Bhagwat et al., 2017). Glass fibre composites are more resistant to damage and can provide lower stiffness with a higher elongation (Jesthi, Mandal, Rout, & Nayak, 2018).

The mechanical properties of composites reinforced with glass fibre are much lower than these reinforced with carbon fibre, so it can be reasonable to use mixed composite types when designing for optimal results in terms of price-quality (Bhagwat et al., 2017). The combination of the glass and carbon fibres can be used in order to achieve a required mechanical properties of the composite material resulting in an increase of the strength and stability of the material (Bhagwat et al., 2017).

Applying simultaneously two types of fibres can improve the mechanical performance of the composite material and the properties of the hybrid composite will depend on the volume fraction and the sequence of laying the layers of fibres (Jesthi et al., 2018). This can reduce the cost and increase the bearing capacity of the composite structure (Bhagwat et al., 2017). According to research, the tensile strength of a hybrid composite using various reinforced layers is up to 23% higher than the strength of a pure glass fibre reinforced composite (Jesthi et al., 2018).

There are even hybrid carbon /glass fibre / epoxy morphing composites that can change their morphing behavior, which results from a mismatch of thermal expansion coefficient (CTE) between carbon and glass fibres, so the shape of the composite structure can be corrected by temperature. Such composites belong to the class of so-called "smart" materials (Seyyed Monfared Zanjani, Al-Nadhari, & Yildiz, 2018).

In case, when the glass fibre and carbon composites are placed in a water bath to speed up aging, the mechanical properties of the GFRP system deteriorates significantly. After removing the moisture, the strength of CFRP composites increases to 95.75%, while the strength of the GFRP composite reaches approximately 74.65% of the original value (Zhang et al., 2018).

FRP composite materials has good alkaline resistance, and glass fibre reinforced polymer has a relatively small reduction in strength in comparison with carbon fibre (Farooq & Banthia, 2018b).

The FRP laminate composite materials are of interest in this thesis and will be further described in more detail. The fibrous composite type with the continuous fibre used as a reinforcement was chosen for the ecoduct design.

3.4 Physical properties

In this chapter the physical and mechanical properties of FRP composites commonly used in the field of structural engineering are presented. Their physical properties such as density, thermal expansion coefficients and mechanical properties such as tensile strength and stiffness can be found in Table 5.

3.4.1 Temperature and density

FRP is a material where production method and accuracy significantly affect the resulting mechanical properties of the final product. Apart from the resin and fibre involved, the manufacturing process, fibre volume fraction and alignment of the fibres are important factors for the resulting material strength. FRP is generally an anisotropic material, thus, the material properties can differ quite substantially even within the same component but in different directions of the fibre. This chapter does not aim to present all the possibilities but to give a view of the range of possibilities.

Thermal expansion coefficient

The thermal expansion coefficient varies with fibre direction and also fibre volume fraction Table 5 gives the values for different configurations.

Table 5. Thermal expansion coefficient for different configurations of fibres (Friberg & Olsson, 2014).

	Unidirectional	Unidirectional	Bidirectional	Mat + roving
Fibre volume fraction V_f [%]	65	65	65	37
Coefficient of thermal expansion [$10^{-6}/^{\circ}\text{C}$]	8,6	14,1	9,8	11

Glass transition temperature.

Glass transition temperature (G_t) of the polymer matrix and the fibre is an important parameter affecting the overall mechanical properties of FRP laminate. G_t of the polymer resin is much lower than that of the fibre. It is the temperature when the polymer matrix loses stiffness and become more flexible. This is the reason why the mechanical properties of the resin are governing parameters while choosing the resin type for the composites.

The operating temperatures of the designed structure should be taken into account. As an example, the glass transition temperature for the Polyester resin is around 60 degrees C, for the Vinylester – 100 degrees C, and 80-150 degrees C for the Epoxy resin (Carattere, 2017). The curing process, curing temperature and time are the main parameters affecting the final mechanical properties of the resin.

Density

The density of FRP generally is between that of timber and Concretes. Table 6 gives an overview of the variation.

Table 6. Range of density for FRP with both normal and more extreme values (Friberg & Olsson, 2014).

	Density
Lower	0,9
Typical,	1,2
Typical,	1,8
Higher	2,3

3.4.2 Mechanical properties

As mentioned before the mechanical properties vary widely for different configurations and directions of FRP. In Table 7 the tensile strength and modulus of elasticity is presented for different materials and fibre orientations. The breaking tension varies from 35 to 1020 MPa and the modulus of elasticity from 2 to 140 GPa. That means that the general term FRP is very useful to describe a specific structural material. The material choice and fibre orientation influences the properties of the material.

Table 7. Influence of the fibre orientation in FRP composite material (Friberg & Olsson, 2014).

Type of FRP composite and orientation	Direction 0 °		Direction 90 °	
	Modulus of elasticity [GPa]	Breaking tension [MPa]	Modulus of elasticity [GPa]	Breaking tension [MPa]
High strength carbon /epoxy				
[0 ₄]	100-140	1020-2080	2-7	35-70
[0 ₁ 90 ₁] _s	55-76	700-1020	55-75	700-1020
[45 ₁ 45 ₁]	14-28	180-280	14-28	180-280
E glass/epoxy				
[0 ₄]	20-40	520-1400	2-7	35-70
[0 ₁ 90 ₁] _s	14-34	520-1020	14-35	520-1020
[45 ₁ 45 ₁]	14-21	180-280	14-20	180-280
High strength aramid/epoxy				
[0 ₄]	46-68	700-1720	2-7	35-70
[0 ₁ 90 ₁] _s	28-34	380-550	28-35	280-550
[45 ₁ 45 ₁]	7-14	140-210	7-14	140-210

In FRP the fibres stand for the major part of the tensile strength, which accounts for the difference in tensile strength transverse to the fibres.

The shear properties are also heavily depending on the fibre orientation. The best orientation is achieved with all fibre orientated $\pm 45^\circ$, this gives however a low tensile strength (see Table 7). In Table 8 the shear properties for different materials are presented.

Table 8. Shear strength and shear modulus for different composite configurations with unidirectional fibre orientations (Friberg & Olsson, 2014).

Material	Shear strength [MPa]	Shear modulus [GPa]
Carbon/ Epoxy	93	7,17
Glass/Vinyl ester	16	5,44
Glass/Polyester		
Aramid/epoxy	34	2,28

In contrast to tensile and shear strength the compressive strength of FRP composites mainly depends on the resin, the fibre resin interface and the modulus of elasticity. Generally the compressive strength of the resin is higher than the tensile strength of the resin.

3.5 Sustainability

Sustainability is a very wide term. Following characteristics are usually quantified in some way (Zoghi, 2014) :

- Resource used
- Environmental impact
- Human and environmental health risks
- Site design strategies
- Performance

FRP can be characterized with two resource types: crude oil for raw material and energy for production. Oil is often viewed as controversial. It is highly usable but with limited availability and high cost in terms of CO₂. The energy use for FRP production is extensive. Depending on exact material, fibres can require temperatures in excess of 1000° C. However, traditional construction materials, such as concrete and steel, need similar temperatures.

Environmental impact is of different nature. There are different toxic gases released during the life cycle as well as gases associated with global warming.

To quantify the life cycle cost for a whole material group is nearly impossible. However, it is worth knowing that there is evidence that FRP bridges perform better in terms of energy use and CO₂ emissions than traditional steel and concrete bridges (Mara et al., 2014). Nevertheless, this may vary from case to case.

Another important issue is recycling possibilities. FRP cannot be reused as a building material, and material recycling is only partially possible. Thermoplastic resins can be melted and reused to some extent. There is also a possibility to use a granulate from FRP as filler or to chemically recover the material. Those processes are however either very energy consumptive or give a less valuable material.

A possible way to deal with FRP waste is to incinerate it. FRP can release a high amount of energy by burning. This creates new toxic emissions which can lower the attractiveness of this solution (Mara et al., 2014).

A common practice is to store FRP in a landfill. The polymer in FRP adds to the growing amount of plastic “trapped” in nature. The normal abrasion of FRP also adds to that, in comparison to steel and concrete, this impact is severe. However, the abrasion of FRP material in ecoducts is limited, since the surface, being under the layer of soil, is not directly exposed to the users of the bridge.

3.6 Durability

FRP structures are often exposed to various external environmental factors, the main ones being humidity and variation of temperatures. These factors can affect the physical and mechanical properties of FRP composites, causing material degradation and deterioration of the bearing capacity of structural members. In accordance with the ESPEC report, about 60% of failures due to environmental factors is caused by humidity and a sharp temperature changes (Glaskova-Kuzmina, Aniskevich, Martone, Giordano, & Zarrelli, 2016). Based on this, factors of presumable influence and possible risks should also be explored.

The largest problem with durability of FRP is degradation of the matrix and changes in the interface between matrix and fibre. This will usually result in a loss of strength and stiffness. Factors influencing the degradation rate are (Friberg & Olsson, 2014):

- Type of resin in FRP composite;
- Type of the fibre;
- Loading conditions;
- Manufacturing methods;
- Moisture uptake;
- Acidity and alkalinity of the environment;
- Temperature and humidity;
- UV radiation;
- Other chemicals.

Most resins change with increasing age. The aging process results in a more brittle and rigid resin structural behavior with time. Thermosetting resins are usually less affected than thermoplastic resins.

The durability of composite structures depends on many factors, and operating temperatures are one of the determining factors between them. In order to increase the hygrothermal properties of composites, the most cost-effective solution is to reduce the possible absorption by the material (Zhang et al., 2018). Also, the use of various hydro and temperature protective coatings may be a possible solution.

Moisture uptake

One of the largest problems with FRP is the ingress of moisture. Usually the resin absorbs moisture, this can result in softening of the matrix and lowering of the glass transition temperature, T_g . The moisture uptake itself can be reversible, the change of mechanical

properties is however often not reversible. The mechanical properties that can be reduced are (Friberg & Olsson, 2014):

- Strain at failure,
- Modulus of elasticity,
- Shear, bond and flexural strength.

There exist synergy effects for moisture uptake together with sustained loading and elevated temperatures. Some reversible effects can be removed by ordinary drying, but complications such as the occurrence of defects in the microstructure of the material and the hydrolysis of the polymer matrix can be permanent (Zhang et al., 2018).

The fibres are less vulnerable towards moisture. Carbon fibres barely absorb moisture. Fibreglass can absorb more, but aramid fibres are most vulnerable to moisture. The absorption of moisture can lead to the swelling of aramid fibres which results in loss of strength (Friberg & Olsson, 2014).

A gelcoat can protect the FRP material against the absorption of moisture but the coat itself must be sufficiently ductile, otherwise cracks can form which lead to local moisture absorption and effects such as debonding of matrix and fibre.

Effects of chemicals

Acidic environment can cause a degradation and debonding process. FRP materials are also vulnerable to alkaline environments. Especially glass fibre can deteriorate in alkaline environments. Both these processes are coupled to the absorption of moisture (Sandahl & Hällerstål, 2018). Since carbon is a nonmetallic conductor, the contact with aluminum or steel can lead to galvanic corrosion (Friberg & Olsson, 2014).

High temperature

Research performed in order to investigate the behavior of composite under increased temperatures showed that the elastic modulus of CFRP composite material decreases with increasing temperatures due to the oxidation of the outer layers. It was concluded that the procedure is closely related to the oxygen content in the environment, since the test results showed that the elastic modulus does not change due to temperature in the inert (nitrogen) environment. The carbon fibre tensile strength decreases by almost 50% when the material is exposed to temperatures in the range 400-700 °C and does not depend on the oxygen content in the environment (Feih & Mouritz, 2012)

Freeze-thaw cycles

Long-term effects of freeze thaw cycles are micro cracking, matrix hardening and the loss of interface between matrix and fibre. Besides the direct loss in strength, the microcracking can result in an increased moisture uptake. The loss of interface can ultimately lead to debonding failure and changes in strength, stiffness and fatigue resistance (Friberg & Olsson, 2014).

Creep

The creep phenomena in FRP structures should be given special attention. The creep of polymer matrix develops with time under the influence of permanent loading and environmental degradation factors such as humidity and temperature variation.

The viscosity of the polymer matrix is an important parameter which influences the durability and reliability of the FRP elements (V. P. Berardi, Perrella, Feo, & Cricri, 2017). The long-term behavior of the FRP laminate and fibres is linearly viscoelastic, which means that creep strains

increase linearly with time, however the creep behavior of the resin is nonlinear. The creeping rate can be significantly increased with rise in temperature or mechanical loads on the FRP elements (Yang et al., 2018).

Creep phenomena should always be considered when designing structures made of FRP to ensure the safety requirements for the material strength throughout the entire service life of the structure.

Fire

There are two main problems that fire presents for FRP structures. First, the growing creep and delamination of the material and, secondly, the poisonous gases omitted by the process.

Depending on the exact material composition FRP is very susceptible to creep and loses strength at between 100°C to 200° C. At higher temperature of about 250°C to 400° C the material starts to decompose. In most cases the resin is the most critical component both with regard to stiffness, decomposition and flammability (Friberg & Olsson, 2014).

Each material has a different response. As an example: Phenolic resin is one of the least flammable resins, but the time to failure is still very quick because it loses strength quickly.

There are different measures to increase the fire performance of FRP (Friberg & Olsson, 2014). A Phenolic skin decreases the flammability of the surface (Phenol is a type of resin, see 3.2.). Additions into the resin can act as flame retardants. They can also change the physical properties of the composite. Flame retardant coats can be applied.

3.7 Production Methods

The production method is one of the governing factors for the properties of the resulting product. The range goes from highly industrialized methods to handmade. The issues to be considered vary from the level of standardization, the required fibre content, the number of components, the shape of the components, and the available knowledge of existing workers. Something that should be mentioned for all methods is the importance of avoiding voids in the laminate during production. Several methods applicable to bridge construction are presented below (Friberg & Olsson, 2014).

Hand lay-up

In the hand-layup method, the form is an assembly. Laminate is composing manually, alternately applying fibre and resin. The method is characterized by (Friberg & Olsson, 2014):

- Low fibre content.
- Varying quality.
- Possibility for complex forms.
- Low investment cost.
- Labor intensive production.
- Easy to teach new staff.

A possibility to increase the fibre content is to use a vacuum- or pressure-bag during curing. In that way the fibre content can be increased to about 55 % and 65 % respectively (Domone & Illstho, 2010).

Resin Transfer Molding (RTM)

Resin Transfer Molding is classified as a semi-automatic method. The stacked fibres are prepared and placed between two molds. The resin is then injected into the mold. Sometimes the injection is assisted by a vacuum pump. The method is characterized by (Friberg & Olsson, 2014):

- Fibre content of up to 65 %.
- Tolerances between hand lay-up and pultrusion can be achieved.
- The initial investment cost is between that of hand lay-up and pultrusion methods.
- Low viscosity resins.

The size of the components produced is usually in the range of 0.5 m² and up to 10 m².

Resin Injection Molding (RIM)

The resin injection molding works similar to the RTM methods mentioned earlier. The fibre is prepared in a form. The form is then sealed with a vacuum bag and the resin is infused under the pressure. One of the problems with the RIM method is that it is more difficult to achieve full fibre impregnation with resin.

Pultrusion

The pultrusion process is a highly automated process that can produce a variety of constant sections. The process requires advanced machinery and good knowledge of the process. A high-quality product in terms of strength and tolerances can be achieved. The process works by pulling continuous fibre through a guiding system. Then the fibre is injected or passed through a resin bath. Then the fibre impregnated with resin pass through the heated die, the composite is cured and cut to the required element length. The method is characterized by:

- High fibre content,
- Small tolerances,
- High investment cost,
- Fast setting and low viscosity of the resin (Friberg & Olsson, 2014).

Only continuous sections can be produced by this method. Their average size can vary from 3 mm to 900 mm (Strongwell, 2019). Polyester or vinylester resins are usually used in pultrusion. Epoxy can be used but the composite has a longer curing time (Sandahl & H  llerst  l, 2018).

Prepreg

Prepreg FRP production process is usually used for the high-performance composite structures, for example, in the aerospace applications. It is an autoclave process. The face sheets or layups of partially cured resin with fibres are placed in autoclave to cure.

With the prepreg process it is possible to place additional fillers, details or elements into the layup before curing. In that case, the integrated parts will be strongly bonded into the laminate. If the additional element was partially cured, then it is called co-curing. If the element has been fully cured or incurable elements must be used – the process is called co-bonding.

Prepreg offers a wide range of layup solutions with infinite number, sequence and fibre directions of FRP plies which can be placed in autoclave. Any geometry of the structural members can be produced. The main disadvantages of this process are its relatively long production time and high cost, since the process of preparing the laminate before being placed in an autoclave is performed manually.

3.8 Connections

The design of structural joints is an important aspect related to the sustainability and durability of the structure over its intended service life. Whereas FRP is not a conventional building material, there exists a limited knowledge that can be used as a guideline for designing joints of FRP elements.

Three different categories of FRP structural joints can be considered: mechanical, bonded and combined joints. Each of these categories has its specific safety requirements that should be fulfilled in safe and efficient design. Different types and configurations of the connections for structural members can be found in the following sections.

3.8.1 Structural joints for FRP elements

As stated by the Eurocomp specification, structural joints of the designed ecoduct were classified into:

Primary structural connections

It is expected that this type of connection will provide strength and stiffness of the assembly of structural members over the entire service life of the ecoduct. It requires a highest strength and durability of the joint since the failure of this type of joint can have a significant impact on the structural performance and its further exploitation capability.

Secondary structural connections

This connections type provides the strength and stiffness to the assembly, however, its failure will not cause significant damage and will not affect the overall structural behavior. Such a local failure of an ecoduct sections can be repaired or strengthened.

Non-structural connections

Decorative panels can serve as a good example of this type of connection; the failure of the joint of non-bearing elements will not cause any damage and is not expected to be dangerous to human life. Non-structural connections were not considered in this thesis.

Three categories of structural connections must be considered when designing joints of FRP elements of the ecoduct:

- Mechanical joints;
- Bonded joints;
- Combined joints.

In order to choose the most appropriate solution for the joint design, the following table can be reviewed comparing the various categories of structural joints based on Eurocomp recommendations (Table 9).

Table 9. Characteristics of joint categories.

	Mechanical	Adhesive	Combined
Stress concentration at joint	high	medium	medium
Strength to weight ratio	low	medium	medium
Water tightness	no	yes	yes
Thermal insulation	no	yes	no
Aesthetic (smooth surface)	bad	good	bad
Sensitive to peel loading	no	yes	no
Disassembly	yes	no	no
Inspection	easy	difficult	difficult
Time to develop full strength	immediate	long	long

Mechanical connections

Consequently from Table 9, low requirements for the surface preparation, the possibility for disassembly and easy inspections are the evident advantages of the mechanical joints, nevertheless, high stress concentrations and the need to use special gaskets and sealants to protect against environmental influences, such as fluid and weather, can become the main drawbacks of this type of connection.

It should be noted that the bolts for mechanical connection can be produced of metal or FRP, however, PNG Design guideline do not permit the use of FRP bolts to join FRP elements (Carattere, 2017).

Bonded connection

In conclusion to Table 9 it can be highlighted that the bonded connection proposes a high joint strength and minimization of the possible corrosion problems owing to the fact that the joint surface is not directly exposed to the environment. These are the main advantages of this type of connection. But in spite of that, bonded connection cannot be disassembled, requiring a special attention to the inspections, which is difficult to proceed, and the strength of the joint can be affected by the influence of environmental degradation factors such as temperature and humidity.

Combined connections

This type of connection combines the advantages of the mechanical joining type, providing support and pressure while assembling the members by bolts, and the bonded connection, reducing the bondline defects by bolts, although bolts carry no load after the assembly and acts

only as backup elements. However, this type of combined connections is not permitted by PNG Design guideline to be used in design of the joints of the FRP composite elements (Carattere, 2017) and was not considered in this thesis.

3.8.2 Failure modes of structural joints of FRP elements

To better understand the behavior of different joint types under loading conditions, possible failure modes of FRP members will be further described.

Mechanical connection

On the authority of Eurocomp statements, four failure modes should be considered in the design of mechanical bolted joints for FRP elements: net-section failure, bearing failure, shear-out failure and bolt shear failure (The European structural polymeric composites group, 1996). These failure modes are illustrated in Figure 13.

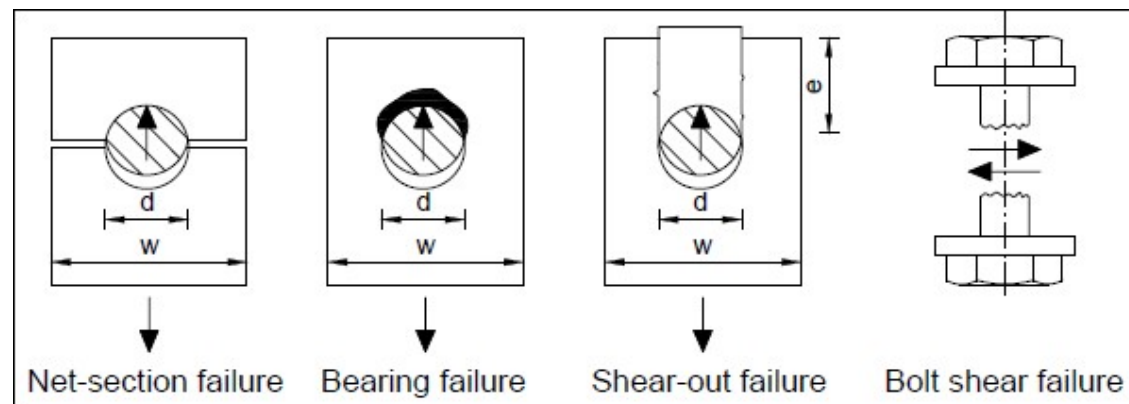


Figure 13. Basic failure modes in bolted laminate connection.

The main characteristics of the failure modes of the joints were studied in this section, taking into account factors affecting the bearing capacity of the joints in order to maximize the safety of the structure and improve the design efficiency.

Net-section failure

This type of failure forms transversally to the direction of loading between the bolt holes and the edges of the element. Tensile or compressive stresses at the edge of the hole from uniaxial loading are the main causes of this failure mode. The diameter of the holes and the width of the plate are decisive parameters affecting the strength of the joint, and with a large ratio of the diameter of the hole to the width of the plate, a net-section failure mode may take place.

Bearing failure

Occurs due to compressive stresses in the contact area of the bolts and the composite material. Most likely it can happen when the ration of the diameter of the hole to the width of the plate is low. In order to avoid compressive crushing failure, the fasteners should not be over-tightened, and their strength should be lower than the strength of the laminate.

Shear-out failure

Is caused by shear stresses and can occur when the strength of fasteners is substantially higher than that of the plate. This is the failure of the laminate with a short end distance, but it's also typical for the pultruded highly orthotropic laminate profiles with no dependence on the end distance.

Bolt shear failure

The main reason for this failure mode is a high shear stress in the fasteners. Bolt shear failure can occur when the strength of the fastener is much lower than the strength of the plate.

Next section will outline the general recommendations for the design of mechanical connections based on Eurocomp and PNG Design statements.

Bonded connection.

Five possible loading modes of the bonded connection are illustrated in Figure 14.

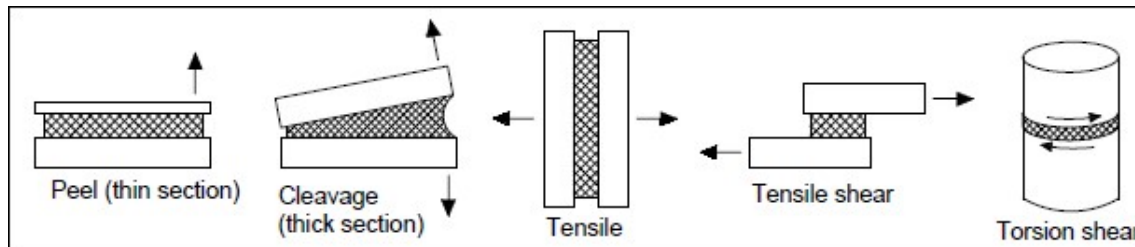


Figure 14. Loading modes of the bonded connection.

However, tensile and tensile-shear loading modes can be regarded as governing loading modes considered in the joints design of FRP elements.

It should be noted that adhesive joint configuration can experience three modes of failure: adhesive failure, cohesive failure of adhesive and cohesive failure of adherend.

Adhesive failure

This failure mode is characterized by the rupture of the adhesive bond between structural components. To avoid adhesive failure, the appropriate adhesive materials should be used, and a high-quality surface treatment should be performed.

Cohesive failure of adhesive occurs when loads reaches the adhesive strength. Cohesive failure of the adherend occurs when the out-of-plane loads or the interlaminar shear loads reaches the strength of the adherend and usually starts from the matrix between the lamina.

It should be noted that the length of the lap, the thickness of the adhesive and an orientation of the fibre in the laminate are governing factors influencing the predominant failure mode of the adhesive joint.

Adhesive connections are generally stiffer than mechanical connections. There is however a lack of knowledge over the long-term behavior of adhesive connections (Friberg & Olsson, 2014).

3.8.3 Choice of configurations of structural joints

Paying attention to the main loading direction acting on a bridge, the following typical joint configurations can be observed for the design task of this thesis, which are presented in Figure 15.

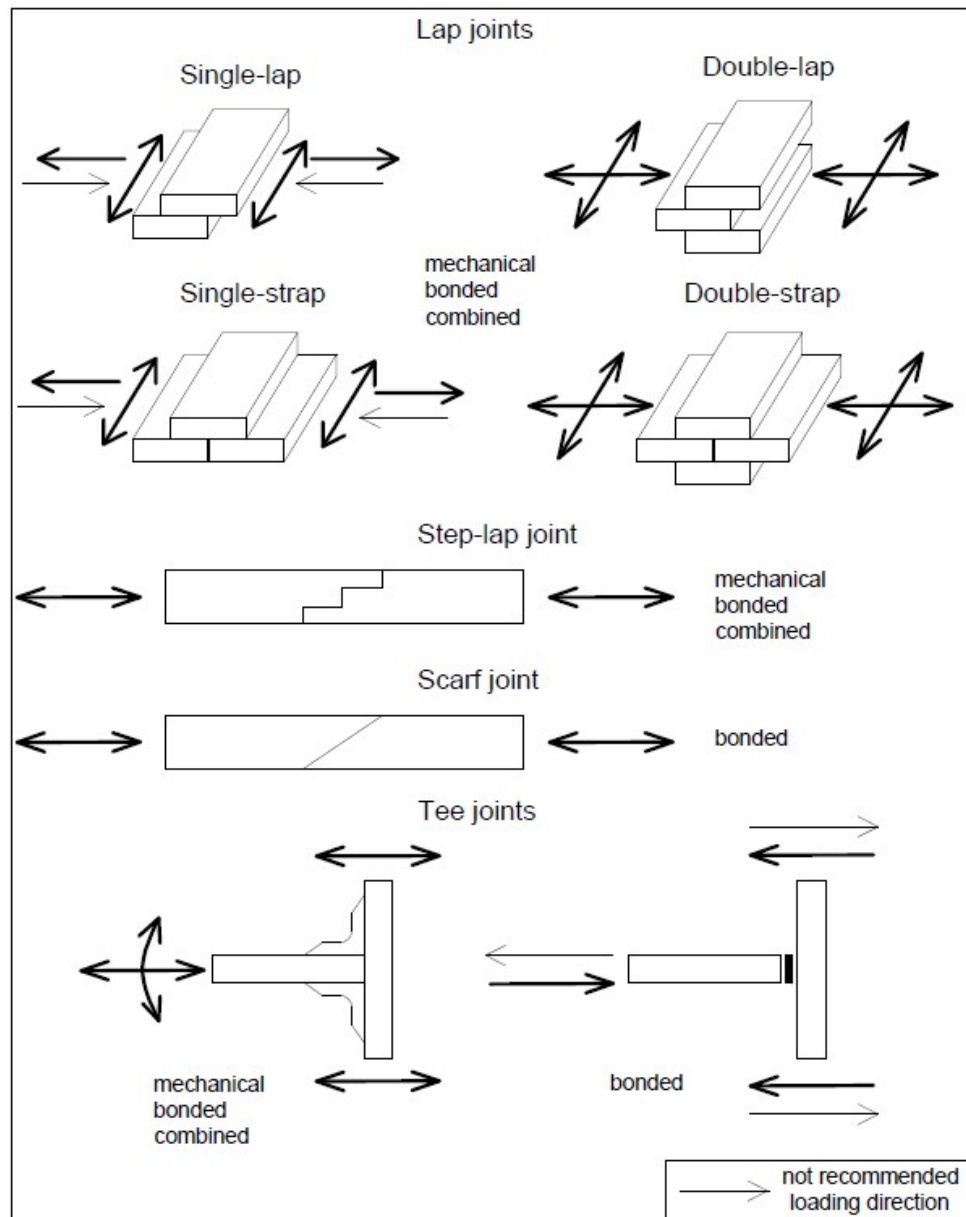


Figure 15. Typical joint configurations (The European structural polymeric composites group, 1996).

Other joint configurations, such as angle joints, butt joints, molded joints, cast-in joints were considered as not appropriate for joining of the load-bearing FRP bridge elements because of the unfavorable loading directions and inapplicability in the particular design case and were disregarded in this thesis.

Pursuant to Eurocomp guideline, single and double lap joint configurations are inefficient if the composite laminate has a thickness greater than 5 mm. The step-lap joint configuration was recognized the most appropriate for the design purposes.

3.9 Guidelines and codes

While developing the ecoduct design the following European codes, guidelines and recommendations were used:

1. Barrier effects and estimated places of the highest need on ecoducts in Swedish conditions were identified by Swedish transport administration.
2. Geometry requirements on ecoducts were provided by:
 - Swedish transport administration (Calluna AB, 2012);
 - The regulations for road design (Vägars och gators utformning, 2015);
 - The old Swedish transport administration (Vägverket & Banverket, 2005);
 - Trafikverket.
3. Loads and combination of actions on an ecoduct were identified according to:
 - EN 1991 Actions on bridges;
 - EN 1990 Basis of structural design, combinations of actions;
 - EN 1992-1995 Design of structures.
4. The FRP composite material properties were identified according to:
 - Eurocomp Design Code and Handbook (The European structural polymeric composites group, 1996);
 - Prospects for New Guidance in the Design of FRP structures (Carattere, 2017).

4 Case study

This section outlines the main geometrical parameters and loading conditions of the ecodeuct based on Eurocode recommendations, as well as the material properties of the composite elements of the bridge in relation to short-term and long-term loading and the environmental degradation effects based on Eurocomp and PNG Design guidelines.

4.1 Bridge geometry and loading conditions

Span

Based on the previous study, the simply supported bridge with the span of 20 m will be designed. Such a design can then be used for both highway and motorways as presented in Table 3.

Width

Minimum width, accessible for animals: 30 m

Minimum width, structural: $W = 30 + 2 \times 5 = 40$ [m]

Fences & Screens

Fastening possibilities for fences are provided at the edge as well as 1,5 m from the edge.

Variable load

Load for pedestrian bridges in equation 2 according to Eurocode 1, part 2:

$$q_{fk} = 2 + \frac{120}{L+30} \text{ kN/m}^2 \quad \text{With } L = 40 \text{ m} \quad q_{fk} = 3.71 \text{ kN/m}^2 \quad (2)$$

Vehicle loads

Service vehicle defined in Eurocode 1 part 2 section 5.6.3. Figure 16 presents how the loads from the service vehicle are applied. Figure 17 presents how the load from the vehicle is distributed to the bridge.

$Q_1 = 80$ [kN], where Q_1 is the load from service vehicle, axis 1 in SLS

$Q_2 = 40$ [kN], where Q_2 is the load from service vehicle, axis 2 in SLS

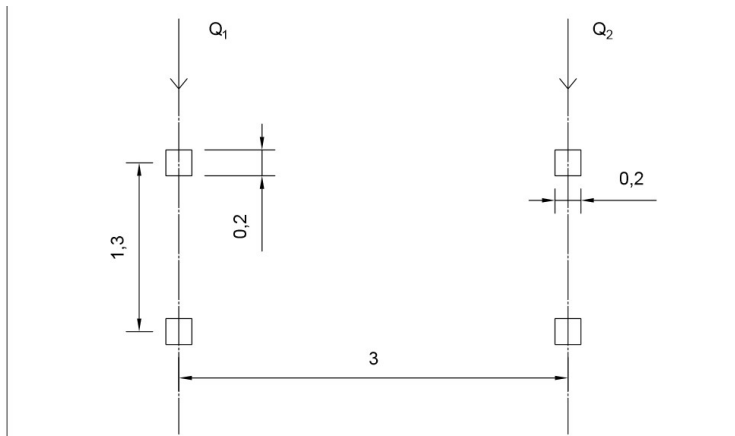


Figure 16. Service vehicle.

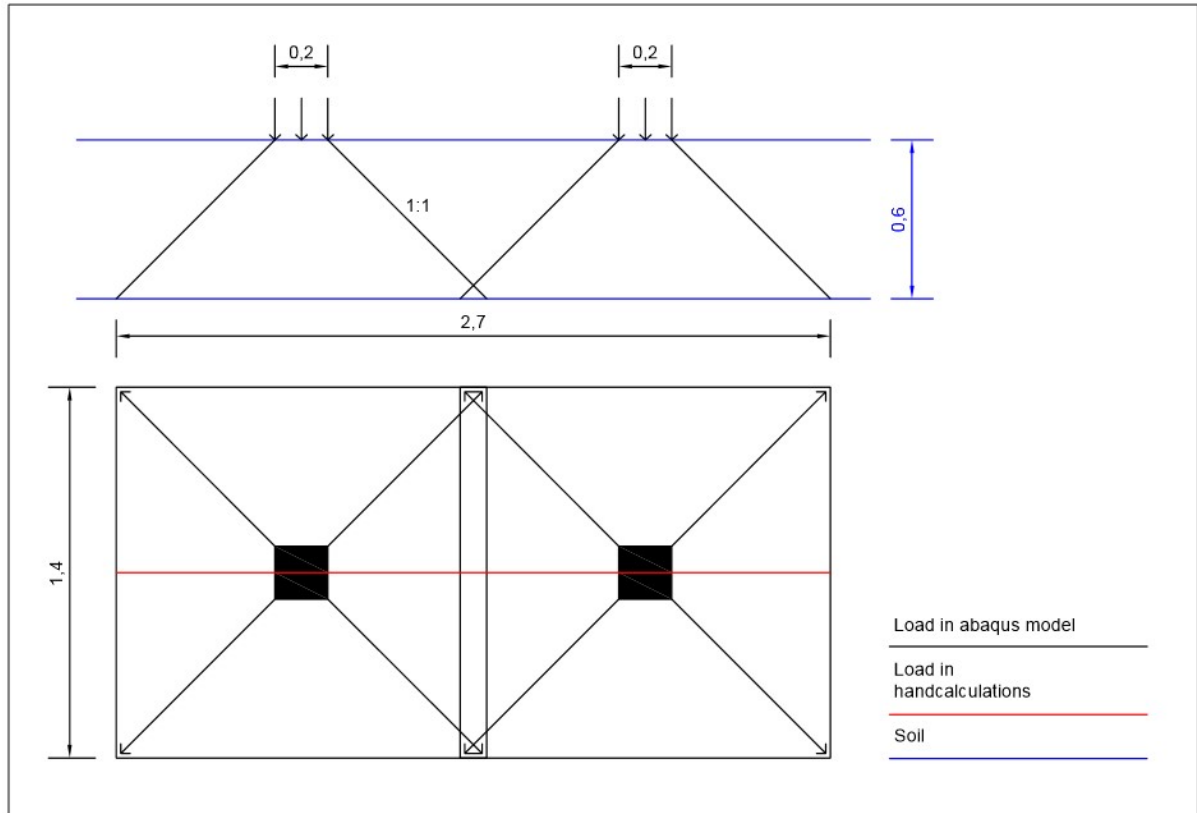


Figure 17. Distribution of load from vehicle.

Snow load

Variable fixed action EN1190:2002 4.1.1 (1) and (4) Eurocode doesn't specify snow load for bridges (EN 1991-1-3 section 1.1 (8)). The snow load will be taken as the characteristic snow load on the ground as defined for the calculation for buildings.

To get a snow load that is relevant for Swedish conditions, three different maps were evaluated. The snow zone map and an elevation map were combined with a map of barriers. The results can be paraphrased as:

- Most parts of Sweden are in Zone 2.
- There are large areas along the eastern coast in zone 3.
- There are some small parts in zone 1 and 3.5.
- The largest parts of Southern Sweden is under 300 m above sea-level.
- The largest parts of Northern Sweden with major roads are under 600 m above sea-level.
- Most of the barriers are in southern Sweden.
- In the north there are barriers along the eastern coast.

In Table 10 some different characteristics with respect to snow zone and elevation above sea-level as well as their relevant importance are presented. According to that a characteristic snow load of $s_k = 2,5 \text{ [kN/m}^2\text{]}$ was chosen.

Table 10. Characteristic snow load for some combinations of snow zone and elevation above sea-level.

S_k [kN/m ²]		Elevation above sea-level [m]			
Zone		0	300	600	900
	1	0,828	1,720	2,613	3,506
	2	1,618	2,510	3,403	4,296
	3	2,408	3,300	4,193	5,086
	3,5	2,803	3,695	4,588	4,581
Color code:		Large areas with substantial barriers.	Substantial areas with barriers.	Small areas with some barriers.	Very small area with some barriers or areas with very few barriers.

The different combinations are marked according to relative area in Sweden. The categorizing is done with the help of three maps showing snow zone, elevation above sea-level and potential barriers respectively (Andreas Seiler et al., 2015; SS-EN 1991-1-3, 2003; “Sverige elevation map,” 2019).

Soil load

The soil load is one of the major loads on the bridge. A suggested soil section is presented in Figure 18. The main part of the bridge will be covered in 0,6 m of soil. 0,6 m is recommended as enough for small bushes and grass, see Section 2.2. At the edges earth mounts of 1,5 m height will be put, which will provide both screens and enough soil to grow larger vegetation. The top of the earth mounts will be 2 m wide. Firstly, this height provides screening sufficient for all animals except moose. The high mounts will screen of noise more effectively than thin screens or trees. The width of mounts will ensure the possibility of planting trees. The inner slope is a natural slope, the outer slope should be reinforced by geotextiles according to Björkman (2019).

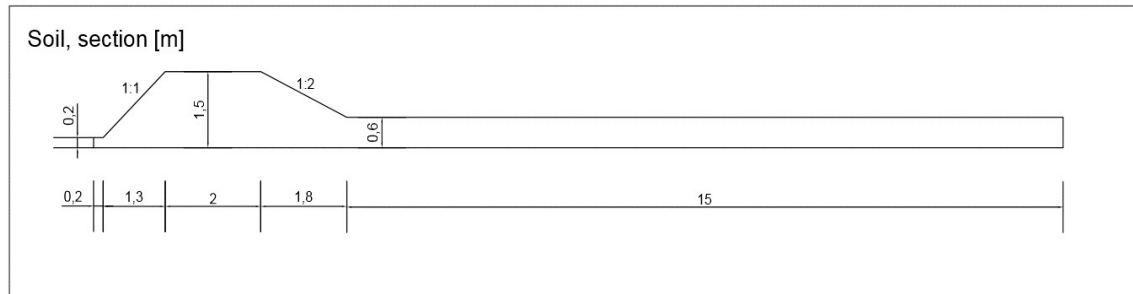


Figure 18. Half-section of proposed soil thickness on ecoduct.

The load is calculated according to equation 3:

Density of soil: $\rho_{\text{soil}} = 20$ [kN/m³] (Trafikverket, 2011)

Soil load, middle: $q_{\text{soil}} = h_{\text{middle}} \times \rho_{\text{soil}} = 0.6 \times 20 = 12$ [kN/m²] (3)

Soil load, edge: $q_{\text{edgesoil}} = h_{\text{edge}} \times \rho_{\text{soil}} = 1.5 \times 20 = 30 \text{ [kN/m}^2\text{]}$

Where:

ρ_{soil} - Density of soil

q_{soil} - Load from soil in the middle section of the ecoduct

q_{edgesoil} - Load from soil in the edge section of the ecoduct

h_{middle} - Hight of soil in middle section of the ecoduct

h_{edge} - Hight of soil in edge section of the ecoduct

The soil is taken with “natural moist” water content, to avoid a total saturation of the soil a draining layer should be provided in the bottom of the soil layer.

The load q_{edgesoil} was used for the total extent of the mount. This gives a load on the safe side and makes it possible to place smaller boulders on the slopes.

Self-weight

The self-weight of the FRP ecoduct is taken as $g = 2 \text{ [kN/m}^2\text{]}$ for check of the load combinations. For the preliminary dimensioning the load was increased. Either to $5 \text{ [kN m}^2\text{]}$ or individually.

Wind load

The ecoduct is higher than most of the bridges, there will also be more hindrs for the wind, thus increasing the wind load. Because of its high width/length ratio and large number of supports the bridge will have a large resistance against horizontal forces. The bridge deck will not take up horizontal forces as a beam but rather as a plate. Therefore, the action from the wind was ignored for the purposes of this thesis.

Total load on a bridge

In Figure 19 all loads on the bridge are presented. The height of each load gives the approximate size.

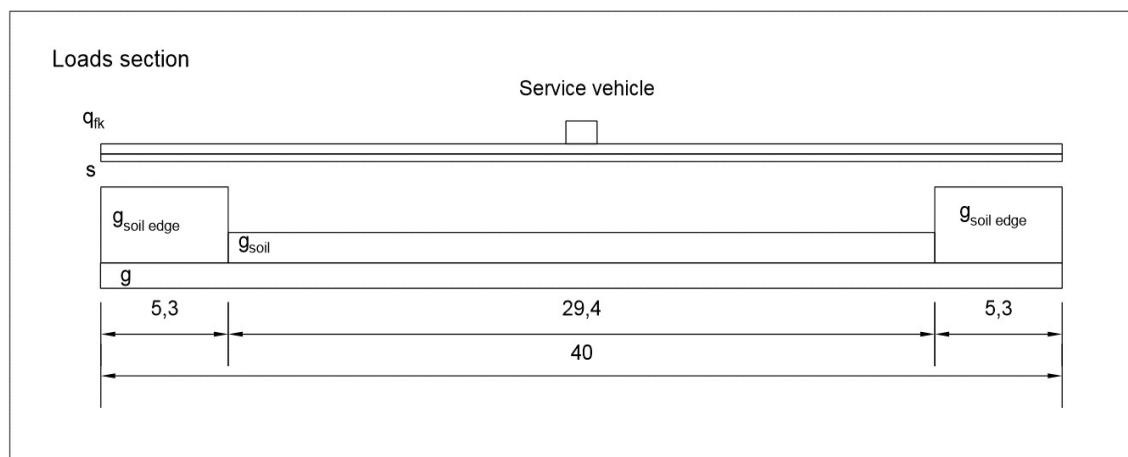


Figure 19. Loads on section of bridge. Height of the loads in the figure gives an approximate impression of the relative value of the loads compared to each other. The position of the service vehicle can be at any place between the edge section.

4.1.1 Load combinations

The two standardized methods used in this thesis to choose relevant load combinations are:

1. Eurocode SS-EN 1990;
2. The European structural polymeric composites group - Eurocomp Design Code and Handbook, 205AD.

The difference between them is however minor. The loads considered as permanent were: self-weight and soil load. The variable loads considered were: live load (see Section 4.1 pedestrian loading), snow load and load from service vehicle.

Representative values of the variable action were determined by multiplying the characteristic values by the combination factors according to EN1990:2002 Table A 2.2. Combination factors can be found in Table 11.

Table 11. Combination factors for variable loads.

	Live	Snow	Vehicle
ψ_0	0,4	0,8	0
ψ_1	0,4	0,6	0
ψ_2	0	0,2	0

Partial safety factor were chosen according to EN 1990 for Actions and can be seen in Table 12.

Table 12. Partial safety factors.

	ULS	SLS
$\gamma_{G,j}$	1,35	1
$\gamma_{Q,j}$	1,5	1
$\gamma_{Qf,j}$	1,35	1

Calculation were performed for different load cases, which included: quasi-permanent, frequent, serviceability and ultimate limit states. The load combinations for Eurocode and Eurocomp differ only in ULS load combination. Eurocomp recommends that some of the reductions in Eurocode be omitted.

Characteristic combination

$$\sum g_{k,j} + q_{k,1} + \sum \psi_{0,i} q_{k,i} \quad (i > 1) \quad (4)$$

Frequent combination (Fr.)

$$\sum g_{k,j} + \psi_{1,1} q_{k,1} + \sum \psi_{2,i} q_{k,i} \quad (i > 1) \quad (5)$$

Quasi-permanent combination (Q.P.)

$$\sum g_{k,j} + \sum \psi_{2,i} q_{k,i} \quad (i \geq 1) \quad (6)$$

Load combination for ultimate limit state (ULS), from Eurocomp.

$$\sum \gamma_{G,j} g + \gamma_{Q,q} q_{k,1} + \sum \gamma_{G,i} \psi_{0,i} q_{k,i} \quad (i > 1) \quad (7)$$

Load combination for ultimate limit state (ULS), from Eurocode

$$\sum \gamma_{G,j} g + \sum \gamma_{G,i} \psi_{0,i} q_{k,i} \quad (i \geq 1) \quad (8)$$

$$\sum \xi_{G,j} \gamma_{G,j} g_{k,j} + \gamma_{Q,q} q_{k,1} + \sum \gamma_{G,i} \psi_{0,i} q_{k,i} \quad (i > 1) \quad (9)$$

For the ultimate limit state the load combination from Eurocomp was used since it gives a higher loading situation. These formulas were accounted for persistent and transient design situations.

The maximum values of shear force and bending moment for unfavorable load situations on the bridge can be found in Table 13. The calculations performed can be found in Appendix E.

Table 13. Maximum shear and bending moment values.

		Q.P.	Fr.	Characteristic	ULS
Mid section	$V_{ed} [kN/m^2]$	155	169,9	256,9	349,8
	$M_{ed} [MNm]$	0,775	0,849	1,465	1,803
Edge section	$V_{ed} [kN/m^2]$	577,6	592,4	629,7	823,1
	$M_{ed} [MN m]$	2,888	2,962	3,149	4,116

The load on the ecoduct is shown in Table 14.

Table 14. Load on an ecoduct in different states.

	Q.P. [kN/m^2]	Characteristic		ULS	
		Distributed [kN/m^2]	Q1/Q2 [kN]	Distributed [kN/m^2]	Q1/Q2 [kN]
Middle section	15,5	18,49	80/40	25,26	108/54
Edge section	33,5	38,71	-	49,56	-

4.1.2 Design requirements

Deflection

Eurocomp states deflection limits, which can be seen in Figure 20 (The European structural polymeric composites group, 1996):

$$\delta_2 = \frac{L}{250} \quad \text{and} \quad \delta_{max} = \frac{L}{300}$$

δ_1 – the instantaneous deflection of the deck section under the permanent loads.

δ_2 – the variation of the deflection of the beam, due to the variable loading plus any time dependent deformations due to permanent loading;

δ_{max} – the sagging in the final state relative to the straight line joining the (supports).

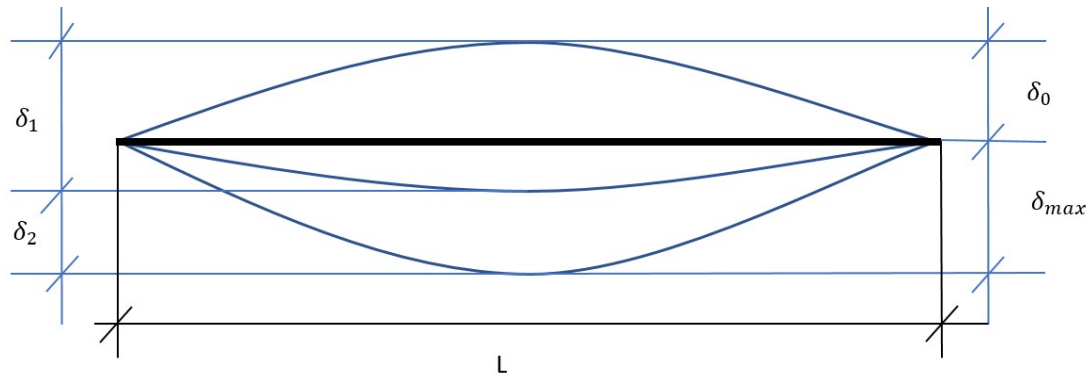


Figure 20. Deflections according to Eurocomp.

Which with: $L = 20$ [m] gives:

$$\delta_2 = 80,0 \text{ [mm]} \quad \text{and} \quad \delta_{max} = 66,7 \text{ [mm]}$$

Stresses

Both Eurocomp and PNG design guideline proposes the calculation for the ultimate cross-sectional resistance in bending and shear. The recommended equations for the design strength and required area A and section modulus W are given in Table 15.

Table 15. Cross-sectional constants calculation from Eurocomp and PNG Design.

	Eurocomp (Sections 4.3, 4.5)	PNG Design (Sections 6.2.2, 6.2.3)
Design strength (in tension)	$f_{dt} = \frac{f_{kt}}{\gamma_{M,Eurocomp}}$	$f_{dt} = \eta_c \times \frac{f_{kt}}{\gamma_{M,PNGdesign}}$
Shear area	$A_{web} = \frac{V_{uls} \times \gamma_{M,Eurocomp}}{f_{k\tau}}$	$A_{web} = \frac{V_{uls}}{f_{d\tau}}$
Section modulus	$W = \frac{M_{uls} \times \gamma_{M,Eurocomp}}{f_{k\tau}}$	$W = \frac{M_{uls}}{f_{d\tau}}$

f_{kt} , f_{dt} - characteristic and design tensile strength of the laminate;

$f_{k\tau}$, $f_{d\tau}$ - characteristic and design shear strength of the laminate;

η_c – conversion factor accounting for the long-term influence of temperature, humidity, creep on laminate (see following Section 6.1.1);

V_{uls} - ultimate shear force acting on a bridge;

M_{uls} - ultimate bending moment on a bridge at ultimate state.

Analyzing the results of calculations using the formulas of the table, it can be concluded that Eurocomp does not take into account the long-term behavior of the FRP composites under the influence of environmental degradation effects and sustained load (η_c). The reason behind that was the lack of practical experience at the time of writing Eurocomp regarding long-term changes in the properties of FRP composites. PNG Design, in its turn, takes these correction factors into consideration.

According to the PNG Design recommendations, the creep rupture of the FRP laminate should be checked in quasi-permanent load state considering the long term behavior of the laminate under the static load.

The design material strength should satisfy the following requirement, where f_{ed} is the design strength of the laminate:

$$f_{ed} < \eta_{ct} \times \eta_{cm} \times \frac{0,3 \times f_{kt}}{\gamma_{M,PNGdesign}} \quad (10)$$

$$f_{ed} < \eta_c \times \frac{0,3 \times f_{kt}}{\gamma_{M,PNGdesign}} \quad (11)$$

Buckling

In order to receive the efficient design, the criteria of the load factor $\lambda > 1$ is used in this thesis. Here λ is the first positive eigenvalue for buckling of the entire bridge section. The load was taken in ULS and the material properties are reduced with γ_M and $\eta_{c.md}$.

$\eta_{c.md}$ – conversion factor taking into account the short-term temperature and humidity effects on a FRP laminate material properties.

Since the ecoduct is expected to undergo bending, the following failure types in the section should be checked: facing failure of the flanges, transverse and horizontal shear failure. The failure modes are depicted in Figure 21.

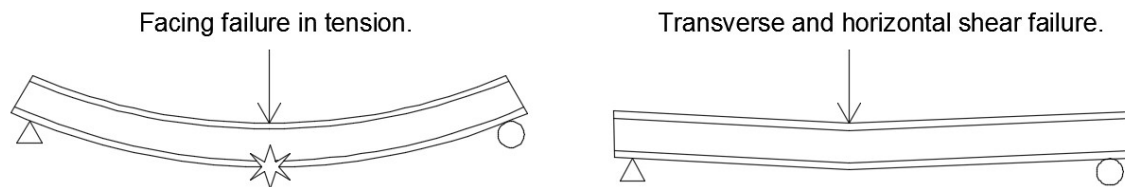


Figure 21. Failure modes of the ecoduct section in bending and shear.

Facing failure

The facing failure of the bottom flange of the ecodeuct section in bending is shown in Figure 21. This type of the section failure should be checked with normal stresses:

$G_{ed} < f_{ed}$ (Section 6.4.1 PNG Design).

Where f_{ed} is the design strength of the laminate.

Transverse and horizontal shear failure

This failure type should be avoided in design and the check of the cross section should be performed with shear stresses:

$$\tau_{ed} < f_{\tau d} \quad (12) \text{ (Section 6.4.2 PNG Design)}$$

Where τ_{ed} is the shear stress and $f_{\tau d}$ the corresponding design shear strength of laminate.

The shear stresses in section should be lower than the design material strength in tension.

The other failure modes of the ecodeuct section, such as flexural crushing of the core, local crushing of the core, shear crimping, facing wrinkling, intracell buckling of the section were not considered in this thesis due to unsuitable load conditions causing these types of failure.

4.1.3 Joint design requirements for FRP ecodeuct members

In order to develop an efficient joint design for the FRP composite ecodeuct elements, the Eurocomp and PNG Design recommendations should be taken into consideration.

The main task of the connection is the distribution of internal forces and moments between the connected elements so that the internal and designed forces and moments remain in static equilibrium (PNG Design; Eurocomp). The deformability of the joint depends on the deformation capacity of the fasteners in mechanical connections and adhesion in adhesive connections, which eventually means that intended design forces and stresses at the joint should be below the design strength of the connectors.

Mechanical connection

According to the PNG Design guideline, the mechanical joints should be used in connections of the primary load bearing FRP ecodeuct elements.

The joint should be design with respect to the conditions in which it is predicted to be loaded: in shear, in tension or in combination of both. The types of loading conditions are depicted in Figure 22.

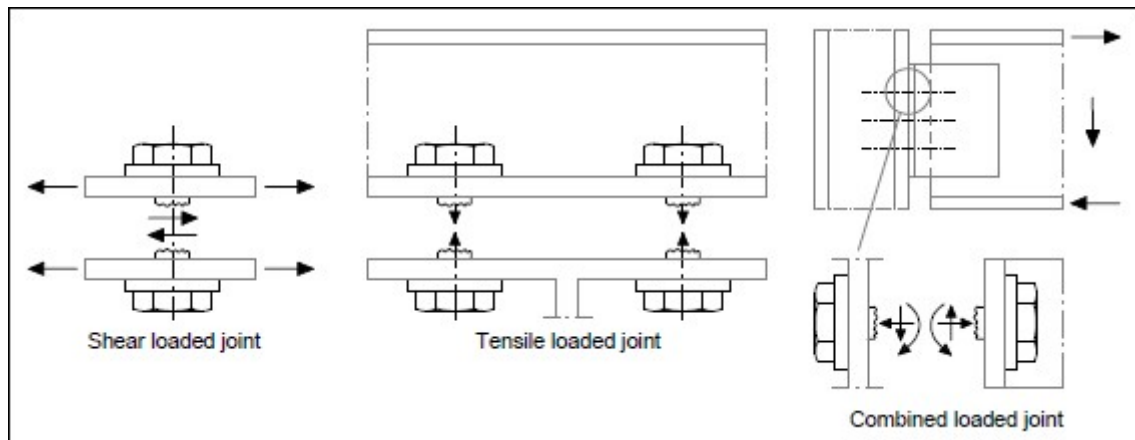


Figure 22. Loading types of bolted connection.

General requirements to the design:

- The local x-axis directions of the connected elements should converge to a single point.
- Bolts made of FRP are not permitted (PNG Design).
- Bolts with constant diameter should be used, otherwise the applicability of variable diameter bolts should be determined by testing. The bolt thickness should be no lesser than the one of the thinner connected element.

Adhesive connection

According to the PNG Design guideline, the adhesive connections should not be used in the primary load-bearing elements (Section 8.4.1 PNG Design). However, Eurocomp has no limitations in this case (Section 5.3.7.4 Eurocomp).

The secondary structural connections of the ecodeut sections can be designed as adhesive connections.

4.2 Discussion: the case study

To design an efficient structural solution, it is necessary to know the requirements that the structure should fulfill. In chapter 0 the context in which a typical ecodeut should be built in Sweden is described. In Section 4.1 a specific case is formulated suiting that context and the requirements. This discussion aims at explaining the choices made in this case.

Span

As it was shown in Section 2.3, the span over the road varies between 28,0 and 40,6 meters for motorway bridges and 16,1 and 29,7 m for highway bridges. That results in a span for motorway bridges between 16 m and 20,3 m. The minimal length of the bridge span in this case is based on the safety regulations for roads. The supports are placed only 1 m beside the safety railing. Since the values give the span length from the actual structural support, the minim length required is only achievable if the supports have some sort of inclination. There is also an argument against using the minimum span length as to how the bridge will be perceived from the road. A narrower ecodeut will be perceived as very near to the road. Since the bridge is also very wide, the experience for the driver will be similar to a tunnel. Therefore, a choice of the span of 20 m was judged to give both the necessary space to build foundations as well as give a more open driving experience.

Width

The ecoduct width of 40 m is the suggestion of this thesis. That is based on the requirements to have the minimum allowed width of 30 m and the possibility to plant trees as screens against noise and light at the edges of an ecoduct. According to the literature study this sort of environment is preferable in design of ecoducts. Since the design solution in this thesis is modular, it is however possible to construct narrower bridges with the same solution. The goal with this ecoduct design solution was to create the best possible basis for a typical ecoduct design.

Loads

There are several loads that must be considered. The largest of these, the soil load, is critical since it is a permanent load and, therefore, will cause a large creep deformation in FRP laminate.

The requirements for the depth of the soil layer vary according to the sort of plants that supposed to be planted. Since trees are desirable only at the edges, there is the greatest need for soil there. This means that it was possible to optimize the material use in the bridge by limiting the amount of soil load in the middle and only dealing with larger soil load at the edges.

Ecoducts are treated as pedestrian bridges in Eurocode, that means that a variable load as well as a service vehicle must be taken into account. Since the traffic on the bridge is expected to be minimal, the smallest possible variable load was chosen. The load of the usual service vehicle according to Eurocode was taken in the design. The reason for this is that the bridge should be able to allow the maintenance vehicles to drive on the bridge. The service vehicle was limited to the middle part of the bridge, thus it was not considered together with the larger soil load on the edges.

The snow load was chosen so that most of the areas where ecoducts may be of interest were considered and a reference value was chosen. This means that most areas in Sweden are included in this load case but that there might be some places, especially in the north, where there it is necessary to take larger snow loads into account.

Design requirements

The requirements on the deflections and allowable stresses in the ecoduct sections were described in Section 4.1.2. The possible failure modes of the bridge sections were studied, and the requirements were considered in order to ensure the safety limits in the design.

Material properties

The ecoduct design includes preliminary designs and the final design decision. Material properties for the preliminary designs were taken from the Chalmers master thesis work (Sandahl & Hållerstål, 2018). Material properties for the final design were calculated with a Classical laminate theory in accordance with Eurocomp and PNG Design recommendations.

The possible combinations of different types of the fibre and polymer matrixes were studied and the most suitable FRP composite material decision was made for the design of an ecoduct. The chosen materials (fibres and resins) and their parameters (fibre volume, fraction, orientation in the laminate, number of layers of different directions) are described in detail in Section 6.1.

5 Preliminary design

The preliminary design is presented in this chapter. 19 concepts are developed and evaluated on the basis of material use and production possibilities. As a result, 3 designs in 2 different materials are chosen. More details such as joining technique and production methods were investigated. Finally, a new evaluation was done, choosing a final design.

Since there does not exist a Eurocode for FRP at this date, the Eurocomp design code and PNG Design guidelines were used for the design. The Eurocomp design code is compatible with Eurocode. Material properties were calculated according to “Prospect for New Guidance in the Design of FRP Structures (Carattere, 2017)” (PNG design guidelines). The reason behind this is that the method described there is more developed and specific than that proposed by Eurocomp. The deflection limits were used as the only criterion during the preliminary stage of design.

5.1 FRP composite material properties used for the preliminary design

The material properties of the FRP composite for preliminary conceptual design solutions were taken as reference values from the Chalmers Master's work “Design of an FRP Eco-bridge” (Sandahl & Hållerstål, 2018).

When verifying the deformability of composite material, the average (arithmetic mean) value of Young's modulus for all the number and directions of plies should be taken into consideration. Calculation of material properties for GFRP and CFRP was performed at the Master thesis study from Chalmers (Sandahl & Hållerstål, 2018). Based on this work, the following values of material properties of the composites presented in Table 16 were selected for the preliminary design.

Table 16. Material parameters used in preliminary design.

	Glass fibre	Carbon fibre
$E_{instant} [MPa]$	35,6	113,2
$E_{creep} [MPa]$	16,7	53,2
$G_{instant} [MPa]$	3,6	4,0
$G_{creep} [MPa]$	1,7	1,9

5.1.1 Preliminary design proposals

Based on the requirements stated by Eurocode and Eurocomp for the design of the bridge, 13 preliminary design solutions were developed and compared in the evaluation matrices. Together with different material choices, this gave a total of 19 proposals.

The preliminary designs of the ecoduct proposed two types of structural system:

- bridge deck structural system;
- beam-deck structural system.

The concepts can be seen in Table 17. Material need for the different conceptual designs., which represents the need of material for the sections of 1 m width for different design solutions. The approximate values of the area and sections height gives an impression of material requirements and design efficiency.

Bridge deck

Firstly, bridge deck constructions were considered. A bridge construction means in this case two flanges and a lightweight web as the main bearing structural elements. The principal is presented in Figure 23.

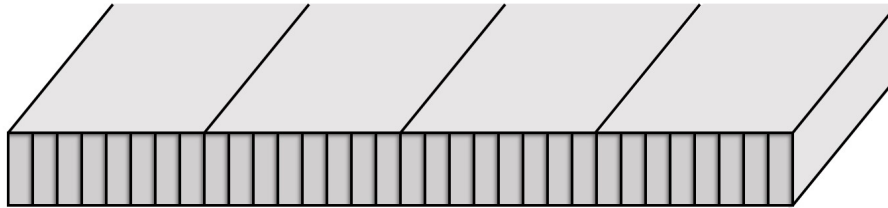


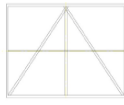


Figure 23. Principal construction of beam-deck structural system.

The main advantages of the bridge deck construction are that most of the assembly can be achieved in the workshop. The width of each singular panel is limited by the possibilities of transportation. The maximum width was assumed to be 3 m, which is slightly less than the maximum allowed width of transport without special equipment (“Villkor - Trafikverket,” 2019).

In Table 17 different bearing deck sections for the ecoducts are presented. The area of the cross-section as well as the height are given. Table 18 includes information on possible production methods for various sections and suggestions on the assembly of structural parts from the individual sections.

Table 17. Material need for the different conceptual designs.

N	Figure	Material used.		Height [m]	
		Area [m ²]		Glass	Carbon
1		11,8	8,1	1,0	0,6
2		11,6	7,9	1,0	0,6
3		5,9	4,3	1,1	0,7


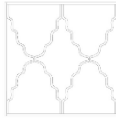
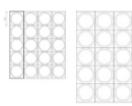
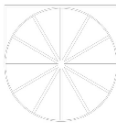
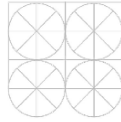


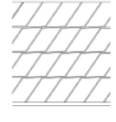
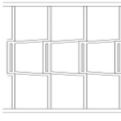

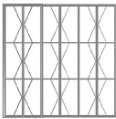
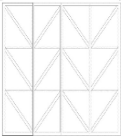
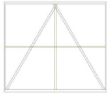
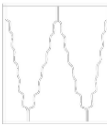
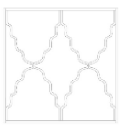
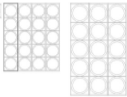
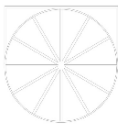
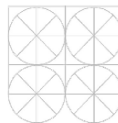
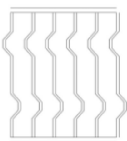
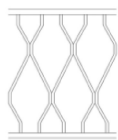
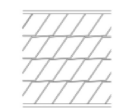
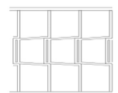
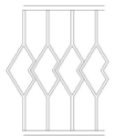
4		7,75	5,43	1,1	0,7
5		7,77	5,38	1,1	0,7
6		11,2	9,44	1,3	0,8
7		15,3	3,63	1,0	1,0
8		14,3	4,17	1,0	1,0
9		9,5	4,88	1,3	0,77
10		12,7	-	1,2	-
11		9,8	-	1,3	-
12		10,1	-	1,3	-
13		8,9	-	1,4	-

Table 18. Production methods for different design solutions.

N	Figure	Production method	Production technique	Assembly
1		Pultrusion /Prepreg	1) Pultrusion of three vertical sections made of 3 box elements. Adhesion of the sections.	Three vertical sections can be bonded with adhesion at the factory and a deck section with 1m width will be achieved. Then it is possible to bond together three sections in order to receive one deck section with a width of 3 m.
2		Pultrusion /Prepreg	2) One box element can be produced with pultrusion, RTM or VIP. Then all three elements will be wrapped around with plies until the thickness of the webs will be reached. Afterwards, adhesion of all three sections.	
3		Prepreg	Whole section should be made simultaneously.	Sections of 1 m width can be bonded together in order to receive one deck section with a width of 3 m.
4		Pultrusion	Pultrusion of sheets and bonding them together in the places of their connections.	
5		Pultrusion		
6		Pultrusion/RTM/VIP/ Prepreg	One box element can be produced with pultrusion, RTM, VIP or Prepreg. Then wrapping around all three elements with plies until the thickness of the webs will be reached.	All vertical sections can be bonded with adhesion at the factory and a deck section with 1m width will be received. Then it is possible to bond together three sections in order to receive one deck section with a width of 3 m.

7		Prepreg	Production of the whole section.	Sections of 1 m width can be bonded together in order to receive one deck section with a width of 3 m.
8		Prepreg	Production of the whole section.	Sections of 1 m width can be bonded together in order to receive one deck section with a width of 3 m.
9		Prepreg/ autoclave/ RIM	Webs and flanges are produced separately. Webs can be produced in an autoclave with foam between 2 webs. The flanges can be produced in a autoclave. The flanges can be produced using RIM.	Webs and flanges are joint adhesively to 3 m wide sections.
10		Prepreg/ autoclave/ RIM	Webs and flanges are produced separately. The webs can be produced in an autoclave. The flanges can be produced using RIM.	
11		Prepreg/ autoclave/ RIM		
12		Prepreg/ autoclave/ RIM		
13		Prepreg/ autoclave/ RIM	Webs and flanges are produced separately. Webs can be produced in an autoclave with foam between 2 webs. The flanges can be produced in a autoclave. The flanges can be produced using RIM.	

As can be seen from Table 18, some elements of concepts can be prefabricated with pultrusion and easily assembled into structural components at the factory or on site, while the production of others, despite their efficient geometries from the point of view of stress distribution and deformability, can become a significant issue since the sections should be produced as a whole sections.

Beam-deck structural system

The beam system consists of smaller parts that are easier to process and assemble on site. The principle is shown in Figure 24.

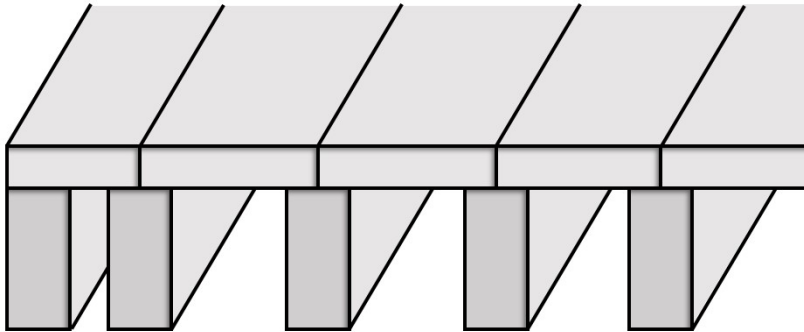








Figure 24. Principal construction of beam solution.

Different configurations of shape and materials were considered. An overview over different possibilities is presented in Table 19.

Table 19. Material need and production method for different beam solutions.

N	Figure	Composite material use, Area [m ²] (Area of beam + area of deck)		Distance between beams [m]	Height [m]	Production method	Assembly
		Glass	Carbon				
14		3,5 + 1,5 = 5,0	-	2 / 1	1,9	RIM/ (pultrusion or autoclave)	The beam is assembled by mechanical connections and adhesion.
		1,5	2,6	2 / 1	1,2		
15		3,6 + 1,1 = 4,7	-	1 / 0,5	1,9	RIM/ (pultrusion or autoclave)	-
		1,5	1,9	2 / 1	1,5		
16		8 + 1,1 = 9,1	-	1 / 0,5	1,35	RIM/ (pultrusion or autoclave)	The beam is assembled by adhesive joints
		1,1	4,5	1 / 0,5	0,9		
17		3,4 + 1,5 = 4,9	-	2 / 1	1,7	RIM/ (pultrusion or autoclave)	The beam is assembled by mechanical connections and adhesion.
		1,5	3,4	2 / 1	1,1		
18		5,5 + 1,1 + 1,1 = 7,7	-	2 / 1	1,5	RIM/ (pultrusion or autoclave)	
		1,1 + 1,1	2,5	2 / 1	1,3		
19		3,9 + 1,1 = 5,0	-	2 / 2,5	1,8/2,6	RIM/ (pultrusion or autoclave)	-

Production technique: beam elements are produced using RIM; decks are produced either by pultrusion or using autoclave. Logistics & Construction: beams are lifted in place separately; decks are placed on beams.

5.1.2 First evaluation

This section presents the evaluation criteria and the results of the first evaluation. The evaluation method is also discussed. The evaluation criteria presented in Table 20 are used for both assessments. Only the criterion marked in blue are used for the first evaluation. The reason for this was that the design at this stage was less advanced.

Table 20. Evaluation criteria. For the first evaluation only the criteria's marked with blue were used.

Criteria	Features
Production complexity	Ranging from difficult to manufacture to established and effective production technique with minimal manual labor.
Transport	Evaluation of the features of structural elements regarding their transportation complexity from the factory to the construction site.
Risk of damage	During transportation, joining of parts and erection of the bridge elements.
Difficulty of assembling	Complexity of assembling the bridge. Large elements or elements that are difficult to fit in are assessed as worse.
Maintenance	Assessing the possibility and complexity of performing safety checks and maintaining structural elements.
Traffic disturbance	Possible traffic disturbance during bridge erection. A more complex assembling process with larger elements requires a longer period where the traffic is disturbed.
Design cost	Ranging the design complexity depending on the structural system used in the design and simple/complicated geometry of structural elements.
Material use	The amount of the composite material required in the design by cost. (Carbon fibres 10 times more expensive compared with glass fibres).
Risk of moisture ingress	Depending on the amount and configurations of structural joints.
Dependency on connections	Adhesive joints are assessed as more dangerous than bolted connections.
CO ₂ footprint	Depending on the amount of material needed for production of each concept.
Risk of abrasion	Depends on how many parts
Possibilities of recycling	Depends on the recycling possibilities of the material.

The criteria were weighted against each other as shown in Table 21. The weighting is done in these steps:

Each criteria is compared to each in turn. Example: Criteria 1 to criteria 2. Here criteria 1 is taken as more important than criteria 2. Therefore Criteria 1 gets 3 points and criteria 2 gets 1 point.

All points for each criteria are summed up.

The total points for all criteria given is summed up.

The percentage of points from the total points given is calculated for each criteria.

Table 21. Weighting of evaluation criteria for first evaluation.

Criteria	Complexity	Transport	Risk of damage	Difficulty of assembling	Design cost	Material use (cost)	Sum	
	1	2	3	4	5	6		
1		3	3	2	3	1	12	15%
2	4		2	1	3	1	12	15%
3	4	2		1	3	1	12	15%
4	4	3	3		3	1	16	20%
5	4	1	1	1		1	9	11%
6	4	3	3	3	3		19	24%
1 = less important; 2 = equal; 3 = more important							80	100%

The evaluation was done regarding the information given in Section 5.1. The complexity of the geometry, number of joints required, and the material use were the criteria for comparing the designs with each other.

The cost for the material was calculated using a conversion factor of 10 together with the area for respective cross section.

$$\text{Cost glass fibre} = A_{\text{glass}} \quad (13)$$

$$\text{Cost carbon fibre} = 10 \times A_{\text{carbon}}$$

Three different solutions were chosen for further study. The weighted score for some concepts was not the highest, the choices were also made to achieve a variation of solutions. 3 general concepts were chosen to be further developed (marked in red in Table 22):

- A pultruded sandwich construction.
- A prepreg produced sandwich construction.
- A beam-deck structural system using the entire soil-depth of the ecoduct.

Table 22. Results from first evaluation.

Criteria		Complexity	Transport	Risk of damage	Difficulty of assembling	Design cost	Material use (cost)	Weighted sum
		1	2	3	4	5	6	
Design		15%	15%	15%	20%	11%	24%	100%
1	glass	3	3	3	2	2	2	2,45
	carb	3	3	3	2	3	0	2,09
2	glass	3	3	3	2	3	2	2,56
	carb	3	3	3	2	3	0	2,09
3	glass	3	2	2	2	2	3	2,39
	carb	4	2	2	2	2	1	2,06
4	glass	3	2	2	2	2	3	2,39
	carb	3	2	2	2	2	1	1,91
5	glass	3	2	2	2	2	3	2,39
	carb	3	2	2	2	3	1	2,03
6	glass	2	2	2	2	1	3	2,13
	carb	2	2	2	2	1	0	1,41
7	glass	1	2	2	2	1	2	1,74
	carb	1	2	2	2	1	1	1,50
8	glass	1	2	2	2	1	2	1,74
	carb	1	2	2	2	1	1	1,50
9	glass	3	3	3	3	2	2	2,65
10	glass	1	2	2	2	2	2	1,85
11	glass	1	2	2	2	2	3	2,09
12	glass	1	2	2	2	2	2	1,85
13	glass	1	2	2	2	2	3	2,09
14	glass	2	3	2	3	2	4	2,83
	carb	2	3	2	3	2	2	2,35
15	glass	3	3	1	3	3	4	2,94
	carb	3	3	1	3	3	2	2,46
16	glass	2	3	2	3	2	3	2,59
	carb	2	3	2	3	2	1	2,11
17	glass	2	3	2	3	2	4	2,83
	carb	2	3	2	3	2	1	2,11
18	glass	2	3	2	3	2	4	2,83
	carb	2	3	2	3	2	2	2,35
19	glass	2	2	2	3	2	4	2,68
0	Unsatisfactory							
1	Just tolerable							
2	Adequate							
3	Good							
4	Very good							

5.1.3 Detailed description and evaluation of 3 chosen concepts

Design 1 - Pultruded bridge deck design solution

The design solution is shown in Figure 25. The main advantage of this concept is the possibility to pultrude hollow sections with a width of 250 mm and to bond them together in the factory. The sections of one meter width should be connected to each other with a lap-snap adhesive joints (see Section 3.8.3).

The webs and bracings will provide an effective shear transfer, and longitudinal stiffeners will ensure the absence of the local buckling of the webs.

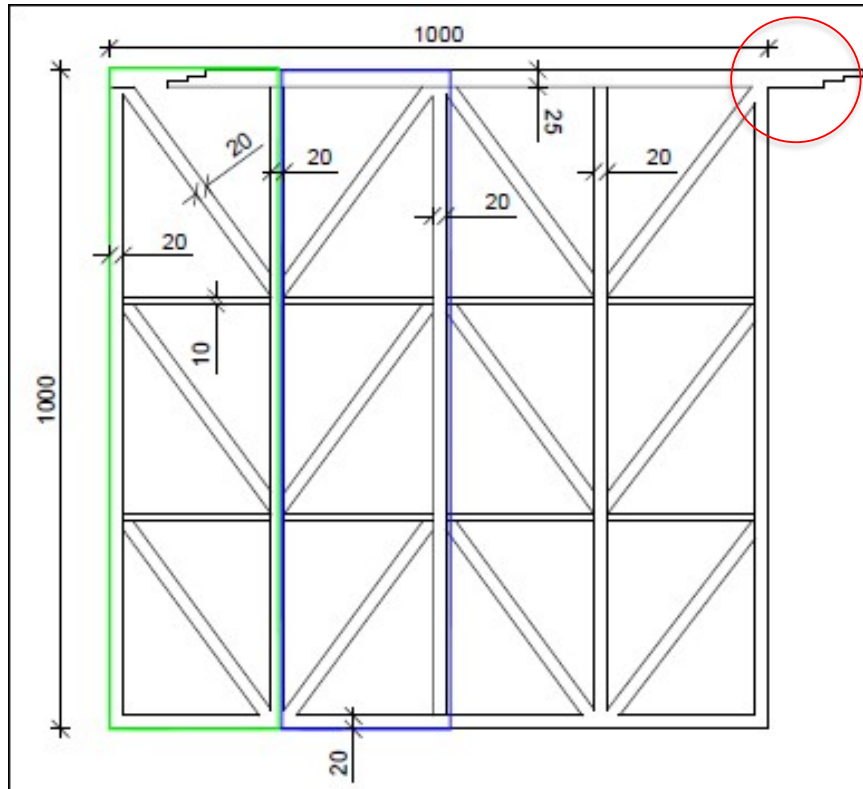


Figure 25. Pultruded bridge section design solution.

Design 9 - Prepreg sandwich solution

Webs with a non-structural foam filling will be produced with prepreg in an autoclave (Figure 26). The flanges will be produced either by the same methods or a RIM/RTM process. The flanges and webs will be joined adhesively in a controlled environment. 3 m wide sections will be produced and then mechanically bonded during the final assembling.

the beam-deck structural system the mechanical type of connections should be used for joining beams together with the bridge deck which should be fixed on top of the beams. Adhesive bonds are used to bond the beams themselves. Several proposed solutions can be seen in the following section.

Connections for bearing-deck sections

There are several solutions proposed for connecting the bearing deck sections. There are two different types of connections. Firstly, 1 m wide members are bonded adhesively. This gives a high-strength connection between the sections and form one section three meters wide. Those connections can be done in a workshop before the assembly of the bridge. Secondly, the 3 m wide sections are connected with mechanical connection type on site.

Adhesive connections

The one-meter wide bridge deck sections should be connected with a lap-strap joint type, as shown in Figure 28. Parts should be prefabricated in such a shape and connected to each other with an adhesive bonding.

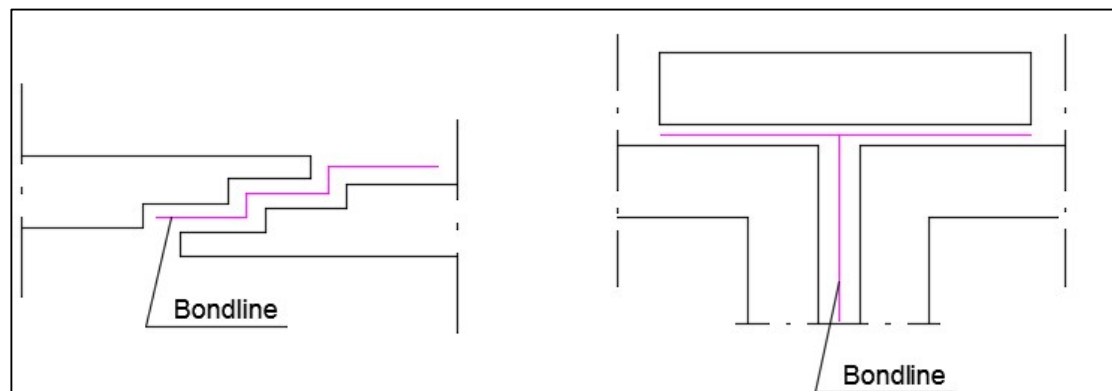


Figure 28. Adhesive connection possibilities for bearing deck structural system.

Bolted connections

There are several solutions for connecting the sandwich sections that can be handled separately in transport. In Figure 29 and 30 three different methods are presented.

The first (right) one is more complicated in geometric terms. That can result in a stress concentration. Blind bolts are necessary to be used since it is not possible to reach the inside part of the cross section. The blue lines present a possibility to transfer the force more effectively and give more dimensional stability.

The second (left) solution is simpler in geometric terms. A disadvantage with this solution is that area of friction is smaller than for the first solution. Of course, the area could be increased but that would mean that the connection flanges are more vulnerable towards damage.

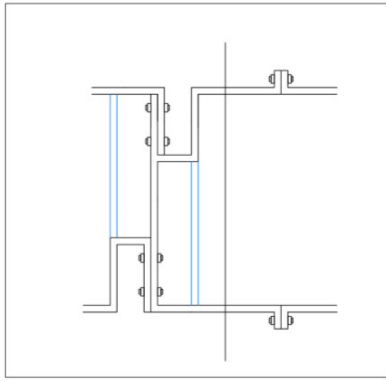


Figure 29. Mechanical connections for bearing deck system.

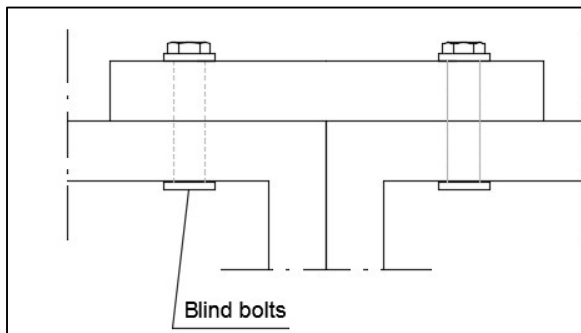


Figure 30. Mechanical connections for bearing deck system.

Connections for beam deck system

The joint should be designed for the beam-deck structural system concept for the beam to deck connections. This connection type can be seen in Figure 31. The angles with a thickness of no lesser than that of the beam web should be used. The angles should be connected to the structural elements with blind bolts because of the closed shapes of the beam sections.

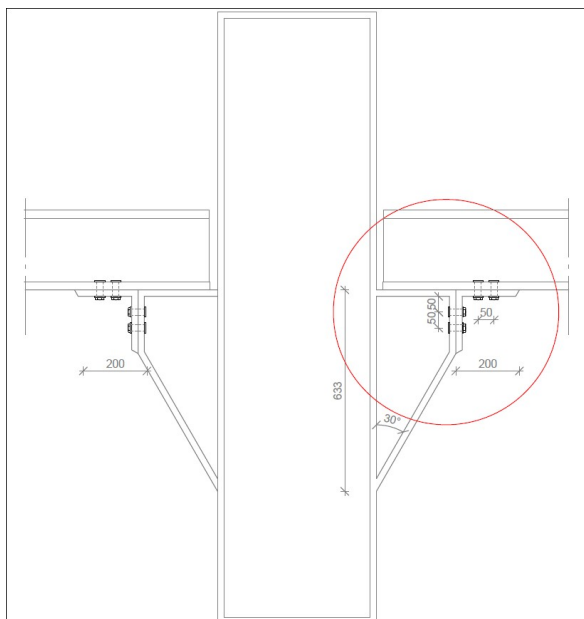


Figure 31. Mechanical connection of the beam to the deck of an ecoduct.

Beam assembly connections

The large beams of design 19 cannot be produced in one piece. In Figure 32 four different connections are presented. Following positive and negative properties have been identified:

Version A

- + high buckling capacity
- + 3 double flanges
- high material use
- small tolerances

Version B

- + large are of adhesion
- + easy to apply pressure for assembling
- box sections produced by pultrusion

Version C

- + few parts
- + easy to apply pressure
- complicated geometry
- small tolerances

Version D

- + smaller parts
- depends very much on adhesive bonding
- small tolerances

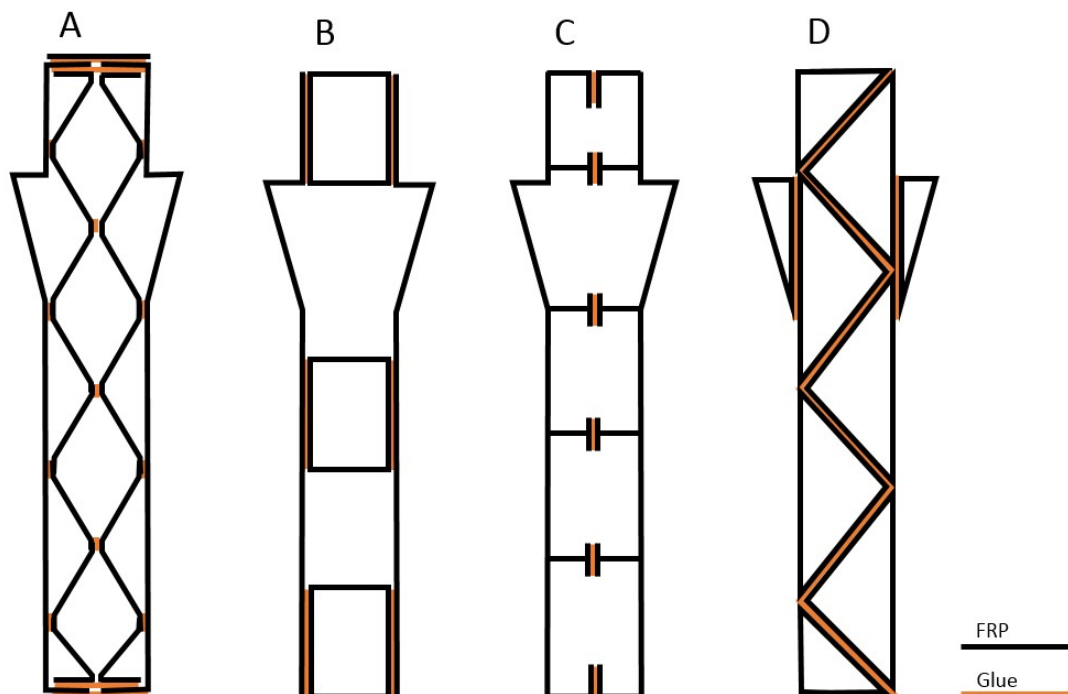


Figure 32. Different possibilities for manufacturing design 19.

5.1.4 Second evaluation

In the second evaluation all criteria presented were taken into account, see Table 23.

Table 23. Evaluation criteria for second evaluation.

Criteria	Manu- facture	Assembling and transport					Economy		Durability		Sustainability			Sum	
	Production complexity	Transport	Risk of damage	Difficulty of assembling	Maintenance	Traffic disturbance	Design cost	Material use (cost)	Risk of moisture ingress	Dependency on connections	CO2 footprint	Risk of abrasion	Possibilities to recycle		
	1	2	3	4	5	6	7	8	9	10	11	12	13		
1		3	3	2	2	3	3	2	3	2	2	3	2	30	11%
2	1		2	1	1	2	3	1	2	1	1	3	1	19	7%
3	1	2		1	1	2	3	1	2	1	2	2	1	19	7%
4	2	3	3		3	3	3	2	3	2	2	3	2	31	11%
5	2	3	3	1		3	3	1	3	2	2	3	2	28	10%
6	1	2	2	1	1		3	1	2	1	1	3	1	19	7%
7	1	1	1	1	1	1		1	1	1	1	1	1	12	4%
8	2	3	3	2	3	3	3		3	2	2	3	1	30	11%
9	1	2	2	1	1	2	3	1		1	2	2	2	20	7%
10	2	3	3	2	2	3	3	2	3		3	3	3	29	10%
11	2	3	2	2	2	3	3	2	2	1		2	1	24	9%
12	1	1	2	1	1	1	3	1	2	1	2		1	16	6%
13	2	3	3	2	2	3	3	3	2	1	3	3		30	11%
1 = less important; 2 = equal; 3 = more important														277	100%

As seen in Table 24, the rates for the different designs are very similar to each other. The chosen design, Nr. 9 has, however, the highest rates.

Table 24. Second evaluation.

Criteria			Design				
			2		9		19
			Glass	Carbon	Glass	Carbon	Glass
1	Constructability, complexity	11%	2	2	3	3	3
2	Transport	7%	2	2	2	2	3
3	Risk of damage	7%	3	3	3	3	2
4	Difficulty of assembling	11%	2	2	2	2	3
5	Maintenance	10%	3	3	3	3	2
6	Traffic disturbance	7%	3	3	3	3	4
7	Design cost	4%	2	2	3	3	2
8	Material use (cost)	11%	3	1	4	2	4
9	Risk of moisture ingress	7%	3	3	3	3	2
10	Dependency on connections	10%	4	4	3	3	2
11	CO2 footprint	9%	2	3	2	3	2
12	Risk of abrasion	6%	2	2	2	2	1
13	Possibility to recycle	11%	2	3	2	3	2
Weighted sum			2,84	2,82	3,00	2,98	2,80
0	Unsatisfactory						
1	Just tolerable						
2	Adequate						
3	Good						
4	Very good						

5.2 Discussion of preliminary design

The aim of the preliminary design was to investigate a wide range of suggestions and different possibilities. Focus was on the choice of the bridge structural system. The twostep evaluation process was used, this made it possible to have a large amount of designs as well as investigating some preliminary design solutions more in depth.

The first evaluation of the design was considered as a guideline for the further discussions. The goal was also to achieve a variation in different designs. Therefore, three very different concepts were chosen for further investigation. Before the final evaluation, production possibilities were investigated more in depth. In the end the concept chosen also had the highest rates. The main reasons for the choice of this design (and also the high rates) were:

- Cost and production method are the best. The production method is more conventional than for design two.
- The size of the elements produced are smaller and can thus be produced by more manufacturers.
- The webs can be produced by both pultrusion and prepreg/autoclave.

6 Final design

The final design solution is developed in this section. The material properties of the FRP laminate are calculated for flanges and webs of the bridge deck section. The different geometries with different angles of inclination of the stiffening parts of the webs will be further studied. The buckling behavior of the developed sections will be investigated with finite element analyses.

6.1 Material properties of FRP laminate

The material properties of FRP composite for the final design decision were calculated according to the classical laminate theory and with regard to Prospect for New Guidance in the Design of FRP Structures (Carattere, 2017). The recommendations of Eurocomp and PNG Design were compared, and the differences were highlighted (see Section 4.1.2).

6.1.1 Relevant conversion factors

Ensuring structural safety throughout the entire service life of the bridge is an important issue that must be given careful attention. To this end, the behavior of FRP composite material under the influence of environmental degradation effects and long-term load were considered by conversion factors applicable to the material properties of the laminate to predict a reduction in strength over time and to ensure the safety limit.

To perform the limit states analyses, the total conversion factor was calculated. It considers the effects of changes in temperature and humidity, creep and fatigue.

$$\eta_c = \eta_{ct} \times \eta_{cm} \times \eta_{cv} \times \eta_{cf} \quad (13) \text{ (eq- 2.6, section 2.3.6)}$$

η_c - total conversion factor, shall be used to convert the test results into values which can be assumed to represent the behavior of the material or the product in the structure or the ground;

η_{ct} - conversion factor for temperature effects;

η_{cm} - conversion factor for humidity effects;

η_{cv} - conversion factor for creep effects;

η_{cf} – conversion factor for the fatigue effects.

Since the ecoduct is expected to experience mainly a static loading over its entire service life, caused by the soil load and self-weight of the structural members, the fatigue loading effects was disregarded in this thesis. The largest influencing loads were assessed as the permanent loads, which mainly cause bending of structural elements. The variable loads, apart from the service vehicle are comparatively small.

Temperature effect

FRP materials have a temperature-dependent behavior due to the polymer matrix. It is assumed that the designed FRP composite structure should function at an ambient temperature of -40...+40°C.

$$\eta_{ct} = 0,9$$

η_{ct} – conversion factor for the verification of strength and stability under the influence of temperature (2.3.6.1);

Humidity effect

The value of conversion factor should be determined according to Table 2.5 (section 2.3.6.2, Carattere, n.d.). The designed structure belongs to the exposure class II with an outdoor climate $T_s < 30^\circ\text{C}$.

$$\eta_{cm} = 0,9$$

η_{cm} – conversion factor for the verification of strength and stability under the influence of moisture (2.3.6.1).

Creep.

Creeping effect should be calculated for permanent and quasi-permanent loading conditions (accumulated duration of characteristic load more than 10 years, Table 2.6).

For the pultruded profiles with properties in the direction parallel to the direction of pultrusion the conversion factor for creep was taken according to Table 10.2 (Carattere, 2017).

$$\eta_{vc20} = 0,5$$

η_{vc20} – conversion factor to account for creep effects for the reference period of 20 years.

Design working life of the structure was taken 100 years SS-EN 1990 Table 2.1.

$$tv = 24 \times 365 \times 100 = 8,76 \times 10^5$$

tv - accumulated load duration (hours);

$$T = 0,253 + 0,141 \log(tv) = 1,091$$

The conversion factor for the creep effect can be calculated with an equation 15:

$$\eta_{cv} = \eta_{cv20}^T = 0,469 \quad (15)$$

Total conversion factors used in design

In accordance with Table 2.4 (Carattere, 2017) conversion factors shall be used for the next checks which is shown in Table 25:

Table 25. Conversion factors to be taken into account.

Influencing factor	Strength (ULS)	Stability (ULS)	Creep (SLS)	Momentary deformation (SLS)
η_{ct}	+	+	+	+
η_{cm}	+	+	+	+
η_{cv}	+	-	+	-

The total conversion factor can be found with equation 16:

$$\eta_c = \eta_{ct} \eta_{cm} \eta_{cv} = 0,38 \quad (16)$$

Momentary deflection:

$$\eta_{cmd} = \eta_{ct}\eta_{cm} = 0,81 \quad (17)$$

The total conversion factors for different checks can be found in Table 26.

Table 26. Total conversion factors.

Conversion factor	Strength (ULS)	Stability (ULS)	Creep (SLS)	Momentary deformation (SLS)
η_c	0,38	0,81	0,38	0,81

6.1.2 Partial safety factors

Comparing the choice of the safety coefficients for the structural safety verification, applicable according to Eurocomp and PNG Design recommendations, the difference in methods of calculation can be pointed out which is represented in Table 27. The table includes safety factors for pultrusion and prepreg manufacturing processes.

Table 27. Comparison of safety factors from Eurocomp and PNG Design recommendations.

Material partial safety factors	Eurocomp (Tables 2.4, 2.5, 2.6)	PNG Design (Table 2.1)
γ_{M1} - coefficient related to the level of uncertainties in the laminate, depending on the properties being derived from tests or the statistical/theoretical data	1.15	1.35
γ_{M2} - coefficient accounting the accuracy of the production process	1.1	1.35
γ_{M3} - coefficient considering the operating design temperature range and heat distortion temperatures of the laminates	2.5	-
Calculation	$\gamma_M = \gamma_{M1} \times \gamma_{M2} \times \gamma_{M3}$ $= 3.163$	$\gamma_M = \gamma_{M1} \times \gamma_{M2}$ $= 1.823$

Apparently, Eurocomp proposes higher material safety requirements compared to PNG Design.

Taking into consideration statements of the Sections 4.1.2 and 6.1.2 and performing the simple calculation, it can be concluded that the method proposed by PNG Design guideline is more conservative having smaller value of the total material safety factor γ_M , but taking into account the deterioration of the laminate material properties with time considering the sectional bending and shear resistance of the eco-bridge FRP members.

For the verification of the structural safety in ULS partial safety factors were determined according to PNG Design (Carattere, 2017).

$$\gamma_M = \gamma_{M1} \times \gamma_{M2} \quad (18)$$

Partial safety factors for material was chosen according to Section 2.3.4.1, PNG Design.

Since material properties in the preliminary design was derived from the theoretical models for prepreg and pultrusion production methods, the quality is expected to correspond to $V_x < 0.1$, where V_x is the variation coefficient.

$$\gamma_{M2uls} = 1,35$$

$$\gamma_{M2global.stab} = 1,35$$

Partial safety factors were chosen for the verification of global and local structural stability.

6.1.3 Glass and carbon fibres material properties

E-glass and HS carbon fibres were chosen to be used in the preliminary design.

Material properties were selected according to Table 11.1 of Prospect for New Guidance in the Design of FRP Structures (Carattere, 2017). Material properties of fibre types can be seen in Table 28.

Table 28. Typical values of fibre properties.

Tension in fibre direction				
Prop.	Units	E-glass	HS-carbon	Meaning
E _{f1}	GPa	73,1	238	Young's modulus in fibre direction
E _{f2}	GPa	73,1	15	Young's modulus perpendicular to fibre direction
ν _f	-	0,238	0,3	Poissons ratio
ε _{f1}		0,038	0,015	Ultimate tensile strain of fibre in 1st and 2nd directions
ε _{f2}		0,024	0,009	
Compression in fibre direction				
ε _{fc}	-	0,024	0,009	Ultimate compressive strain of fibre in two
Shear				
G _f	GPa	30	50	Shear modulus
ρ _f	kg/m ³	2570	1790	Density of the fibre
α	-	5*10^-6	-4E-07	Thermal expansion coefficient

6.1.4 Resin material properties

Polyester is one of thermoset polymers. It was chosen as a polymer matrix for the fibre reinforced composite elements of the ecodeuct based on the following comparison of the different types of resin.

Resin types comparison (WPL, 2013)

- Polyester resin has comparatively lower strength than Vinylester and Epoxy. Polyester is more susceptible to corrosion and chemical environment, having lower operating temperatures. Higher mechanical properties makes Vinylester resin more expensive than Polyester. Vinylester is mainly used for the wind turbine production and automotive industries.

- Epoxy resin, comparing to Polyester and Vinylester resins, has higher strength and better performance under the influence of environmental degradation effects. Epoxy has higher electrical resistance, heat deflection temperatures, lower shrinkage over the curing process and lesser toxic emission. Epoxy has better adhesion to the fibres in composites. Having a great versatility, epoxy can be modified adding agents (increasing the fire resistance or material toughness), and fillers (nanotubes, increasing the electrical resistivity). Because of such high material characteristics epoxy resin is the most expensive thermoset polymer type.

Based on the comparison of the three thermoset polymers types, Polyester resin was accepted as the most suitable material for the prefabrication of the bridge composite members with material properties that meet the design purposes and are sufficient for the design requirements.

The corresponding material properties of the Polyester resin was selected according to the Table 11.2 (Carattere, 2017) and can be seen in Table 29.

Table 29. Polyester resin material properties.

Prop.	Polyester resin	Meaning
E_r [GPa]	3,55	Young's modulus
G_r [GPa]	1,35	Shear modulus
ν_f	0,38	Poisson's ratio
ρ_r [kg/m ³]	1200	Density

6.2 Relevant material properties of the FRP laminate

The material properties for the final design solution of the deck structural system was considered with respect to the Eurocomp and PNG Design recommendations.

The FRP bridge deck section with a balanced symmetric laminate were designed, which means that the layers of the same direction were placed symmetrically regarding the mid-surface of the sections (6.3.1.2 PNG Design; 2.5.4.1 Eurocomp).

The following criteria should be satisfied in the laminate design (The European structural polymeric composites group, 1996):

- In view of that the laminate is considered a orthotropic material with different material properties in longitudinal and transverse directions of the fibre, the amount of the reinforcement with the direction of ∓ 45 degrees should be no less than 20% of the total amount of reinforcement.
- The grouping of the plies with 0 and 90 degrees orientation should be avoided.
- The plies of 45 degrees orientation should separate the plies oriented with 0 and 90 degrees in order to minimize the interlaminar shear and through-thickness stresses when the laminate is predicted to experience in-plane loads.
- It is desirable to dispose the layers of the outer surface at an orientation of 45 degrees, thereby reducing the effects of interlaminar shear.

Now, in light of the previously described requirements, the bridge sections material properties were calculated regarding the number of plies in different directions in flanges and webs, which can be seen in Figure 33.

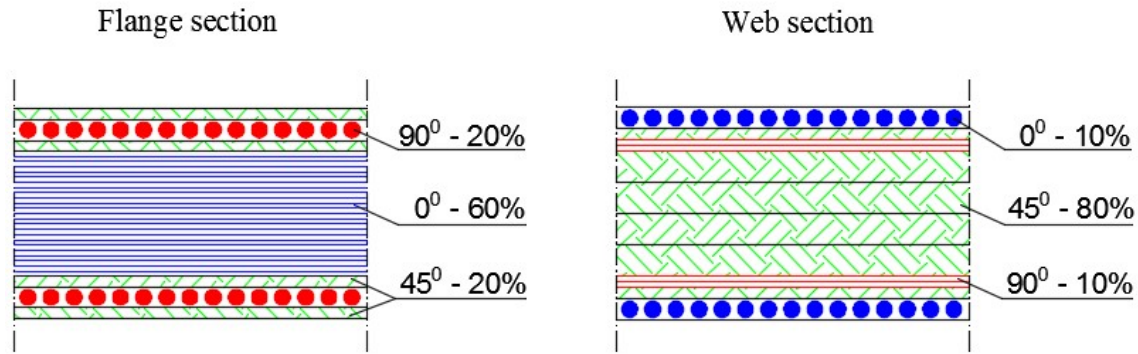


Figure 33. Laminate layers for flanges and webs in the deck section.

Flanges

The bending strength of the section can be achieved by adding a increased number of plies of the 0 degrees orientation in flanges. The plies with 90 degrees orientation were added to assure the material strength in flanges in transverse direction. The plies oriented in 45 degrees was added to provide an efficient shear transfer between the plies of 0 and 90 degrees orientations.

Webs

Plies oriented in 45 degrees are added to hold the shear forces transferred through the webs and are the governing plies orientation in the web-section. The plies with 90 and 0 degrees orientation were added to increase transverse material strength in the webs.

The material properties for the web and flange sections of the bridge deck cross section were calculated according to the Classical Laminate Theory. The fibre volume fraction, number and sequence of layers of different fibre orientations in the laminate were considered.

The flanges were designed as 25 mm thick. It is a reasonable thickness to assure the bending capacity of the deck section and production possibilities.

The web thickness varies in different proposed geometries depending on the height of the deck cross section, which means the higher section – the thinner webs. However, the material properties of the laminate depend on the ratio of the number and thickness of the layers with different orientations in it. The material properties remain the same when the laminate thickness changes keeping the ratio of the number and thickness of the same oriented layers in webs in proportion.

The characteristic values for the material strength in tension were selected as a reference values for GFRP laminate with 0,55 fibre volume fraction.

$$f_{kt} = 470,7 \text{ MPa}$$

$$f_{k\tau} = 70 \text{ MPa}$$

The final material properties are presented in Table 30.

Table 30. Material properties of FRP for flange and web sections of the bridge deck.

Section	Property	Units	Longterm behaviour ¹ (QP, SLS)	Instantaneous deflection ² (characteristic, SLS)	Ultimate capacity ³ (ULS)
Flange	Ex	GPa	12,317	26,235	14,395
	Ey		3,228	12,532	6,876
	Gxy		1,179	4,577	2,512
	v	-	0,31		
Web	Ex	GPa	5,787	12,327	6,764
	Ey		3,522	13,674	7,503
	Gxy		2,128	8,263	4,534
	v	-	0,444		
Edge web	Ex	GPa	8,206	17,491	9,597
	Ey		6,686	14,251	7,820
	Gxy		3,192	6,805	3,734
	v	-	0,388		

¹ Long-term behavior of the FRP composite material under the durable influence of permanent loads, such as solid weight and self-weight of the structure. The calculation takes into account the influence of the creep of the polymer matrix that develops over the service life of the ecodeck, and deterioration of material properties under the influence of humidity and temperature variation.

² Material properties of the FRP composite material immediately after loading at the beginning of the service life of the structure.

³ Material properties taking into account the deterioration of material strength under the influence of environmental degradation factors such as humidity and changes in temperature calculated for the ultimate loading conditions on a bridge.

6.3 Handcalculations: optimization of the section and verification of deflections

To optimize the chosen solution some key geometry parameters were analyzed in hand calculations. The parameters considered were:

- Height of cross-section,
- Thickness and spacing of webs.

The design requirements used to optimize the geometry of the bridge section are described in section 4.1.2. In Table 31 the different design parameters are presented together with the geometry parameters depending on those requirements.

Table 31. Design requirements with corresponding design and geometry parameters.

	Design parameter	Geometry parameter
Deflection	I	h, t _f , t _w , b
Strength in bending	W	h, t _f , t _w , b
Strength in Shear	A _{shear}	h, t _w , b

Where b is the spacing of the webs.

Since the shear strength is only dependent on the shear area, the thickness and spacing of webs were analyzed primarily. As seen in Figure 34 and Figure 35, the resulting thickness is very small. For the middle section it ranges from 0,1 to 1,75 mm, for the edge section it ranges from 0,5 to 8 mm. From a production point of view the webs of 1.75 mm are very thin.

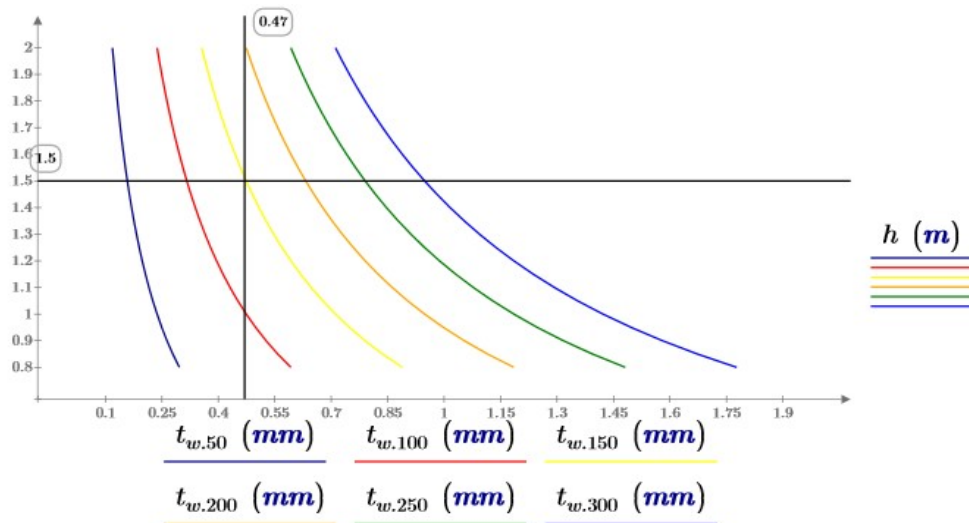


Figure 34. Possible configurations of web thickness and spacing as a function of height (middle section). The index numbers give the spacing of the webs.

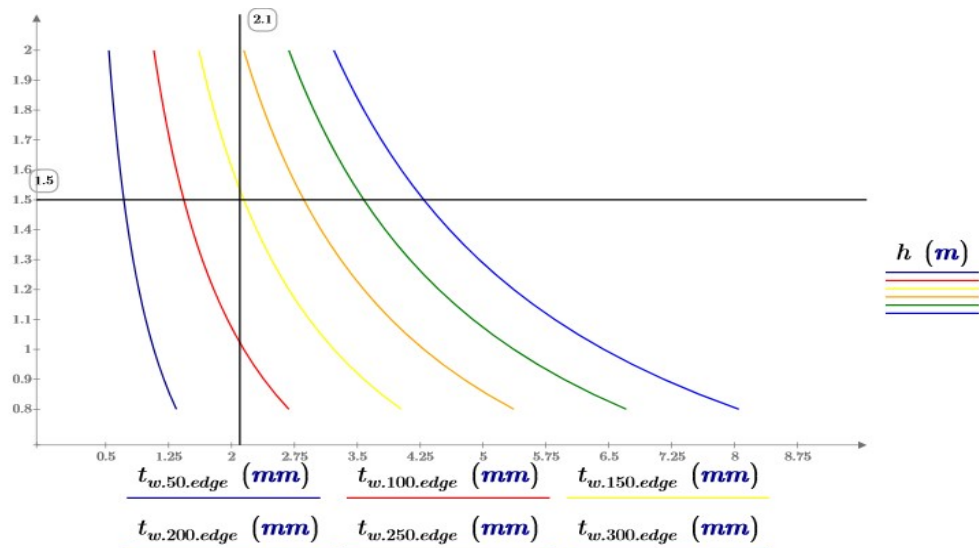


Figure 35. Possible configurations of web thickness and spacing as a function of height (edge section).

In Figure 36 the height of the cross-section is presented as a function of the flange thickness. From a production point of view the thickness should not exceed 25 mm. That results in a height of 1,48 m. In Figure 37 the corresponding graph for the edge section is presented. The flange thicknesses ranges from 25 to 175 mm with height ranging from 0,8 to 2 m. To achieve the necessary capacity in the edge section the web area and spacing is therefore increased.

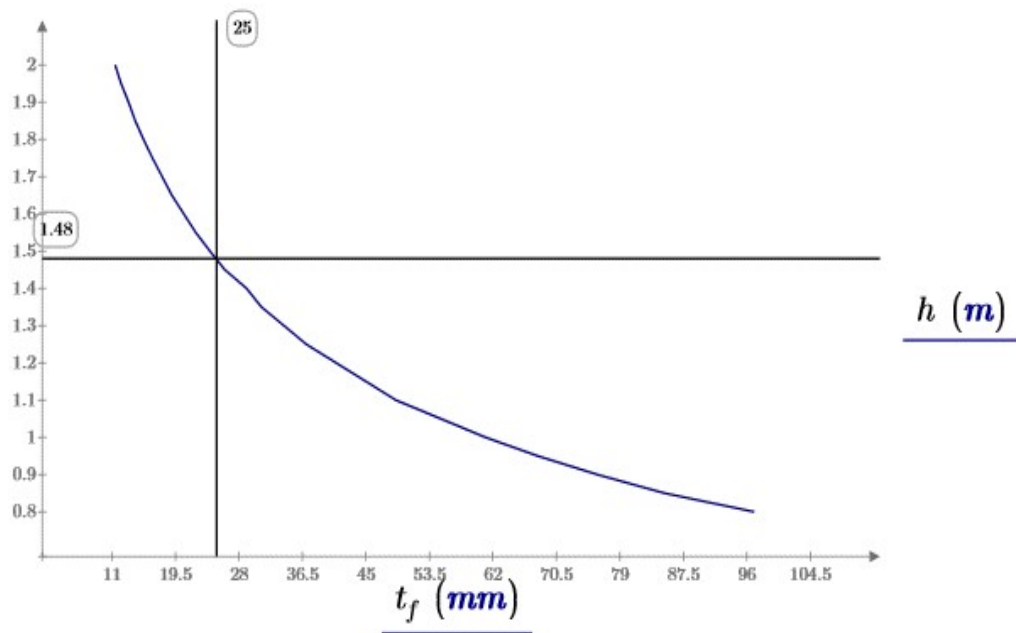


Figure 36. Height of cross-section as a function of flange thickness.

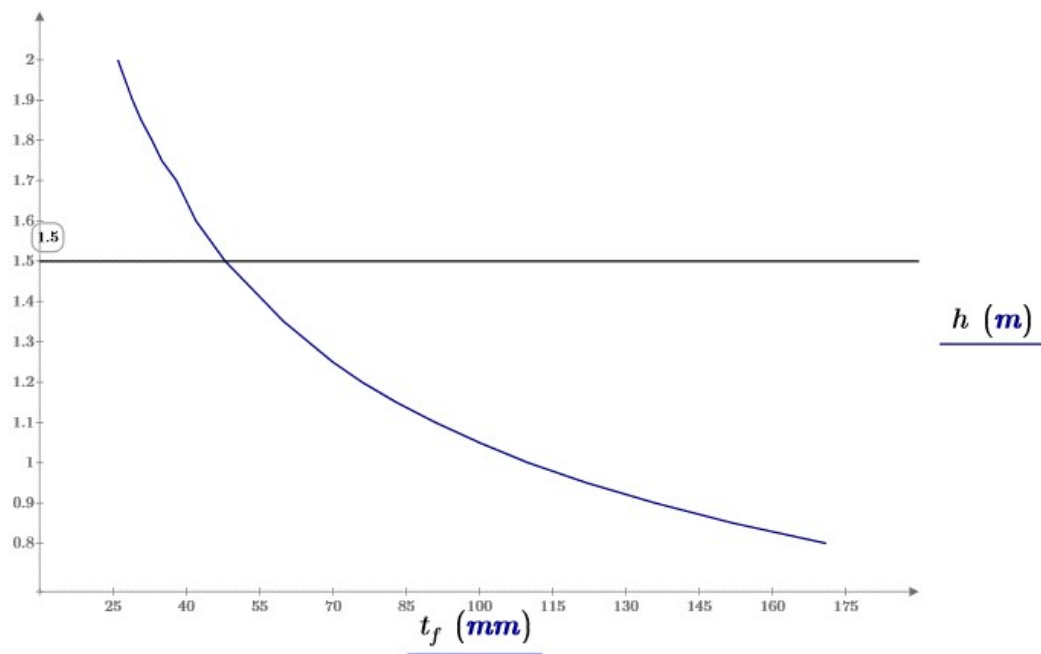


Figure 37. Height of cross-section as a function of flange thickness (edge section).

Figure 38 presents the possible spacing and thickness of the webs in the edge section.

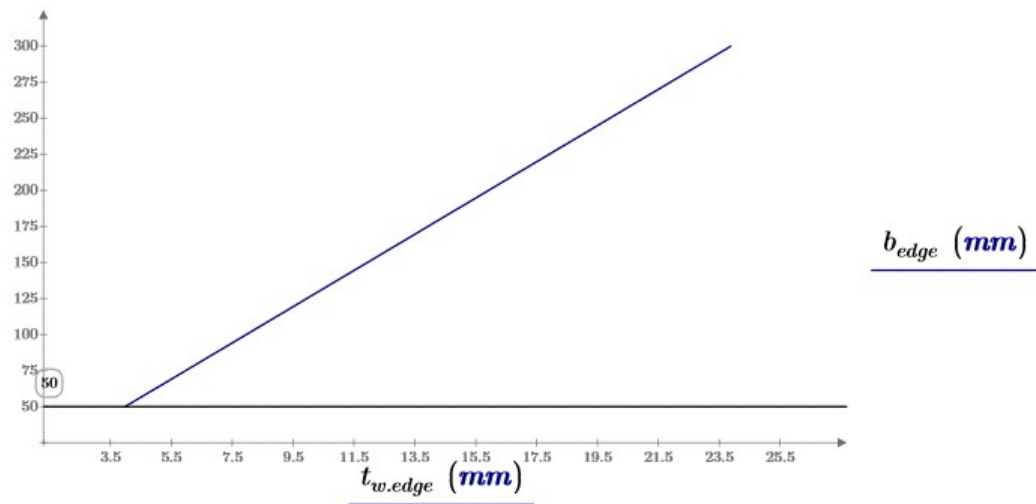


Figure 38. Web spacing as a function of web thickness in edge section.

In Table 32 the most efficient geometry according to the hand calculations is presented. A pre-cambering of 30 mm is assumed. Which means that the bridge is produced so that the initial deformation without any loads (even self-weight) is +30 mm. Figure 34 to Figure 38 the minimum configuration for a height of 1,5 m has been marked. In the final design the minimum web thickness is not used. In the middle section the web thickness is increased because of production considerations. In the edge section the web thickness is increased to lower the height of the total cross-section.

Table 32. Final geometry according to hand calculations. Pre-cambering = 30mm.

	Middle section	Edge section
h	1500	1500
t_f	25	25
b	150	50
t_w	5,7	8,8

Table 33 presents the deflection in the middle of the ecoduct and the requirements on those deflections.

Table 33. Deflections and deflection requirements for handcalculations.

	Middle section	Edge section [mm]	Requirement [mm]
Quasi permanent load combination	58,5	75,0	80,0
Short term variable load action + long term part of permanent load action	18,6 + 45,5 = 64,0	8,2 + 53,8 = 62,0	66,7

6.4 Modeling in Abaqus

The modeling technique in Abaqus software will be described in this section.

6.4.1 Material properties

The material properties of the FRP laminate were introduced into the system in accordance with calculations made for flanges and webs separately for different load conditions on an econduct. The material properties and its detailed description can be seen in Table 30.

6.4.2 Material orientations

Three different coordinate systems are used in the model. They are presented in Figure 39. The global orientation is the same as in hand calculations. The material orientations are used to assign the material properties and are also related to the stress result parameters.

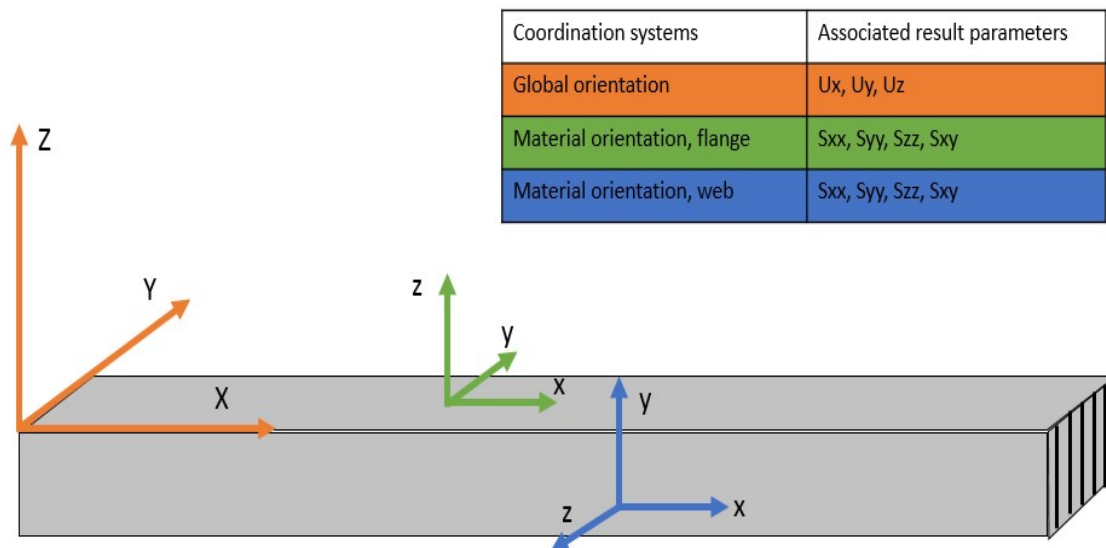


Figure 39. Coordinate systems used for Abaqus model.

6.4.3 Loads

The loads described in Section 4.1.1 are assigned to 1 m wide cross-section in Abaqus. In Figure 40 the load distribution is presented. The distributed load from self-weight, soil load and variable load is assigned to the whole beam. The loads from the service vehicle are recalculated to distributed load on an area of 2,7 m \times 1,4 m and then assigned according to Figure 40. See Section 4.1 for thorough explanation of how the vehicle load is distributed.

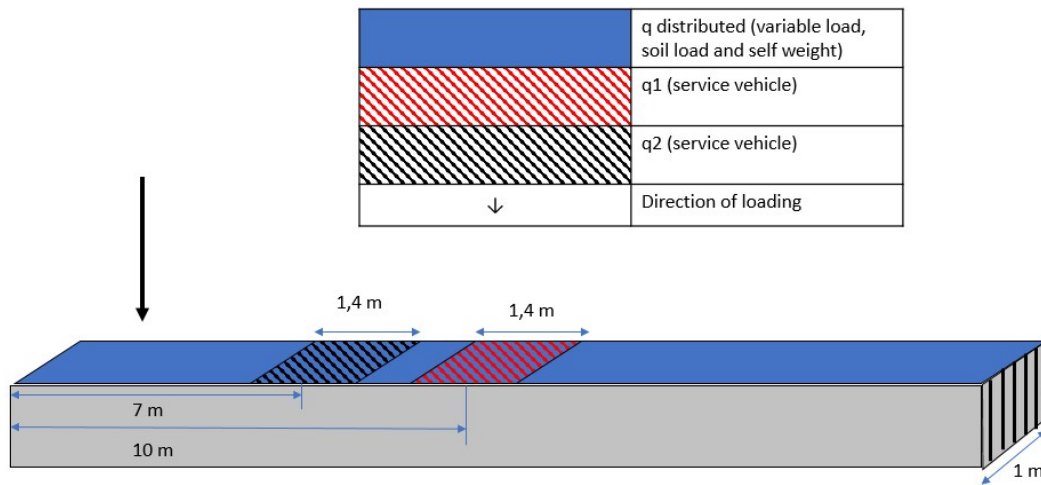


Figure 40. Load distribution on model in Abaqus.

6.4.4 Boundary conditions

The deck section was restrained as a simply supported beam. Two possible solutions for boundary conditions BC1 and BC2 were studied in order to choose the one with better performance regarding lateral deflection of the webs under the loading. The boundary conditions are shown in Figure 41.

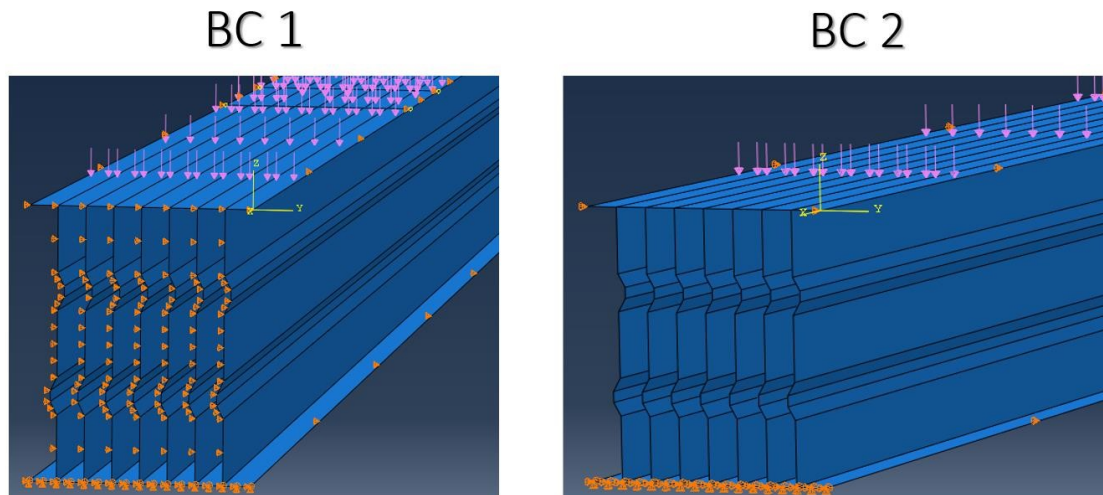


Figure 41. Boundary conditions for the 1 m width bridge deck section.

The support edges were restrained from movement in all the translations on one side and from lateral and vertical movements on the other side. The flange edges were restrained from movement in lateral direction (Y).

As it can be seen in Figure 41 for BC1, the webs over the support was restrained to prevent lateral deflection, however in the set BC2 the webs were allowed to move freely.

The results of the study showed that the lateral deflection of the webs in service loading state was 3 times lesser for the set of BC1 (Figure 42).

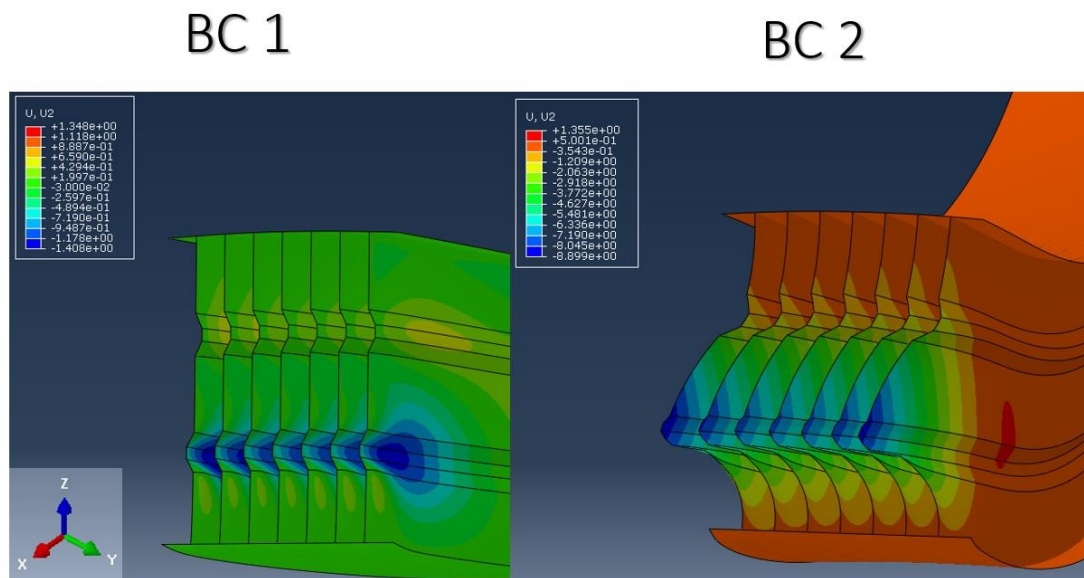


Figure 42. Lateral deflection of webs over the support for BC1 and BC2.

All the further investigation was made with a boundary conditions set BC1 presented in Figure 43.



Figure 43. Conditions for BC1.

6.4.5 Geometries

A range of different geometries was investigated. The hand calculations presented in Section 6.3 were used as limits for the geometry.

The geometries investigated are presented in Figure 44 and Table 34. It was necessary to increase the web thickness in some cases due to buckling issues.

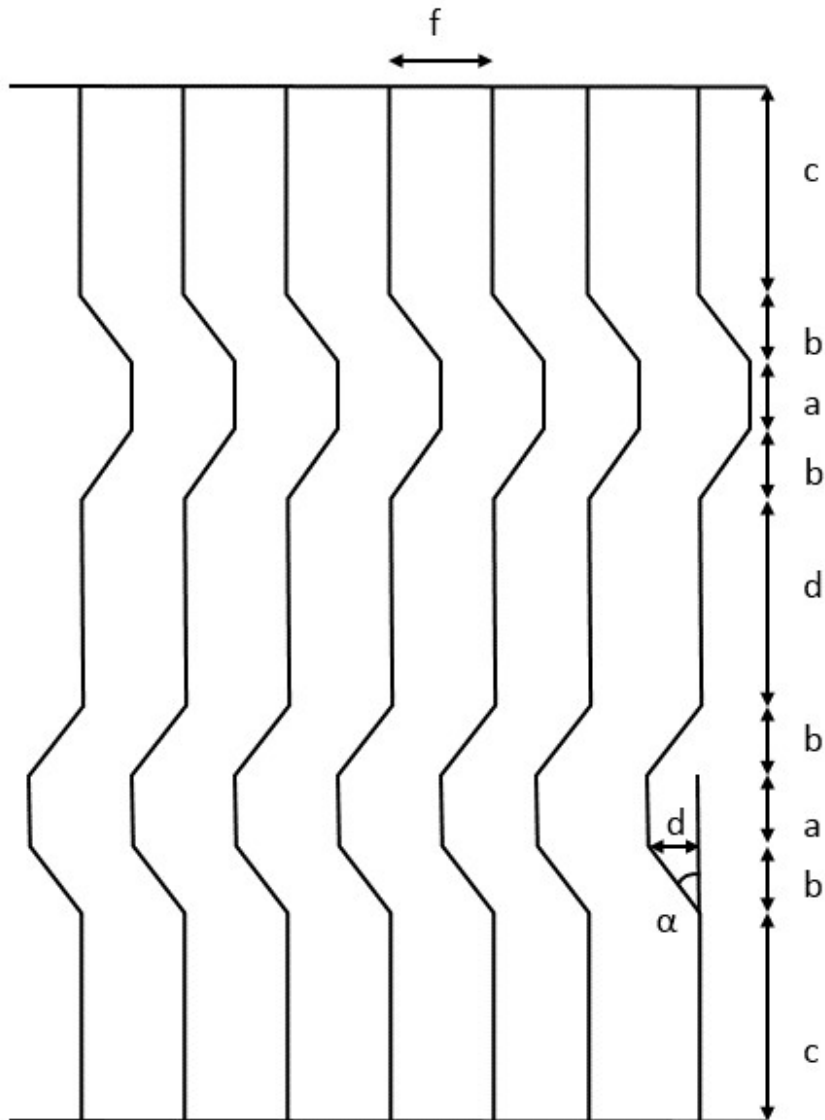


Figure 44. Cross-section of the final ecoduct design.

Table 34. Geometry of crosssection.

Model nr.	α	a [mm]	b [mm]	c [mm]	d [mm]	e [mm]	Height [mm]	t_w [mm]	Area [m ² /m]	f [mm]
G1	30	100	60	290	180	34,6	1250	8,5	0,152	142
G2	45					60			0,16	
G3	60					103,4			0,176	
G4	30			335	213	34,6	1350	6,5	0,127	
G5	45					60			0,132	
G6	60					103,4			0,145	
G7	15			390	280	16,1	1500	8	0,094	150
G8	30					34,6			0,095	
G9	45					60			0,095	
G10	60					103,4			0,097	
G11	15	100	100	350	200	26,8			0,088	
G12	30					57,7			0,088	
G13	45					100			0,090	
G14	30	140	140	300	140	80,8			0,082	
G15	45					140			0,084	
G16	30			260	140	80,8			0,082	
G17	45					140			0,084	
G8 Edge	30	100	60	390	280	34,6	1500	8,8	0,254	50

6.5 Results

In this chapter the results from Abaqus analysis for the different geometries from Table 34 are presented.

6.5.1 Static analysis

The static analysis performed for the thesis had three different purposes:

- Confirming the results from the hand calculations.
- Compare different geometries to each other. The deflection and stresses for different geometries were evaluated in the characteristic and ultimate limit state load combination respectively.
- Check of the safety requirements. The strength of FRP material in ULS and quasi permanent load combination was verified according to PNG Design recommendations. The requirements on deflections are a combination of instant deflection from the permanent loads directly after loading (δ_1) with the deflection from the variable loads together with longterm influence of permanent loads (δ_2) (see Figure 20). Since material properties for both load cases cannot be assigned to the deck model simultaneously, the deck section was modeled for both cases separately, and the results of the Abaqus simulation were confirmed by manual calculations for the same loading conditions.

The results are presented in Table 35 and in figures later in the chapter. The simulation was performed for the characteristic load case. The maximum stresses were in the bottom flanges of the section and the values were also checked to assure the material strength requirements. Shear stresses were calculated for the concepts of 1.5 m height.

Parameters investigated are:

S_{xy}	Shear stresses in XY direction
S_{xx}	Normal stresses in X direction
U_z, U_y	Deflection in Z and Y directions respectively

The coordinate system is according to Figure 43.

Table 35. Static analysis results (Abaqus), deflections in Y and Z directions are presented, normal stresses in X direction, shear stresses in XY plane with regard to the material orientation in the webs are also presented.

Static analysis (characteristic load combination)							
N of the concept	Height (mm)	α	Deflection (mm)			Stresses (MPa)	
			Uy max	Uy min	Uz	Sxx	Sxy
G1	1250	30	0,95	-0,93	-66,49	26,2	-
G2		45	1,49	-1,08	-67,0	26,1	
G3		60	2,63	-1,42	-68,69	25,7	
G4	1350	30	1,7	-1,6	-59,6	24,7	
G5		45	1,9	-2,9	-60,4	23,9	
G6		60	2,4	-5,1	-63,9	23,2	
G7	1500	15	2,4	-4,0	-50,7	24,3	-6,1
G8		30	4,7	-4,5	-52,2	24,2	-7,1
G9		45	8,1	-5,2	-56,1	24,0	-10,3
G10		60	15,7	-7,2	-65,7	23,5	-8,7
G11		15	4,4	-4,5	-51,6	24,3	-8,9
G12		30	8,9	-4,7	-55,1	24,0	-12,4
G13		45	17,0	-5,2	-63,4	23,7	-15,4
G14		30	15,4	-4,3	-59,2	23,9	-11,8
G15		45	33,6	-4,0	-76,4	23,5	-13,3
G16		30	17,9	-4,8	-60,8	24,1	-14,1
G17		45	18,1	-4,7	-60,8	23,9	-13,9

Figure 45 presents the maximum tensile stresses in the flange. The data is taken as the highest tensile stress in the bottom flange. All data points in the same color have the same geometry apart from the angle α (see Figure 44). The shape of the marker is used to indicate the angle. The same color and shape code will be used for all the following results.

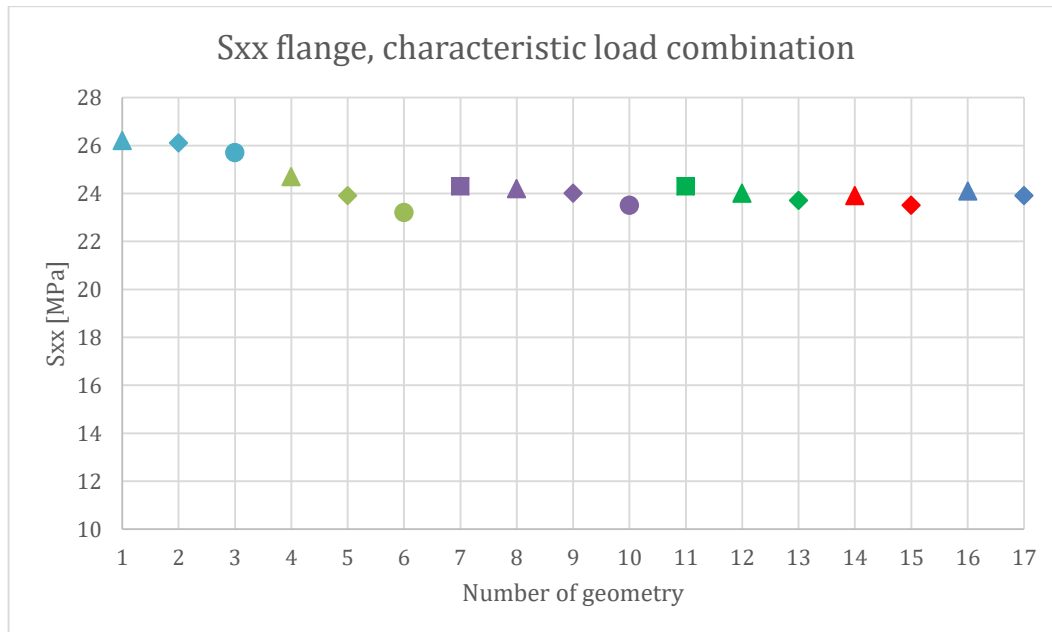


Figure 45 Maximum stresses, normal stresses Sxx in the bottom flange. Characteristic load combination.

Figure 46 presents the largest vertical deflection of the ecoduct. The point is in the bottom flange at the mid-span of the bridge for the instant deflection in the characteristic load case.

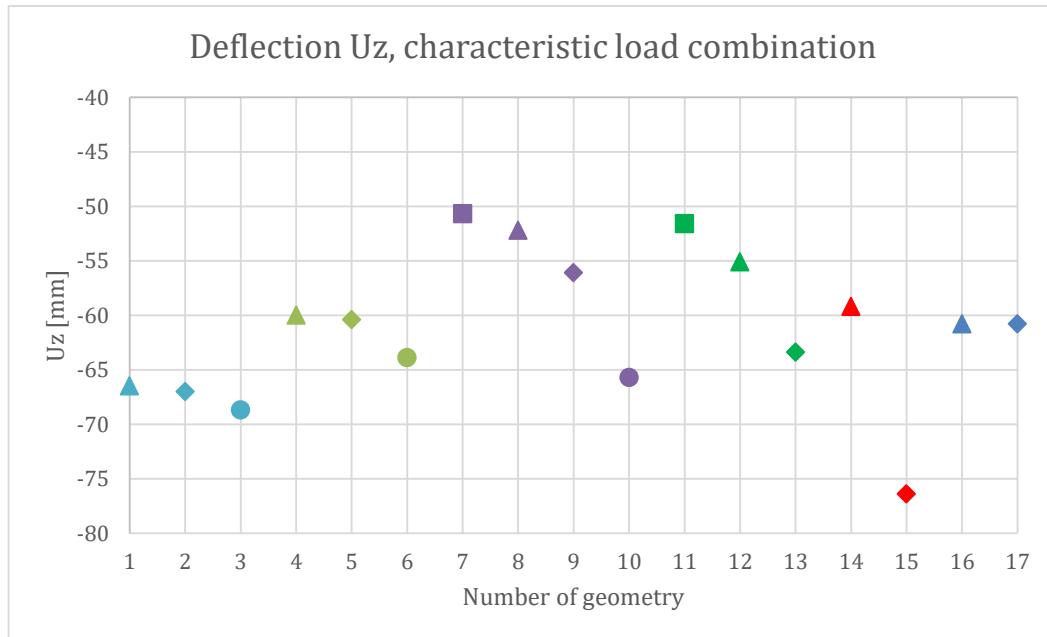


Figure 46. Maximal vertical deflections of the bridge deck in characteristic load combination.

Figure 47 and Figure 48 show the maximum respective minimum deformation of the webs on the stiffeners along the web (part a) of the stiffener, see Figure 44), since the absolute value of the deformation is largest the entire web. The deformation is in y direction, see Figure 39. The maximum value is generally in the middle of the span while the minimum value is found near to the supports. Note that the absolute value for the minimum and maximum does not vary much for some of the geometries.

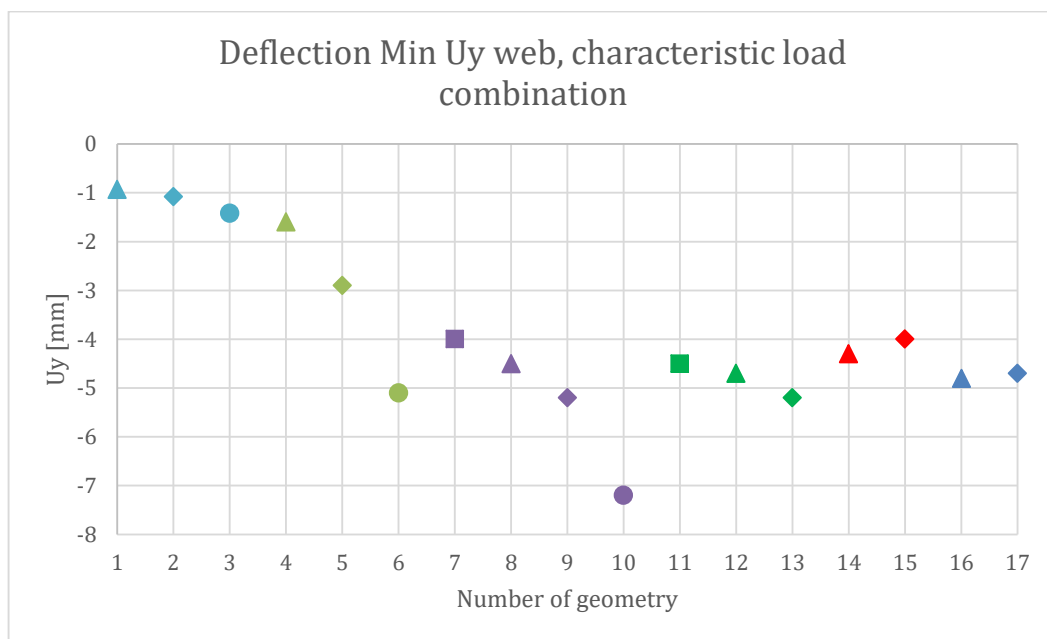


Figure 47. Minimum lateral deflection of web, characteristic load combination.

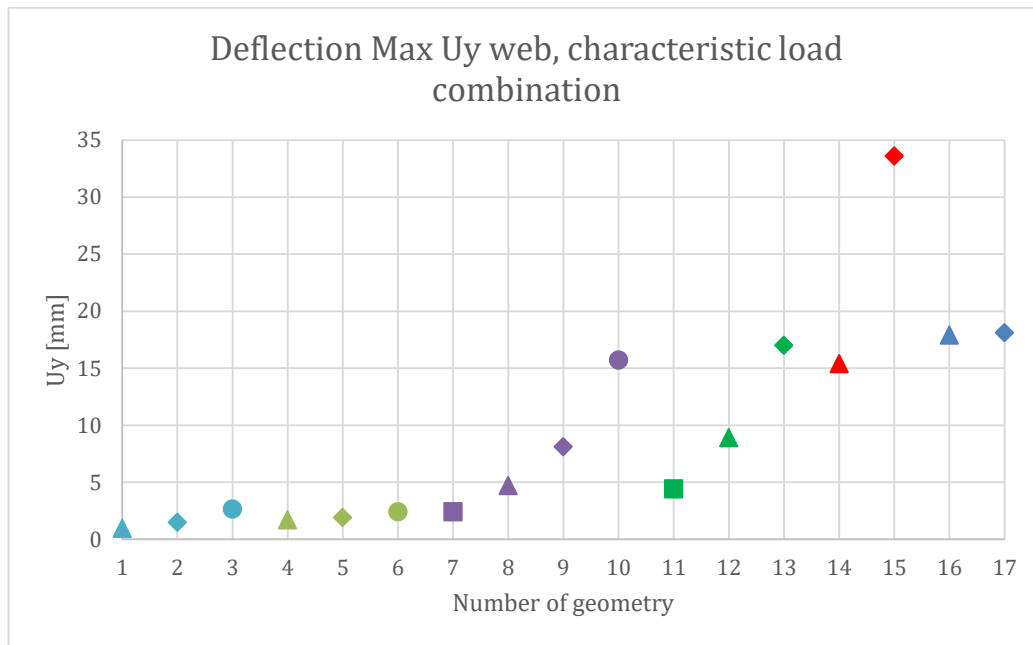


Figure 48. Maximum lateral deflection of web, characteristic load combination.

For reasons discussed in Section 6.6, design nr. 8 was chosen for a more thorough investigation.

Results from different load cases for design nr G8, are presented in Table 36. The ULS and characteristic load case considered instant load while the quasi permanent load case also takes creep into account. Note that deformations are largest for ULS followed by quasi permanent load combination. For the stresses however, the quasi permanent load combination gives the lowest values. It should also be noted that the shear stresses are properly larger than they would be in reality. The boundary conditions used influenced the shear stresses near the supports, where the shear stresses reached the maximum values.

Table 36. Results geometry nr. G8, different load cases.

Load combination	Sxx [MPa]	Sxy [mm]	Uz [mm]	Uy [mm]	Uy [mm]
				Max	Min
ULS	33	-9,14	-129,6	11,6	-11,2
Characteristic	24,2	-7,1	-52,2	4,7	-4,5
Quasi-permanent	15,5	-4,4	-73,7	6,1	-6,7

Results for the edge section in different load cases are presented in Table 37.

Table 37. Results geometry nr G8, edge section.

Load combination	Sxx [MPa]	Sxy [mm]	Uz [mm]	Uy [mm]	Uy [mm]
ULS	31	-4,4	-118,5	4,7	-5,1
Characteristic	24,2	-3,2	-51	2	-2,2
Quasi - permanent	20,9	-2,9	-39,7	3,7	-4

Results for cross section with straight web and corresponding hand-calculations are presented in Table 38. The same load-case, the instant characteristic load is analyzed for both models.

Table 38. Results straight webs, characteristic load combination.

Model	Sxx [MPa]	Sxy [mm]	Uz [mm]	Uy [mm] Max	Uy [mm] Min
Abaqus	24,4	-12,3	-50,0	0,1	-0,1
Hand-calculations	No results	No results	-56,8	No results	No results

In Figure 49 the lateral deformation pattern of the web stiffeners are presented. The results were taken for the geometry G8. The pattern of deformation was similar for all analyzed concepts. The deformations is taken along the middle of part a) of the stiffener. It can be compared with Figure 50 where the whole lateral deformation is presented.

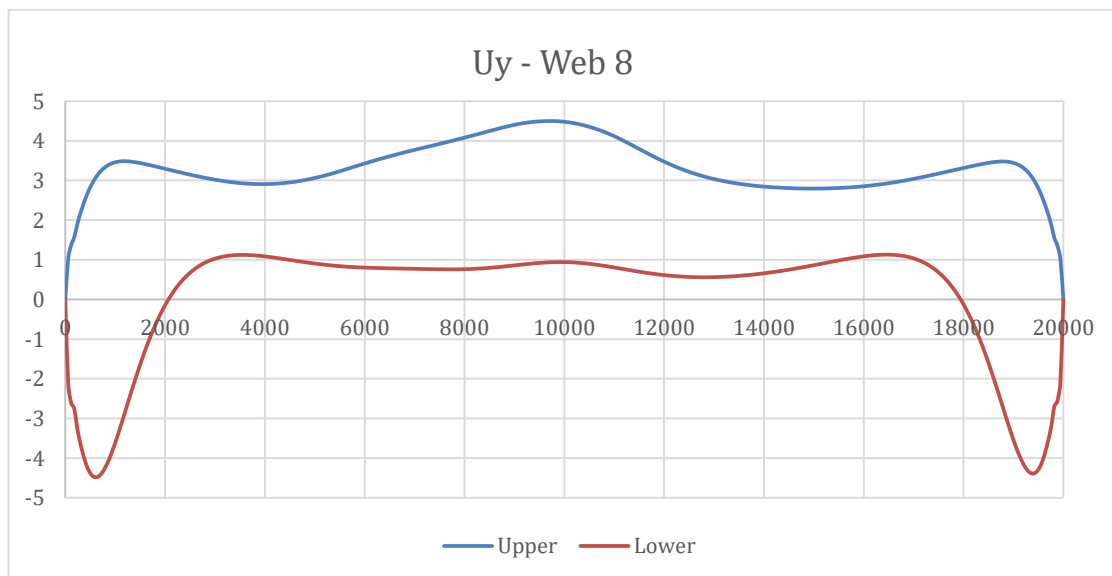


Figure 49. Lateral deflection, Uy, along web stiffeners. Geometry G8 and characteristic load case.

Figure 50 to Figure 54 present the stress and deformation pattern on the cross section. Lateral and vertical deflections are included as well as stresses in x direction and shear stresses.

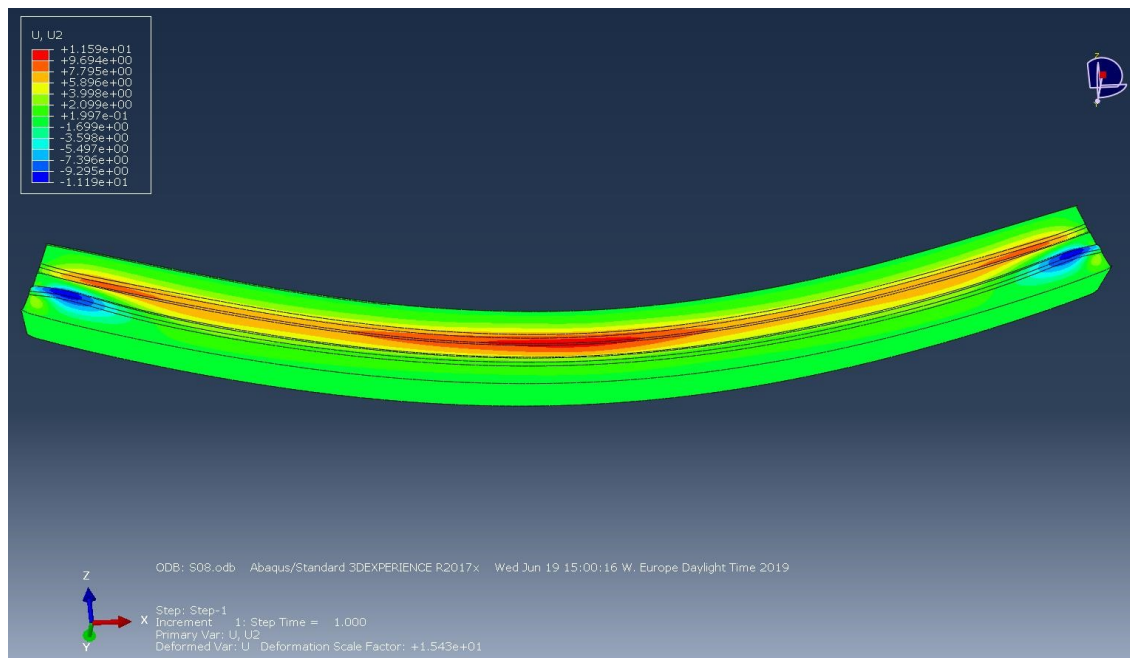


Figure 50. Lateral deflection, design G8. The deflection in y direction ranges from +/- 11 mm. The deflection is most pronounced along the two web stiffeners. The exact form of the deformation along the stiffeners is presented in figure 49.

The vertical deflection (Figure 51) varies only along the Z axis and is largest in the middle of the span.

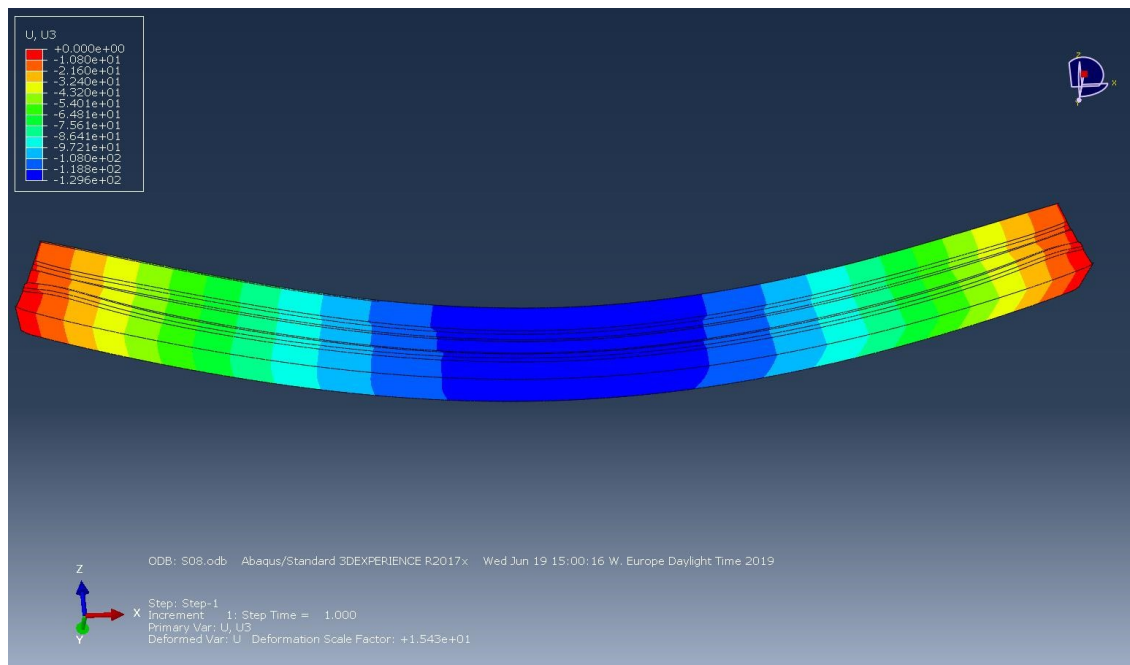


Figure 51. Vertical deflection, geometry G8.

As expected for a simple supported beam the stresses from bending are largest in the flange at the middle of the span (Figure 52).

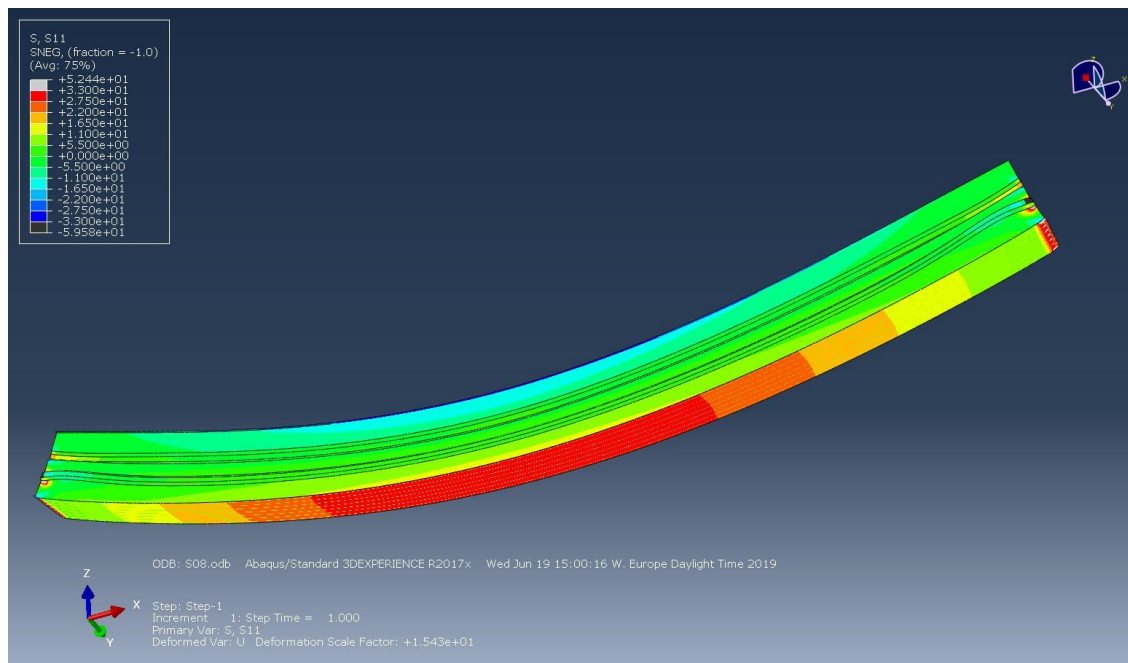


Figure 52. Stresses S_{xx} , geometry G8.

The shear stresses are presented in Figure 53 and Figure 54. In the closeup the location for the highest stresses is visible and marked with two red circles. Note the red arrow, in that position the boundary conditions seem to influence the stresses.

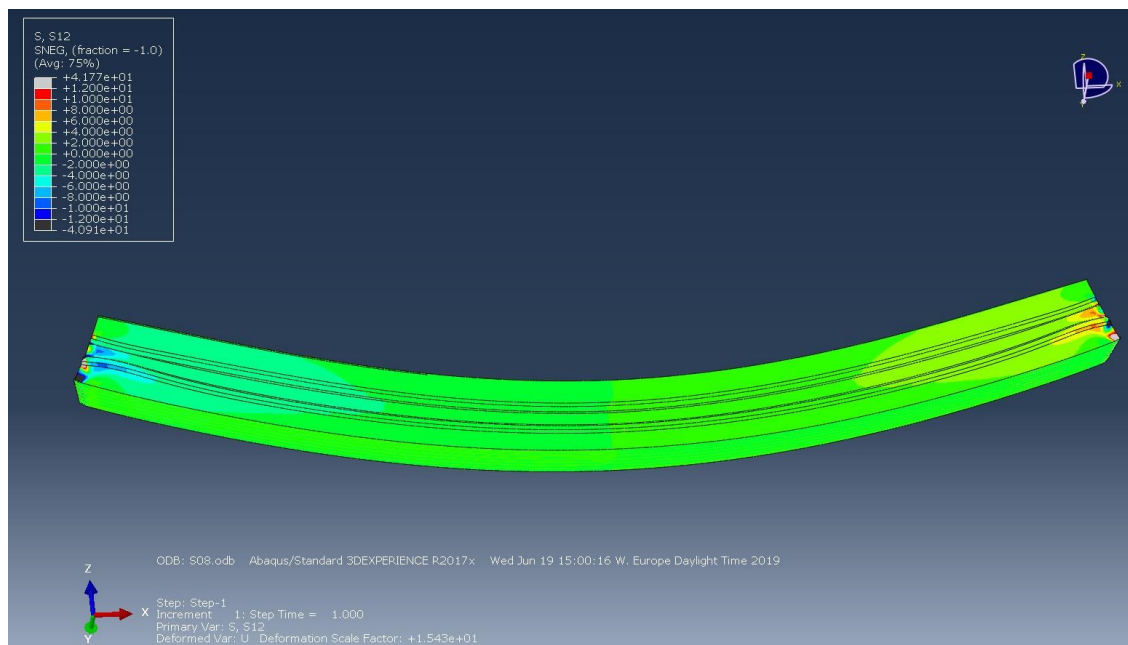


Figure 53. Stresses S_{xy} , geometry G8..

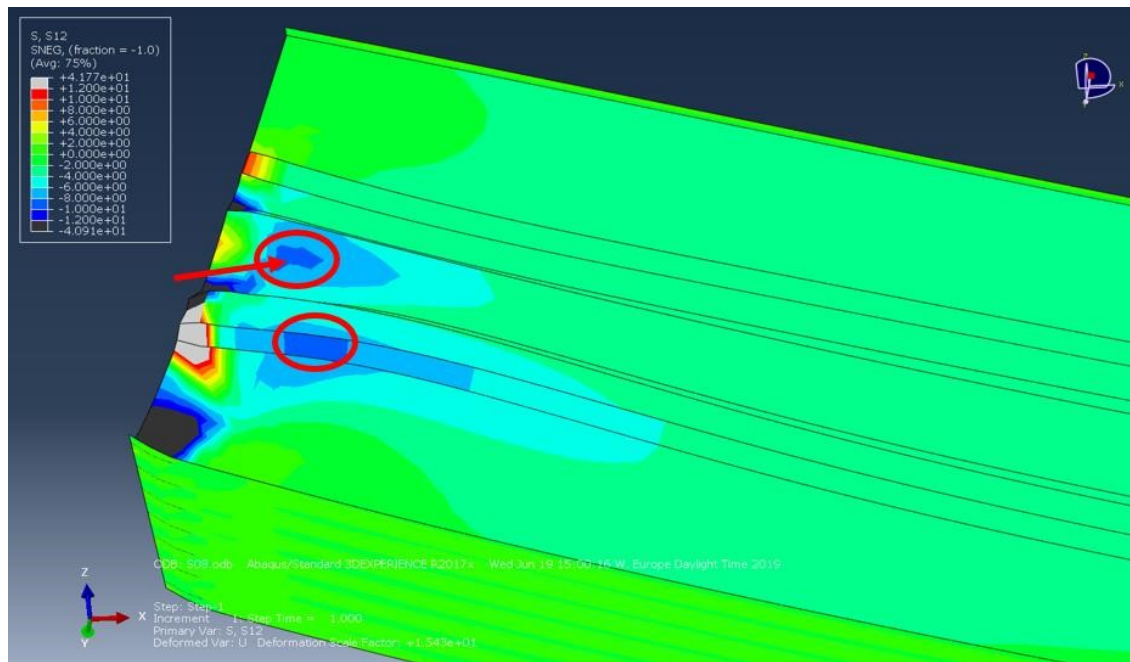


Figure 54. Stresses S_{xy} , geometry G8.

Figure 55 Presents the lateral deflections of the cross section with straight webs.

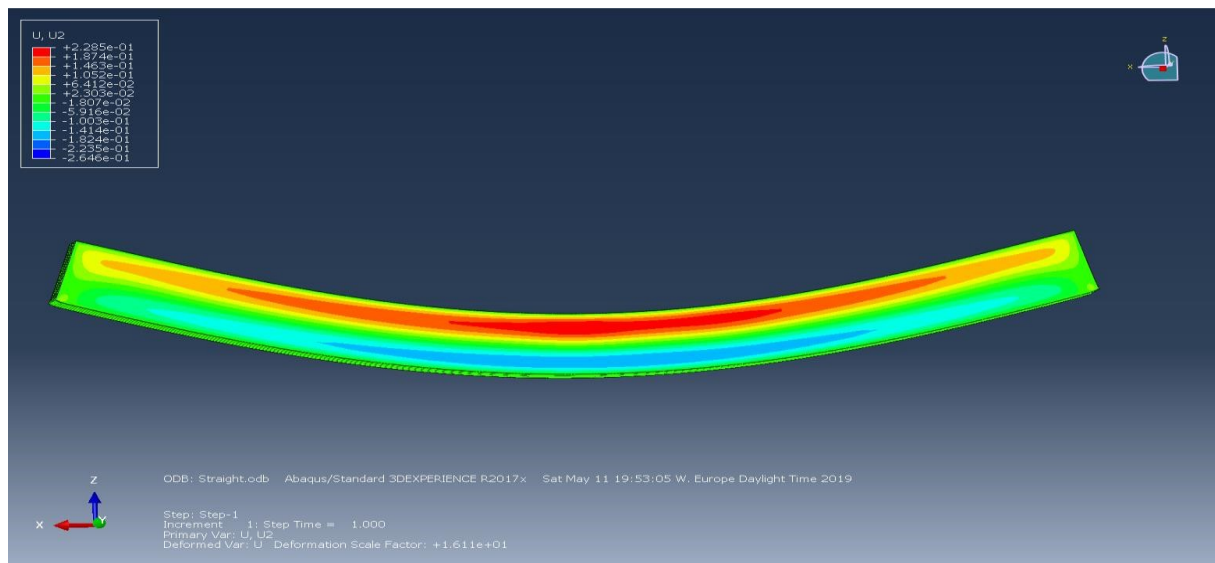


Figure 55. Lateral deflection U_2 , geometry with the straight webs.

6.5.2 Buckling analysis

In this chapter the results from the buckling analysis are presented. The analysis of 17 proposed concepts with different heights and geometries of the bridge deck section was made. The buckling behavior of the deck section was checked in ultimate load state. The load factors for the first 10 buckling modes with the corresponding heights and angles of the inclination of the stiffened parts of the webs are presented in Table 39.

Table 39. Results of the buckling analysis for different geometries of the bridge deck section.

N of the concept	Height (mm)	α	Buckling modes									
			1	2	3	4	5	6	7	8	9	10
			Eigenvalues									
G1	1250	30	3,2	-3,3	3,7	3,8	-3,8	-4	4	-4,3	4,4	4,5
G2		45	2,5	-2,7	3,1	3,1	-3,2	-3	3,5	-3,7	3,9	4
G3		60	1,9	-2	2,4	-2,6	-2,7	2,9	-3	3,3	-3,4	-3,4
G4	1350	30	2,5	-2,6	2,8	-3,1	3,2	-3	3,5	3,6	-3,7	3,8
G5		45	1,9	-2	2,4	2,4	-2,5	-3	2,8	3,1	-3,1	-3,3
G6		60	1,4	-1,5	1,8	1,9	-1,9	-2	2,4	-2,5	2,6	-2,7
G7	1500	15	0,9	0,9	0,9	0,9	0,9	0,9	0,9	0,9	0,9	1
G8		30	1,4	1,4	1,4	1,4	1,4	1,4	1,4	1,4	1,4	1,4
G9		45	1,4	1,4	1,5	1,5	1,5	1,5	1,5	1,5	1,5	1,6
G10		60	0,8	-1	1,2	-1,3	1,3	1,4	1,4	1,4	1,4	1,5
G11		15	1,3	1,4	1,4	1,4	1,4	1,5	1,5	1,5	1,5	1,5
G12		30	1,3	1,6	1,6	1,6	1,6	1,6	1,6	1,6	1,7	1,7
G13		45	0,8	-1,1	1,2	1,3	-1,3	1,5	1,5	1,5	1,6	1,6
G14		30	1	-1,3	1,3	1,4	-1,5	1,8	1,8	1,8	1,8	1,8
G15		45	0,5	-0,7	1	1	-1,2	1,4	-1	-1,7	1,7	1,7
G16		30	0,9	-1,2	1,3	1,3	-1,5	1,7	-2	1,8	2,2	2,2
G17		45	0,9	-1,2	1,3	1,3	-1,5	1,8	1,8	-1,8	2,1	2,2

In Figure 56 the first 10 buckling modes for all deck section geometries are presented. In Figure 57 the first mode eigenvalues are presented as a function of the angle as well as different geometries.

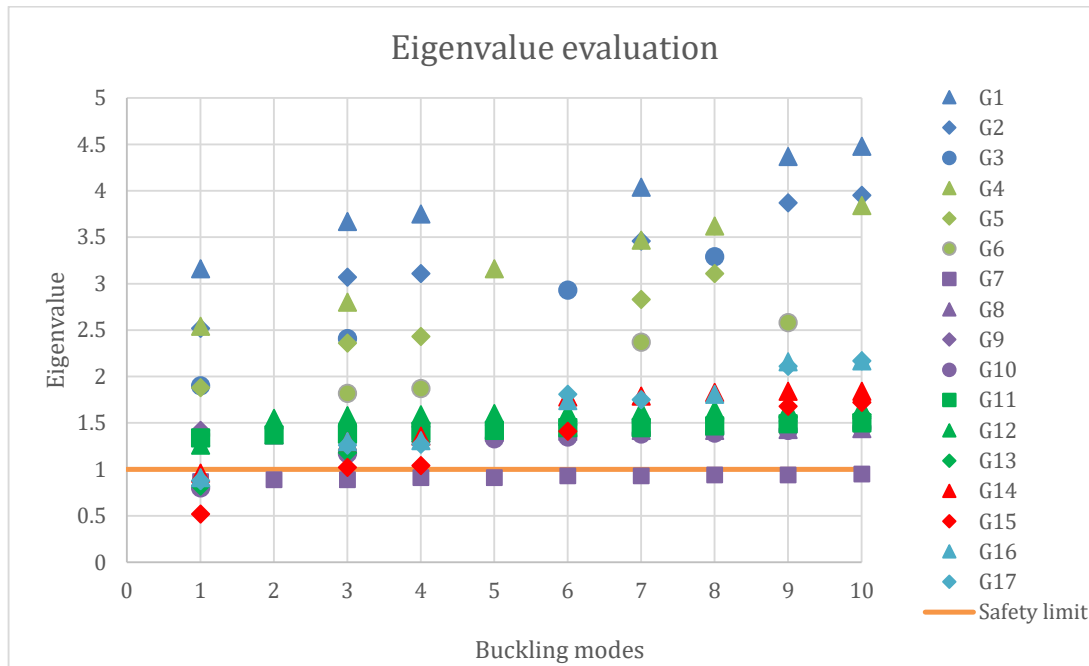


Figure 56. Positive eigenvalues for the first 10 buckling modes for different geometries.

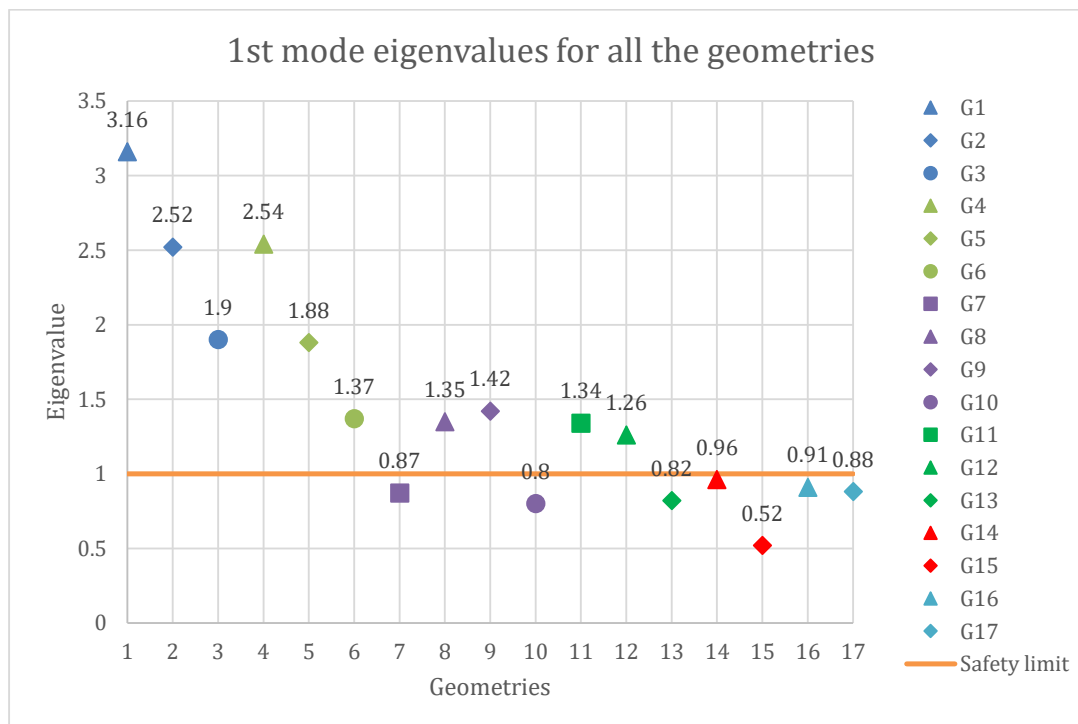
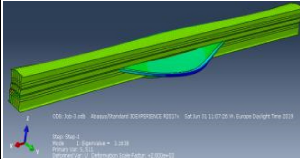
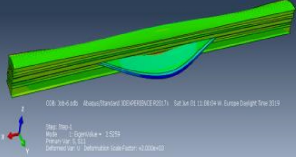
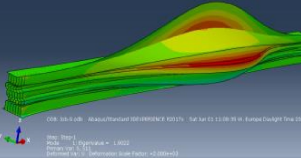
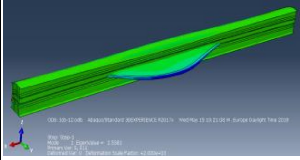
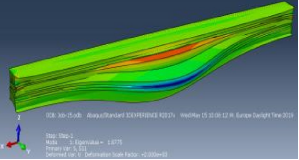
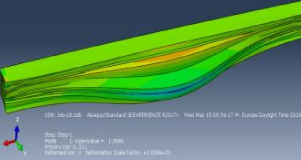
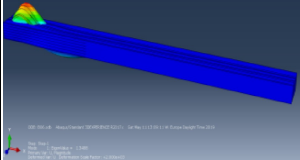
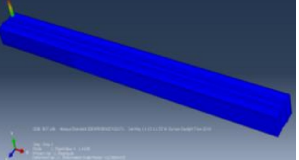
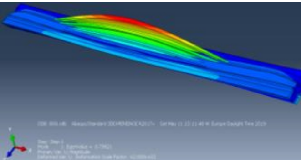
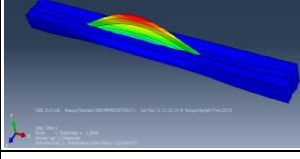
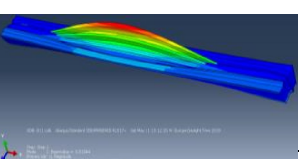
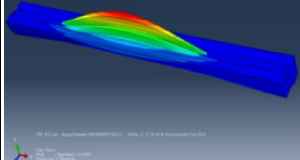
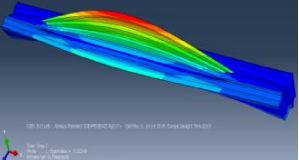
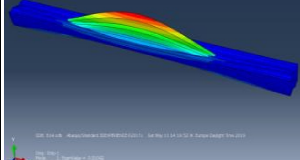
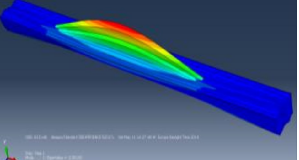


Figure 57. Eigenvalues for first buckling mode for different geometries.

The first buckling modes for the concepts with a height of 1250 mm, 1350mm and 1500 mm and angles of the inclination of the stiffener of 15, 30, 45 and 60 degrees are depicted in Table 40.

Table 40. The 1st buckling modes for the different deck section geometries. The red, green and blue arrows in the pictures are showing the X, Y and Z directions respectively.

N of concept	Height (mm)	$\alpha = 30$ degrees	$\alpha = 45$ degrees	$\alpha = 60$ degrees
G1-G3	1250			
Failure mode		web	web	web
G4-G6	1350			
Failure mode		web	web	web
G8-G10	1500			
Failure mode		web	shear	web
G12-G13				-
Failure mode		web	web	
G14-G15				
Failure mode		web	web	
G16-G17				
Failure mode		web	web	

The first 5 eigenvalues for the edge section are presented in Table 41. In contrast to other analysis, this was done on a cross-section of 0.5 width since the calculation time became excessive for a cross-section of 1 m width for edge sections. The first buckling mode is presented in Figure 58. The buckling modes corresponding to eigenvalue 2-5 were in the same position as for the 1st buckling mode.

Table 41. Five first eigenvalues for the edge section.

	1	2	3	4	5
Eigenvalue	2,0147	2,0147	2,0167	2,0169	2,0213

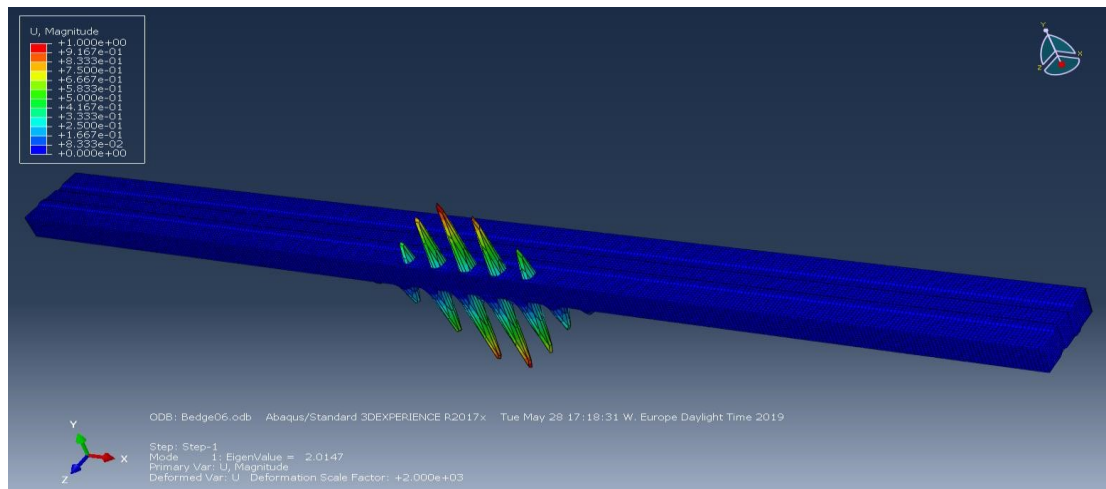


Figure 58. First buckling mode of the edge section (blue arrow in the figure indicate the vertical direction in the global coordinate system).

6.6 Discussion of the final design

Confirming results from hand calculations

The difference between hand calculations and Abaqus in the middle section is:

$$\frac{U_{z \text{ hand}} - U_{z \text{ straight}}}{U_{z \text{ hand}}} = \frac{59 - 52}{59} = 0,12 \quad (19)$$

This difference of 12% seems to indicate that the hand calculations are more conservative in their approach.

Comparing geometries

The difference between an Abaqus model with straight webs and design nr. 8 is:

$$\frac{U_{z \text{ nr 8}} - U_{z \text{ straight}}}{U_{z \text{ nr 8}}} = \frac{52 - 51}{52} = 0,02 \quad (20)$$

This indicates that there is very little difference between those specific geometries. There are however cases where the geometry seems to influence the deformation more. In Figure 45 it can clearly be observed that the angle influences the buckling behavior of the section. For most cases an increased angle means larger deformations.

In Figure 48 it can be seen, that the lateral deflection varies significantly depending on the height of the cross section. For the same load situation, the smallest lateral deflection of the webs was for the lower sections of 1.25 and 1.35 m, and the higher cross sections had higher lateral deformations. The lateral deformations also depend on the angle of inclination of the stiffening part of the webs. Smaller inclination gives smaller lateral deformations. The webs with the angle of 60 degrees had the highest values of lateral deflection. This seems logical since the geometry creates an internal moment (Figure 59) in the stiffeners. This leads to increased deformations.

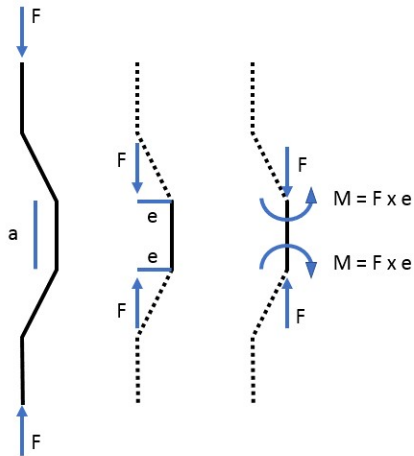


Figure 59. Internal moment in stiffener. Increased a) or e) increases lateral deformation of stiffener.

Deflections

The deflection limits are satisfied for all the deck sections of different heights. However, to assure the safety limits the sections of 1,25 m and 1,35 m height require more composite FRP material to be used. The sections of 1,5 m height are lightweight, fulfilling the deflection limits they need lesser amount of FRP material in the section.

$$\delta_2 = 66,77[\text{mm}] > 64 [\text{mm}] \quad \text{for middle section}$$

$$\delta_2 = 66,77[\text{mm}] > 62 [\text{mm}] \quad \text{for edge section}$$

$$\delta_{\max} = 80,00[\text{mm}] > 58[\text{mm}] \quad \text{for middle section}$$

$$\delta_{\max} = 80[\text{mm}] > 75[\text{mm}] \quad \text{for edge section}$$

As described before, FRP is susceptible to creep, checking the results for the deformation presented in Table 33 gives:

$$\frac{\delta_{\text{creep}}}{\delta_{\max}} = \frac{45,5}{64} = 0,71 \quad \text{for middle section} \quad (21)$$

$$\frac{\delta_{\text{creep}}}{\delta_{\max}} = \frac{53,8}{62} = 0,87 \quad \text{for edge section}$$

Which means that the creep part of the deflection due to permanent load is 71 respective 87 % of the creep part of the permanent load plus the instant deflection of the variable load.

Stresses

The stresses in the proposed section are below the safety limits stated by PNG Design guideline for the material strength of FRP.

FRP material strength with regard to the short-term load in ultimate load state (see table 15):

$$f_{dt} = \eta_{c,md} \times \frac{f_{kt}}{\gamma_{M,PNGdesign}} = 0,81 \times \frac{470,7}{1,823} = 209,1 \text{ [MPa]} > \sigma_{xx} = 33 \text{ [MPa]} \quad (22)$$

$$f_{d\tau} = \eta_{c,md} \times \frac{f_{k\tau}}{\gamma_{M,PNGdesign}} = 0,81 \times \frac{70}{1,823} = 31,1 \text{ [MPa]} > \sigma_{xy} = 9,14 \text{ [MPa]} \quad (23)$$

FRP material strength with regard to creep rupture under the long-term load (see equation 10):

$$f_{dt} = \eta_c \times \frac{0,3 \times f_{kt}}{\gamma_{M,PNGdesign}} = 0,38 \times \frac{0,3 \times 470,7}{1,823} = 29,5 \text{ [MPa]} > \sigma_{xx} = 15,5 \text{ [MPa]} \quad (24)$$

$$f_{d\tau} = \eta_c \times \frac{0,3 \times f_{k\tau}}{\gamma_{M,PNGdesign}} = 0,38 \times \frac{0,3 \times 70}{1,823} = 4,4 \text{ [MPa]} > \sigma_{xy} = 4,4 \text{ [MPa]} \quad (25)$$

The utilization ratios corresponding to those values can be seen in Table 42.

Table 42. Utilization ratios for stresses in ultimate limit stat and quasi permanent limit state.

Load combination	Stress	Utilization ratio
ULS	Bending	16 %
ULS	Shear	29 %
Quasi permanent	Bending	53 %
Quasi permanent	Shear	100 %

The only stress that seems critical is the long-term shear stresses (creep rupture). The stresses at the section approached the material strength limit. Some factors about the reliability of the shear stresses should be mentioned. The material strength values were taken as a reference values provided by manufacturers for FRP materials and should be regarded as approximate. From the design side, the area with the largest shear stresses was allocated close to the supports. The support condition causes a stress concentration. The area directly near to the boundary conditions was ignored when evaluating the shear stresses, since the boundary conditions in the real construction are unknown. But there is however still a chance that there is an influence of boundaries in modeling. Therefore, the analysis regarding creep rupture due to shear stresses remains inconclusive. A more thorough analysis with boundary condictions designed to do not cause stress concentrations may be a way to reach a more conclusive result.

Buckling

As seen in Figure 56, the most efficient geometries regarding buckling are the lower ones with a height of 1.25 m and 1.35 m. This is logical since those sections are less slender than geometries G7 to G17 of 1.5 m height. It is however shown that it is possible to reach enough buckling capacity even with very slender cross-sections. Comparing these sections to each other, an angle of 30 to 45 degrees was found to be the most efficient. In those buckling modes the global buckling has been prevented and local buckling modes become critical.

The buckling analysis was performed without initial deformations. Pre-cambering was not included to the modeling procedure. It was proven in the previous section that creep is an important factor when designing with FRP. In reality the buckling at the end of the lifetime of

the ecoducts will have initial, creep dependent, deformations that must be taken into account when analyzing the buckling behavior. This has not been done in this analysis.

The cross sections with the longer vertical element (a) of the stiffening part (concepts G16, G17) showed worse performance compared to the solutions with the element length of 100 mm and buckled earlier. This may again depend on an internal moment (Figure 59) in the stiffener where the longer vertical part gives an increased initial deformation.

Combined results

The static and buckling analysis of the geometries G8 or G9 showed the most material efficient designs. Taking the lateral deformations into account, design G8 performs better.

7 Discussion

The various stages of each sub-study have been discussed extensively in Sections 4.1.3, 5.2 and 6.6. One of the major challenges in this thesis was the width of the investigation. It ranged from defining a case and context relevant for ecoducts to the preliminary designs evaluation and the definition of the final design solution with the sectional optimization.

Each of those three subjects could have been one thesis. Therefore, it was, of course, necessary to consider each part of the study, however, limiting the investigation in the point when the sufficient knowledge was gained for an efficient design of an ecoduct.

Fauna and infrastructure was treated on a national level. The statistics showed quite clearly which kind of roads were problematic in connection with habitat fragmentation. It was also quite clear what the minimum requirements are on the widths of those roads. There are, however, no guarantees that roads keep to the minimum width. Additionally, there may be an interest in adding more lanes to some roads in future. In the case used here, there is a margin of 3 to 5 meters. This is enough to compensate for smaller increases in road width, but not enough to add a whole lane.

Theoretical requirements and limits do not always confirm with the reality. Not a single real example of an ecoduct was analyzed in this thesis. This is also a weakness in connection with the vegetation design.

For ecoducts more than for any other bridges, it is impossible to really define a typical case. The precise design of the soil and vegetation will always depend largely on local vegetation and terrain.

Preliminary design

The main focus of the preliminary design was on the production method and the deflection limits. Major assumptions were made for both areas of investigation. It was not possible to define exact layout of the FRP laminate or size limits. Each producer has different limits and possibilities and again not a single existing manufacturing proposal regarding the FRP lamina components, number and direction of plies was investigated in depth. The deformation largely depends on the creep behavior, which in turns depends on the exact design of the laminate. Here, the major generalizations were made.

Final design

The final design was approached as an optimization problem for the exact geometry of the cross-section. A material was designed taking up the stresses generated. Two major issues, creep and buckling, were investigated. How creep, developed with time, can affect the buckling behavior of the developed sections was, however, not investigated. There also remains a large number of details, such as connections, that need to be investigated.

One issue that was discovered was the shear stresses, especially for creep rupture. The results remained inconclusive there.

General

In general, the investigation into the design of ecoducts from FRP was successful. A promising design was developed and proved to be functioning up to a certain point. There remain several details that must be addressed: some of them are the shear strength in quasi permanent load combination, connections and fire resistance.

8 Conclusion

An ecoduct design made of fibre reinforced polymer composite material was developed. Several preliminary designs were developed and studied in order to determine the best possible solution for the structural system and sectional geometry.

The bearing deck structural system was chosen for the final design decision. The webs were modeled with the stiffened geometries of a various sizes. The final design was analyzed with a finite element analyses to investigate the buckling behavior of the proposed deck section.

The following conclusions were made based on the study performed:

Fauna and infrastructure

Highways, motorways and railways are the largest barriers in Sweden. The permeability for railways is less well defined than for roads. The bridge span over railways is not as clearly defined and constant as for roads.

In order to ensure a comfortable crossing of the road for animals, landscaping on ecoducts is of great importance. The requirements on vegetation were studied and the case-study was defined with regard to the needs of animals. Generally, the whole ecoduct need vegetation but trees only have a function of screening at the edges of the ecoduct.

Preliminary design

Initial design considered the existing manufacturing possibilities for FRP composite production. These include:

Layup. The possibilities for exact arrangement of the fibres in different production methods governs the material properties of the finished product.

Thickness and size. The thickness and size of individual components are often limiting in design.

The designs were developed with regard to joining technique which should be used to connect structural members. The use of adhesive joints must be considered especially carefully since they must be done in a workshop.

Final design

Production possibilities limit the material. These limits regard both the properties and the dimensions of the sections. Deflection criteria are generally more critical than stress related criteria. This is true for all stress criteria's except the shear stresses in quasi permanent load combination. The shear stresses in quasi permanent load combination are critical. This result could be skewed by the analyzing method which is not very accurate for shear stresses near the support.

The design was developed such as the proposed geometry of the ecoduct section is not complex and the section can be produced with existing manufacturing technologies for FRP production.

The designed ecoduct can be assembled from parts on site. Several solutions are proposed.

It was concluded that buckling is governing in cases of very slender crossections. The section height of 1.5 m was recognized the most efficient from the point of view of bearing capacity, production possibilities and material use.

Stiffeners analyzed in the final design are most effective with a medium inclination of 30 to 45° and of the small size.

General

It is possible to construct ecoducts made of FRP. This can be done with the production methods available nowadays. The size of such cross-sections is reasonable both from the point of view of manufacturing of sections, as well as transport and assembling of the bridge.

In the design of material effective cross-sections, creep deformations and buckling are critical. Small differences in geometry can change the buckling behavior.

Of the designs investigated in this thesis, design nr. G8 in Table 34 is the most material effective.

References

- Älg - Svenska Jägareförbundet. (2019). Retrieved March 1, 2019, from <https://jagareforbundet.se/vilt/vilt-vetande2/artpresentation/daggdjur/alg/>
- Berardi, U., & Dembsey, N. (2015). Thermal and Fire Characteristics of FRP Composites for Architectural Applications, (November), 2276–2289. <https://doi.org/10.3390/polym7111513>
- Berardi, V. P., Perrella, M., Feo, L., & Cricri, G. (2017). Creep behavior of GFRP laminates and their phases: Experimental investigation and analytical modeling. *Composites Part B: Engineering*, 122, 136–144. <https://doi.org/10.1016/j.compositesb.2017.04.015>
- Bhagwat, P. M., Ramachandran, M., & Raichurkar, P. (2017). Mechanical Properties of Hybrid Glass/Carbon Fibre Reinforced Epoxy Composites. *Materials Today: Proceedings*, 4(8), 7375–7380. <https://doi.org/10.1016/j.matpr.2017.07.067>
- Bhatt, P., & Goe, A. (2017). Carbon Fibres: Production, Properties and Potential Use. *Material Science Research India*, 14(1), 52–57. <https://doi.org/10.13005/msri/140109>
- Calluna AB. (2012). *Effektiv utformning av ekodukter och faunabroar*. Trafikverket.
- Carattere, C. (2017). *Prospect for New Guidance in the Design of FRP Structures CONTENTS PART I: POLICY FRAMEWORK I PURPOSE, JUSTIFICATION AND BENEFITS. 9 EXAMPLES OF COMPOSITE STRUTURES IN.*
- Domone, P., & Illsthor, J. (Eds.). (2010). *Construction materials - Their nature and behavior*. (4th ed.).
- Farooq, M., & Banthia, N. (2018a). An innovative FRP fibre for concrete reinforcement: Production of fibre, micromechanics, and durability. *Construction and Building Materials*, 172, 406–421. <https://doi.org/10.1016/j.conbuildmat.2018.03.198>
- Farooq, M., & Banthia, N. (2018b). An innovative FRP fibre for concrete reinforcement: Production of fibre, micromechanics, and durability. *Construction and Building Materials*, 172, 406–421. <https://doi.org/10.1016/j.conbuildmat.2018.03.198>
- Feih, S., & Mouritz, A. P. (2012). Tensile properties of carbon fibres and carbon fibre-polymer composites in fire. *Composites Part A: Applied Science and Manufacturing*, 43(5), 765–772. <https://doi.org/10.1016/j.compositesa.2011.06.016>
- Friberg, E., & Olsson, J. (2014). *Application of fibre reinforced polymer materials in road bridges – General requirements and design considerations*. Chalmers University of Technology.
- Georgii, B., Keller, V., Pfister, H. P., Reck, H., Peters-osten-, E., Henneberg, M., ... Bach, L. (2011). Use of wildlife passages by invertebrate and vertebrate species.
- Glaskova-Kuzmina, T., Aniskevich, A., Martone, A., Giordano, M., & Zarrelli, M. (2016). Effect of moisture on elastic and viscoelastic properties of epoxy and epoxy-based carbon fibre reinforced plastic filled with multiwall carbon nanotubes. *Composites Part A: Applied Science and Manufacturing*, 90, 522–527. <https://doi.org/10.1016/j.compositesa.2016.08.026>

- Jesthi, D. K., Mandal, P., Rout, A. K., & Nayak, R. K. (2018). Effect of carbon/glass fibre symmetric inter-ply sequence on mechanical properties of polymer matrix composites. *Procedia Manufacturing*, 20, 530–535. <https://doi.org/10.1016/j.promfg.2018.02.079>
- Jondelius, E. (2011). *Faunaövergångar i Sverige och Norge*.
- Keck, S., & Fulland, M. (2019). Effect of fibre volume fraction and fibre direction on crack paths in unidirectional flax fibre-reinforced epoxy composites under static loading. *Theoretical and Applied Fracture Mechanics*. <https://doi.org/10.1016/j.tafmec.2019.01.028>
- Kodur, V. R., Bisby, L. A., Green, M., & Chowdhury, E. U. (2005). Fire Performance of FRP Systems for Infrastructure : A State-of-the-Art Report. *Publications Du CNRC (NPARC)*. *Fire and Materials*, 24(1)(May 2014), pp.9-16. <https://doi.org/10.4224/20377587>
- Mara, V., Haghani, R., & Harryson, P. (2014). Bridge decks of fibre reinforced polymer (FRP): A sustainable solution. *Construction and Building Materials*, 50, 190–199. <https://doi.org/10.1016/j.conbuildmat.2013.09.036>
- Naqvi, S. R., Prabhakara, H. M., Bramer, E. A., Dierkes, W., Akkerman, R., & Brem, G. (2018). A critical review on recycling of end-of-life carbon fibre/glass fibre reinforced composites waste using pyrolysis towards a circular economy. *Resources, Conservation and Recycling*, 136(November 2017), 118–129. <https://doi.org/10.1016/j.resconrec.2018.04.013>
- Nationella Viltolycksrådet. (2017). Viltolyckor de senaste 5 åren. Retrieved February 6, 2019, from <https://www.viltolycka.se/statistik/viltolyckor-de-senaste-5-aren/>
- Safe Road Birsta. (2019). Broräcken | Saferoad Birsta AB. Retrieved February 18, 2019, from <https://www.saferoadbirsta.se/produkter/racken/broracken/>
- Safe Road Traffic. (2019). Begreppsterminologi för vägutrustning som vägräcken, krockdämpare, förankringar. Retrieved February 18, 2019, from www.saferoadtraffic.se
- Sandahl, V., & Hällerstål, E. (2018). *Design of an FRP Eco-bridge*. Chalmers University of Technology.
- Seiler, A., & Folkesson, L. (2003). *Habitat fragmentation due to transportation infrastructure. VTI, the Swedish National Road and Transport ...*. Retrieved from <http://scholar.google.com/scholar?hl=en&btnG=Search&q=intitle:Habitat+Fragmentation+due+to+Transport+Infrastructure#7>
- Seiler, Andreas. (2004). Trends and spatial patterns in ungulate-vehicle collisions in Sweden. *Wildlife Biology*, 10(1), 301–313. <https://doi.org/10.2981/wlb.2004.036>
- Seiler, Andreas, Olsson, M., & Lindqvist, M. (2015). *Analys av infrastrukturens permeabilitet för klövdjur*. Retrieved from: <http://trickol.se/bristanalys/>
- Seyyed Monfared Zanjani, J., Al-Nadhari, A. S., & Yildiz, M. (2018). Manufacturing of electroactive morphing carbon fibre/glass fibre/epoxy composite: Process and structural monitoring by FBG sensors. *Thin-Walled Structures*, 130(July), 458–466. <https://doi.org/10.1016/j.tws.2018.05.015>

- SLU. (2019). Retrieved February 20, 2019, from <https://www.slu.se/miljoanalys/statistik-och-miljodata/miljodata/webbtjanster-miljoanalys/markinfo/markinfo/markkemi/ph/>
- Sonnenschein, R., Gajdosova, K., & Holly, I. (2016). FRP Composites and Their Using in the Construction of Bridges. *Procedia Engineering*, 161, 477–482.
<https://doi.org/10.1016/j.proeng.2016.08.665>
- Strongwell. (2019). *EXTREN DWB ® DESIGN GUIDE*. Retrieved from <https://www.strongwell.com/wp-content/uploads/2013/03/EXTREN-DWB-Design-Guide.pdf>
- The European structural polymeric composites group. (1996). *Structural Design of Polymer Composites, EUROCOMP Design Code and Hnadbook*. (J. L. Clarke, Ed.). Taylor & Francis e-Library.
- Trafikverket. (2011). *Trafikverkets tekniska krav för geokonstruktioner - TK Geo 11*.
- Trafikverket. Vägars och gators utformning (2015). Retrieved from https://trafikverket.ineko.se/Files/sv-SE/12046/RelatedFiles/2015_086_krav_for_vagars_och_gators_utformning.pdf
- Trafikverket. (2016). Riktlinje Landskap 20160205 signerad.pdf.
- Trafikverket. (2018). E6, Faunapassager vid Sandsjöbackaområdet, Mölndal–Kungsbacka - Trafikverket. Retrieved April 17, 2019, from <https://www.trafikverket.se/naradig/projekt-i-flera-lan/e6-faunapassager-vid-sandsjobackaområdet-molndalkungsbacka/>
- Vägverket, & Banverket. (2005). *Vilda djur och infrastruktur - en handbok för åtgärder*. Retrieved from <http://www.lansstyrelsen.se/stockholm/SiteCollectionDocuments/Sv/miljo-och-klimat/tillstandet-i-miljon/Sjoar-och-vattendrag/Vilda-djur-och-infrastruktur.pdf>
- Villkor - Trafikverket. (2019). Retrieved May 29, 2019, from <https://www.trafikverket.se/for-dig-i-branschen/vag/Transportdispens/Villkor/>
- Viltolyckor mot ny rekordnivå - Nyheter (Ekot) | Sveriges Radio. (2016). Retrieved May 22, 2019, from <https://sverigesradio.se/sida/artikel.aspx?programid=83&artikel=6576712>
- Wan, B. (2014). *Using fibre-reinforced polymer (FRP) composites in bridge construction and monitoring their performance: an overview. Advanced Composites in Bridge Construction and Repair*. Woodhead Publishing Limited.
<https://doi.org/10.1533/9780857097019.1.3>
- Wenkai, Q. (2015). Analytical method of dynamic properties of FRP based on micromechanical level. *Chinese Journal of Aeronautics*, 28(3), 939–945.
<https://doi.org/10.1016/j.cja.2015.03.008>
- Yang, Z., Wang, H., Ma, X., Shang, F., Ma, Y., Shao, Z., & Hou, D. (2018). Flexural creep tests and long-term mechanical behavior of fibre-reinforced polymeric composite tubes. *Composite Structures*, 193(September 2017), 154–164.
<https://doi.org/10.1016/j.compstruct.2018.03.083>
- Zhang, X., Li, S., Hu, H., Cao, D., Zhong, Y., & Cheng, M. (2018). Hygrothermal durability

of glass and carbon fibre reinforced composites – A comparative study. *Composite Structures*, 211(November 2018), 134–143.
<https://doi.org/10.1016/j.compstruct.2018.12.034>

Zoghi, M. (2014). *FRP Composites in Structures. Assessment* (Vol. 6012).
<https://doi.org/10.1111/j.1574-6941.2007.00310.x>

Appendix A – Interview questions

Interview questions for P. Björkman:

At which kind of roads is the biggest interest in conducts?

Is there a typical surrounding or terrain that is of special interest?

Is there also an interest in Fauna-bridges?

Is there a strategic plan for ecoducts in Sweden?

How does that interest look in terms of:

- Dimensions
- Shapes, connection to surrounding?
- Vegetation

Which features should be taken into account: How can this list be completed?

- Width
- Length
- Screening against noise and light
- Vegetation around and on bridge, also including hiding spaces like stones.
- Topography, do you have any concrete approaches for design here?
- Sightlines
- Disturbance of traffic during construction

About existing projects:

Is there any follow-up on existing projects? What has worked out as intended and what not?

- In construction
- In service

Appendix B – Permeability of Swedish barriers

Permeability of Swedish roads and railways

Vägtyp	barriär (km)	% av totalt	ej barriär (km)	total längd (km)
Europaväg	5 393	70,5%	2 253	7 646
Riksväg	4 412	47,4%	4 895	9 307
Prim. länsväg	1 845	16,6%	9 250	11 095
Sek. länsväg	1 114	1,5%	70 994	72 109
Tert. länsväg	-	0,0%	343	343
Okänt vägtyp	37	8,6%	391	428
Summa	12 801	12,7%	88 127	100 928

Järnväg	barriär (km)	% av totalt	ej barriär (km)	total längd (km)
Arländabanan	23	100,0%	-	23
Bergslagsbanan	415	100,0%	-	415
Botniabanan	182	100,0%	-	182
Citytunneln	7	100,0%	-	7
Godsstråket i Bergslagen	309	100,0%	-	309
Grödingebanan	31	100,0%	-	31
Jönköpingsbanan	112	100,0%	-	112
Malmbanan	426	100,0%	-	426
Mälarmbanan	221	100,0%	-	221
Norra stambanan	336	100,0%	-	336
Nynäsbanan	55	100,0%	-	55
Ostkustbanan	394	100,0%	-	394
Svealandsbanan	114	100,0%	-	114
Södertäljebanan	2	100,0%	-	2
Södra stambanan	592	100,0%	-	592
Umeå-Holmsund	11	100,0%	-	11
Västkustbanan	294	100,0%	-	294
Västra stambanan	465	100,0%	-	465
Öresundsbanan	29	100,0%	-	29
Stambanan i övre Norrland	660	94,9%	35	695
Skånebanan	106	90,1%	12	118
Norge/Vänernbanan	229	77,2%	68	297
Ådalsbanan	154	76,7%	47	201
Sala-Oxelösund	101	66,3%	51	153
Värmlandsbanan	120	59,2%	83	202
Ystadbanan	55	54,9%	45	101
Haparandabanan	139	54,5%	116	254
Övriga järnvägar	293	5,4%	5 157	5 450
Summa	5 874	51,1%	5 614	11 488

Appendix C – Barriers effects

Barrier effects

Source: (A Seiler & Folkesson, 2003)

Table 5-11 - Barrier effects by infrastructure element and animal species.

Infrastructure type/ Infrastructure element	Species affected	Effect on species	Source
<i>All infrastructure</i>			
Infrastructure verge (short grassy habitat with high disturbance levels)	Carabids (ground beetles)	Complete barrier to movement perceived several metres from the edge of the infrastructure	NL-SoA, 5.3.4; Mader, 1984; F-SoA, 5.4.5
Traffic	All species	Mortality due to direct hits and turbulence effects for flying species	F-SoA, 5.4.5
	Amphibians and reptiles	Absolute barrier	Vos, 1997
Roads and railways	Reindeer	Strong barrier effect results in isolation of a reindeer population in a previous summer grazing ground (Snohetta) resulting in lower weight and reduced breeding success of isolated population	N-SoA, 5.4.5
Roads and railways	Epizoid (mammal), synzoic (ant) and ballistic (self) dispersed plant species	Strong barrier effect	Salvig <i>et al.</i> 1997
Major transport links	Wolf and bear	Eastward expansion and recolonisation from Sweden restricted by barrier effect	N-SoA, 5.4.5
<i>Roads</i>			
Concrete drainage ditch	Carabids	Presents a complete barrier at 50cm depth	F-SoA, 5.4.5
Fencing	Wolf	Fenced motorway not important barrier to crossing	Blanco and Cortes, 1999
Part-fenced road	Butterfly	Partial barrier due to the difficulty of manoeuvring in flight	F-SoA, 5.4.5
	Large mammals (Moose, reindeer)	Insignificant effect on populations	S-SoA, 5.4.3
Fenced major road with underpasses			
Fenced major roads	Moose	Barrier effect leading to overgrazing as animals trapped in winter grazing area.	N-SoA, 5.4.5
	Lynx	Dispersal barrier likely to hinder spread of reintroduced populations	CH-SoA, 5.4.5
Road surface	Butterfly (and some other flying species)	Complete heat barrier due to microclimatic effects	Berthoud, 1968
Major road	Mice	Complete barrier	Van der Reest, 1989
Railways			
Railway*	Grasshopper, ground beetles	Absolute barrier	Bergers, 1997 (Cont'd...)

Infrastructure type/ Infrastructure element	Species affected	Effect on species	Source
			(...Cont'd)
	Mice, newts, spiders, ants	Strong barrier	Bergers 1997
	Marten, hedgehog, squirrel, reptiles, frogs, toads, butterflies	Weak	Bergers 1997
	Deer, wild boar, hare, birds	No barrier effect	Bergers 1997
<i>Waterways</i>			
Infrastructure crossing river valleys	kingfisher, dipper, grey wagtail	Risk barrier	Salvig <i>et al.</i> , 1997
River crossings	Fish species	Effects range from complete barrier (dam) to minor effect (pollution, or shaded and altered habitat under bridges)	B-SoA, 5.4.5
Culverts	aquatic fauna	Semi-permeable barrier	Kemper, 1998

Source: National State of the Art reports

* Information not based on field research

Appendix D – Road width

Road width VR110/120 according to VGU, Trafikverket:

A railing along the road is assumed

Railings: 0,5 m

Verge: 2 m

Lane 1: 3,5 m

Lane 2: 3,5 m

Mid-verge: 1 m

Mid: 5 m*

Mid-verge: 1 m

Lane 2: 3,5 m

Lane 1: 3,5 m

Verge: 2 m

Railings: 0,5 m

Total: 26,0 (Trafikverket, 2015)

Which gives the distance between the railings.

The working capacity of the railing is added The capacity H2 is assumed which gives a working width W3 of 1 m (Safe Road Birsta, n.d.; Safe Road Traffic, n.d.).

$$*2 \times 1 \text{ (working width for railing)} + 3 \text{ m for midsupport} = 5 \text{ m}$$

$$\text{Slope : } 2 \times \text{freeheight} = 2 \times \frac{2}{3} \times 5,1 = 6,8$$

The slope goes up to 2/3 of the free height of the bridge.

This makes the total width of an ecoduct to 40,6 m.

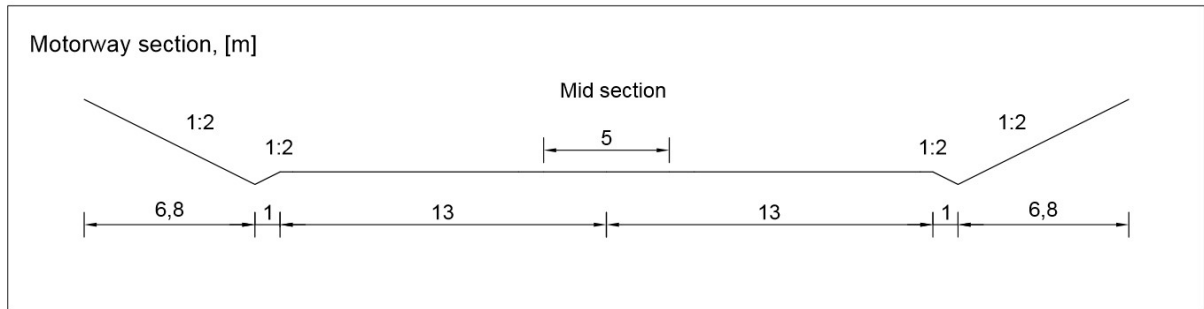


Figure 60. Section of typical motorway in Sweden.

Road width VR110/100 according to VGU, Trafikverket:

2+1 lanes.

Railing along the road are assumed

Railings: 0,5 m

Lane + verge: 5,1 m

Mid: 0,5 m (assumed, total width of railing)

Mid-verge: 0,3 m

Lane 2: 3,5 m

Lane 1: 3,5 m

Verge: 0,2 m

Railings: 0,5 m

Total: 14,1 m (Trafikverket, 2015)

The working capacity of the railing is added. The capacity H2 is assumed which gives a working width W3 of 1 m (Safe Road Birsta, n.d.; Safe Road Traffic, n.d.)

$$\text{Slope} : 2 \times \text{freeheight} = 2 \times \frac{2}{3} \times 5,1 = 6,8$$

The slope goes up to 2/3 of the free height of the bridge.

This makes the total width to 29,7 m.

Appendix E – Load combination

Table 43. Calculation of loads and load combinations for different load cases.

			Permanent			Variable			Midspan		Edge	
		Load	Self weigth	Soil load	Soil (edge)	Live load (Load for pedestrian bridge)	Snow load	Service vehicle*	Ved	Med	Ved	Med
	Governing load:	kN/m ²	2	12	30	3,71	2,51	120	kN/m ²	kN* m	kN/m ²	kN* m
		Q.P.	2	12	30	0	0,502	0				
		Fr	2	12	30	1,48 4	0,502	0				
Qk	Live	SLS	2	12	30	3,71	2,008	0				
Qk	Snow	SLS	2	12	30	1,48 4	2,51	0				
Qk	Vehicle	SLS	2	12	30	1,48 4	2,008	120				
1)	Vehicle	SLS	2	12	30	1,48 4	2,008	120				
2)	Vehicle	SLS	2	12	30	1,48 4	2,008	120				
Qk	Vehicle	ULS	2,7	16,2	40,5							
1)	Vehicle	ULS	2,7	16,2	40,5							
2)	Vehicle	ULS	2,7	16,2	40,5							

Basic geometry

$L := 20 \text{ m}$	Structural span
$W := 40 \text{ m}$	Structural width
$W_{edge} := 5 \text{ m}$	Width of edge section
$I_y(b, h) := \frac{b \cdot h^3}{12}$	$I_r(b, h, r) := b \cdot h \cdot r^2$
$d_{pre} := 0 \text{ mm}$	eventual precambering

Load

$q_{fk} := 2 \frac{\text{kN}}{\text{m}^2} + \frac{120 \frac{\text{kN}}{\text{m}}}{2 \cdot L + 30 \text{ m}} = 3.714 \frac{\text{kN}}{\text{m}^2}$	Variable load
$s := 2.5 \frac{\text{kN}}{\text{m}^2}$	Snowload
$Q_{s.v.1k} := 80 \text{ kN} \cdot \frac{1 \text{ m}}{1.3 \text{ m}}$	Service vehicle
$Q_{s.v.2k} := 40 \text{ kN} \cdot \frac{1 \text{ m}}{1.3 \text{ m}}$	
$q_{soil} := 12 \frac{\text{kN}}{\text{m}^2}$	Soil load in main part of bridge
$q_{soil.edge} := 30 \frac{\text{kN}}{\text{m}^2}$	Soil load in edge section of bridge
$g_k := 7 \frac{\text{kN}}{\text{m}^2}$	Selfweight

Deflection limits

$$\delta_{max} := \frac{L}{250} = 80 \text{ mm} \quad \delta_2 := \frac{L}{300} = 66.667 \text{ mm}$$

Taken from EUROCOMP Table 4.2, General public flooring.
 delta_max: "The sagging in the final state relative to the straight line joining the (supports?)".
 delta_2: "The variation of the deflection of the beam due to the variable loading plus any time dependent deformations due to permanent load".

Variable load:	$\psi_{0f} := 0.4$	$\psi_{1f} := 0.4$	$\psi_{2f} := 0$	SS-EN 1990 (sv) A2:2 p. 63 transportstyrelsen: TSFS 2018:57
Service vehicle:	$\psi_{0fw} := 0$	$\psi_{1fw} := 0$	$\psi_{2fw} := 0$	
Snow load:	$\psi_{0s} := 0.8$	$\psi_{1s} := 0.6$	$\psi_{2s} := 0.2$	
ULS	$\gamma_G := 1.35$	$\gamma_{Qf} := 1.35$	$\gamma_Q := 1.5$	

ULS load combinations SS-EN 1990 table A2:4(B)

$q_{uls.1} := \gamma_G \cdot g_k + \gamma_G \cdot q_{soil} + \gamma_{Qf} \cdot q_{fk} + \gamma_Q \cdot \psi_{0s} \cdot s = 33.664 \frac{kN}{m^2}$	no service vehicle var. load main load
$q_{uls.2} := \gamma_G \cdot g_k + \gamma_G \cdot q_{soil} + \gamma_{Qf} \cdot \psi_{0f} \cdot q_{fk} + \gamma_Q \cdot s = 31.406 \frac{kN}{m^2}$	no service vehicle snow load main load
$q_{uls.3} := \gamma_G \cdot g_k + \gamma_G \cdot q_{soil} + \gamma_{Qf} \cdot \psi_{0f} \cdot q_{fk} + \gamma_Q \cdot \psi_{0s} \cdot s = 30.656 \frac{kN}{m^2}$	service vehicle main load
Service vehicle $Q_{s.v.1} := \gamma_{Qf} \cdot Q_{s.v.1k} = 83.077 \text{ kN}$	Addition to uls load combination (b.3)
$Q_{s.v.2} := \gamma_{Qf} \cdot Q_{s.v.2k} = 41.538 \text{ kN}$	
$q_{uls} := q_{uls.3} = 30.656 \frac{kN}{m^2}$	Se in section "Longitudinalt load actions" below

SLS load combinations + Load for edge section

Middle section Characteristic combination SS-EN 1990 table A2:6	
$q_{char1} := g_k + q_{soil} + q_{fk} + \psi_{0s} \cdot s = 24.714 \frac{kN}{m^2}$	variable load main load, no service vehicle
$q_{char2} := g_k + q_{soil} + s + \psi_{0f} \cdot q_{fk} = 22.986 \frac{kN}{m^2}$	snow load main load, no service vehicle
$q_{char3} := g_k + q_{soil} + \psi_{0f} \cdot q_{fk} + \psi_{0s} \cdot s = 22.486 \frac{kN}{m^2}$	Service vehicle main load
$q_{char} := q_{char3} = 22.486 \frac{kN}{m^2}$	Se in section "Longitudinalt load actions" below

Created with PTC Mathcad Express. See www.mathcad.com for more information.

Quasi permanent combination
SS-EN 1990 table A2:6

$$q_{qp} := g_k + q_{soil} + \psi_{2f} \cdot q_{fk} + \psi_{2s} \cdot s = 19.5 \frac{kN}{m^2} \quad \text{no service vehicle}$$

Edge section

$$q_{uls.a.edge} := \gamma_G \cdot g_k + \gamma_G \cdot q_{soil.edge} + \gamma_{Qf} \cdot \psi_{0f} \cdot q_{fk} + \gamma_Q \cdot \psi_{0s} \cdot s = 54.956 \frac{kN}{m^2}$$

$$q_{uls.b.edge} := \gamma_G \cdot g_k + \gamma_G \cdot q_{soil.edge} + \gamma_{Qf} \cdot q_{fk} + \gamma_Q \cdot \psi_{0s} \cdot s = 57.964 \frac{kN}{m^2} \quad \text{var. load main load}$$

$$q_{uls.edge} := q_{uls.a.edge} = 54.956 \frac{kN}{m^2}$$

$$q_{char.edge} := g_k + q_{soil.edge} + q_{fk} + \psi_{0s} \cdot s = 42.714 \frac{kN}{m^2}$$

$$q_{qp.edge} := g_k + q_{soil.edge} + \psi_{2f} \cdot q_{fk} + \psi_{2s} \cdot s = 37.5 \frac{kN}{m^2}$$

Longitudinal load actions

Moments for middle of span (maximum moments)

Calculation are per meter cross section

$$M(q) := \frac{q \cdot 1 \cdot m \cdot L^2}{8}$$

Bending moment for 1 m wide section.

$$M_{edge}(q) := \frac{q \cdot 1 \cdot m \cdot L^2}{8}$$

Bending moment for 1m wide edge section.

$$M_p(Q, x) := Q \cdot \frac{x}{2}$$

Momen in middle from point load at distance x from support, xmax=L/2

$$x_1 := 10 \text{ m} \quad x_2 := 7 \text{ m}$$

Characteristic load combination

$$M_{s.v.char1} := (M_p(Q_{s.v.1k}, x_2) + M_p(Q_{s.v.2k}, x_1)) = 0.369 \text{ MN} \cdot \text{m}$$

$$M_{s.v.char2} := (M_p(Q_{s.v.1k}, x_1) + M_p(Q_{s.v.2k}, x_2)) = 0.415 \text{ MN} \cdot \text{m}$$

$$M_{s.v.char} := M_{s.v.char2} = 0.415 \text{ MN} \cdot \text{m}$$

Q2 at 7m, Q1 at 10 m

Contribution to moment from service vehicle char. / uls load combination.

$$M_{char1} := M(q_{char1}) = 1.236 \text{ MN} \cdot \text{m}$$

Variable load main load

$$M_{char3} := M(q_{char3}) + M_{s.v.char} = 1.54 \text{ MN} \cdot \text{m}$$

Service vehicle main load

$$M_{char} := M_{char3} = 1.54 \text{ MN} \cdot \text{m}$$

Created with PTC Mathcad Express. See www.mathcad.com for more information.

Quasi permanent load combination

$$M_{qp} := M(q_{qp}) = 0.975 \text{ MN} \cdot \text{m}$$

ULS load combination

$$M_{s.v.uls} := M_p(Q_{s.v.1}, x_1) + M_p(Q_{s.v.2}, x_2) = 0.561 \text{ MN} \cdot \text{m}$$

$$M_{uls.1} := M(q_{uls.1}) = 1.683 \text{ MN} \cdot \text{m}$$

Variable load main load

$$M_{uls.3} := M(q_{uls.3}) + M_{s.v.uls} = 2.094 \text{ MN} \cdot \text{m}$$

Service vehicle main load

$$M_{uls} := M_{uls.3} = 2.094 \text{ MN} \cdot \text{m}$$

Edge section

$$M_{uls.edge} := M_{edge}(q_{uls.edge}) = 2.748 \text{ MN} \cdot \text{m}$$

$$M_{char.edge} := M_{edge}(q_{char.edge}) = 2.136 \text{ MN} \cdot \text{m}$$

$$M_{qp.edge} := M_{edge}(q_{qp.edge}) = 1.875 \text{ MN} \cdot \text{m}$$

Shear force at support

$$V(q) := \frac{q \cdot 1 \text{ m} \cdot L}{2}$$

Shear force, at support, from distributed load

$$V_p(Q, x) := Q \cdot \frac{L - x}{L}$$

Shear force from point load at distance x [m] from support.
xmax=l/2

$$V_{s.v.uls1} := (V_p(Q_{s.v.1}, x_1) + V_p(Q_{s.v.2}, x_2)) \cdot \frac{1 \text{ m}}{1.3 \text{ m}} = 52.722 \text{ kN}$$

$$V_{s.v.uls2} := (V_p(Q_{s.v.1}, x_2) + V_p(Q_{s.v.2}, x_1)) \cdot \frac{1 \text{ m}}{1.3 \text{ m}} = 57.515 \text{ kN}$$

Q1 at 7m, Q2 at 10 m

$$V_{s.v.uls} := V_{s.v.uls2}$$

Contribution to shear from service vehicle

$$V_{s.v.char} := V_p(Q_{s.v.1k}, x_2) + V_p(Q_{s.v.2k}, x_1) = 55.385 \text{ kN}$$

$$V_{uls.1} := V(q_{uls.1}) = 336.643 \text{ kN}$$

$$V_{uls.3} := V(q_{uls.3}) + V_{s.v.uls} = 364.072 \text{ kN}$$

$$V_{uls} := V_{uls.3} = 364.072 \text{ kN}$$

$$V_{char1} := V(q_{char1}) = 247.143 \text{ kN}$$

Variable load main load

$$V_{char3} := V(q_{char3}) + V_{s.v.char} = 280.242 \text{ kN}$$

Service vehicle main load

$$V_{char} := V_{char3} = 280.242 \text{ kN}$$

$$V_{qp} := V(q_{qp}) = 195 \text{ kN}$$

Created with PTC Mathcad Express. See www.mathcad.com for more information.

Edge section

$$V_{uls.edge} := V(q_{uls.edge}) = 549.557 \text{ kN}$$

$$V_{char.edge} := V(q_{char.edge}) = 427.143 \text{ kN}$$

$$V_{qp.edge} := V(q_{qp.edge}) = 375 \text{ kN}$$

Appendix F – Preliminary design

Only design 9 (final design choice) is presented.

Preliminary design - Design 9

Basic geometry

$L := 20 \text{ m}$	Structural span
$W := 40 \text{ m}$	Structural width
$W_{edge} := 5 \text{ m}$	Width of edge section
$I_y(b, h) := \frac{b \cdot h^3}{12}$	$I_r(b, h, r) := b \cdot h \cdot r^2$

Load

$q_{fk} := 2 \frac{kN}{m^2} + \frac{120 \frac{kN}{m}}{2 \cdot L + 30 \text{ m}} = 3.714 \frac{kN}{m^2}$	traffic load
$s := 2.5 \frac{kN}{m^2}$	Snowload
$Q_{s.v.1k} := 80 \text{ kN} \cdot \frac{1 \text{ m}}{1.3 \text{ m}}$	Service vehicle
$Q_{s.v.2k} := 40 \text{ kN} \cdot \frac{1 \text{ m}}{1.3 \text{ m}}$	
$q_{soil} := 12 \frac{kN}{m^2}$	Soil load in main part of bridge
$q_{soil,edge} := 30 \frac{kN}{m^2}$	Soil load in edge section of bridge
$g_k := 5 \frac{kN}{m^2}$	Selfweight

Deflection limits

$$\delta_{max} := \frac{L}{250} = 80 \text{ mm} \quad \delta_2 := \frac{L}{300} = 66.667 \text{ mm}$$

Taken from EUROCOMP Table 4.2, General public flooring.

delta_max: "The sagging in the final state relative to the straight line joining the (supports?)".

delta_2: "The variation of the deflection of the beam due to the variable loading plus any time dependent deformations due to permanent load".

Load combination

Variable load:	$\psi_{0f} := 0.4$	$\psi_{1f} := 0.4$	$\psi_{2f} := 0$
Service vehicle:	$\psi_{0fw} := 0$	$\psi_{1fw} := 0$	$\psi_{2fw} := 0$
Snow load:	$\psi_{0s} := 0.8$	$\psi_{1s} := 0.6$	$\psi_{2s} := 0.2$
ULS	$\gamma_G := 1.35$	$\gamma_{Qf} := 1.35$	$\gamma_Q := 1.5$

$$q_{uls} := \gamma_G \cdot g_k + \gamma_G \cdot q_{soil} + \gamma_{Qf} \cdot \psi_{0f} \cdot q_{fk} + \gamma_Q \cdot \psi_{0s} \cdot s = 27.956 \frac{kN}{m^2} \quad \text{service vehicle main load}$$

Service vehicle

$$Q_{s.v.1} := \gamma_{Qf} \cdot Q_{s.v.1k} = 83.077 \text{ kN} \quad \text{Addition to uls load combination}$$

$$Q_{s.v.2} := \gamma_{Qf} \cdot Q_{s.v.2k} = 41.538 \text{ kN}$$

$$q_{char} := g_k + q_{soil} + \psi_{0f} \cdot q_{fk} + \psi_{0s} \cdot s = 20.486 \frac{kN}{m^2} \quad \text{Service vehicle main load, characteristic value}$$

$$q_{fr} := g_k + q_{soil} + \psi_{1f} \cdot q_{fk} + \psi_{2s} \cdot s = 18.986 \frac{kN}{m^2} \quad \text{var. load main load, no service vehicle}$$

$$q_{qp} := g_k + q_{soil} + \psi_{2f} \cdot q_{fk} + \psi_{2s} \cdot s = 17.5 \frac{kN}{m^2} \quad \text{no service vehicle}$$

Edge section

$$q_{uls.edge} := \gamma_G \cdot g_k + \gamma_G \cdot q_{soil.edge} + \gamma_{Qf} \cdot \psi_{0f} \cdot q_{fk} + \gamma_Q \cdot \psi_{0s} \cdot s = 52.256 \frac{kN}{m^2}$$

$$q_{char.edge} := g_k + q_{soil.edge} + q_{fk} + \psi_{0s} \cdot s = 40.714 \frac{kN}{m^2}$$

$$q_{fr.edge} := g_k + q_{soil.edge} + \psi_{1f} \cdot q_{fk} + \psi_{2s} \cdot s = 36.986 \frac{kN}{m^2}$$

$$q_{qp.edge} := g_k + q_{soil.edge} + \psi_{2f} \cdot q_{fk} + \psi_{2s} \cdot s = 35.5 \frac{kN}{m^2}$$

Load actions

$$M_{uls} := 2.094 \text{ MN} \cdot m \quad M_{uls.edge} := 2.748 \text{ MN} \cdot m$$

$$M_{char} := 1.54 \text{ MN} \cdot m \quad M_{char.edge} := 2.136 \text{ MN} \cdot m$$

$$M_{qp} := 0.975 \text{ MN} \cdot m \quad M_{qp.edge} := 1.875 \text{ MN} \cdot m$$

$$V_{uls} := 364.072 \text{ kN} \quad V_{uls} := 549.557 \text{ kN}$$

$$V_{char} := 280.242 \text{ kN} \quad V_{char} := 427.143 \text{ kN}$$

$$V_{qp} := 195 \text{ kN} \quad V_{qp} := 375 \text{ kN}$$

Created with PTC Mathcad Express. See www.mathcad.com for more information.

Material properties

$E_{sls.g} := 35.6 \text{ GPa}$	$E_{sls.c} := 113.2 \text{ GPa}$	$\rho_g := 2022 \frac{\text{kg}}{\text{m}^3}$	$\rho_c := 1574 \frac{\text{kg}}{\text{m}^3}$
$E_{cr.g} := 16.7 \text{ GPa}$	$E_{cr.c} := 53.2 \text{ GPa}$	All material properties for preliminary design taken from "Design of an FRP Eco-bridge" (E. Hallerstal, V Sandahl, 2018)	
$G_{sls.g} := 3.6 \text{ GPa}$	$G_{sls.c} := 4.0 \text{ GPa}$		
$G_{cr.g} := 1.7 \text{ GPa}$	$G_{cr.c} := 1.9 \text{ GPa}$		
$f_{t.g} := 470.664 \text{ MPa}$	$f_{t.c} := 591.011 \text{ MPa}$	Design strength	

Geometry - Glass fibre

Alla calculations are per meter cross section

$$I_y(b, h) := \frac{\overrightarrow{b \cdot h^3}}{12} \quad I_r(b, h, r) := \overrightarrow{b \cdot h \cdot r^3}$$

flange (Sandwich construction)

$$t_f := 20 \text{ mm}$$

$$t_{f.edge} := t_f$$

$$b_f := 1 \text{ m}$$

Web

$$t_w := 15 \text{ mm} \quad t_{w.edge} := 1.3 \cdot t_w = 19.5 \text{ mm}$$

$$h := 1200 \text{ mm}$$

$$a := h - t_f = 1.18 \text{ m}$$

$$b := 180 \text{ mm}$$

$$b_{edge} := 120 \text{ mm}$$

$$c := 70 \text{ mm}$$

$$d := 270 \text{ mm}$$

$$\text{check } d < \frac{a}{2} = 590 \text{ mm}$$

$$e := 90 \text{ mm}$$

$$\text{check } e < d = 270 \text{ mm}$$

$$L_w := a - 2 \cdot d + 2 \cdot e + 4 \cdot \sqrt{c^2 + \left(\frac{d-e}{2}\right)^2} = (1.276 \cdot 10^3) \text{ mm} \quad \text{length along web}$$

$$L_{w.edge} := L_w$$

Created with PTC Mathcad Express. See www.mathcad.com for more information.

$$d_{pre} := 60 \text{ mm} \quad \text{eventual precambering}$$

$$I_f := 2 \cdot I_y(b_f, t_f) + 2 \cdot I_r\left(b_f, t_f, \frac{h}{2}\right) = 0.014 \text{ m}^4$$

$$I_{f.edge} := 2 \cdot I_y(b_f, t_{f.edge}) + 2 \cdot I_r\left(b_f, t_{f.edge}, \frac{h}{2}\right) = 0.014 \text{ m}^4$$

$$t_{we} := t_w \cdot \frac{L_w}{a} = 16.221 \text{ mm} \quad t_{we.edge} := t_{w.edge} \cdot \frac{L_{w.edge}}{a} = 21.088 \text{ mm}$$

Equivalent thickness of web (thickness* L of web/distance between flanges)

$$I_w := \frac{1}{b} \cdot I_y(t_{we}, a) = 0.012 \text{ m}^4$$

$$I_{w.edge} := \frac{1}{b_{edge}} \cdot I_y(t_{we.edge}, a) = 0.024 \text{ m}^4$$

$$A_w := \frac{1}{b} \cdot L_w \cdot t_w = 0.106 \text{ m}^2$$

$$A_{w.edge} := \frac{1}{b_{edge}} \cdot L_{w.edge} \cdot t_{w.edge} = 0.207 \text{ m}^2$$

$$I := I_f + I_w = 0.027 \text{ m}^4$$

$$I_{edge} := I_{f.edge} + I_{w.edge} = (3.846 \cdot 10^{10}) \text{ mm}^4$$

$$A_f := 1 \text{ m} \cdot t_f$$

$$A := A_w + 2 \cdot A_f = 0.146 \text{ m}^2$$

$$A_{edge} := A_{w.edge} + 2 \cdot A_f = 0.247 \text{ m}^2$$

$$g_{k.actual} := \rho_g \cdot A \cdot g = 2.902 \frac{1}{\text{m}} \cdot \text{kN}$$

gk taken as 7 kN/m²

Deflection

$$\delta_M(k_1, F_V, E, I) := k_1 \cdot \frac{F_V \cdot L^3}{E \cdot I}$$

Deflection due to bending, F total load on beam

$$\delta_V(k_2, F, G_{xy}, A, L) := k_2 \cdot \frac{F \cdot L}{A \cdot G_{xy}}$$

Deflection due to shear, F total load on beam

$$k_1 := \frac{5}{384}$$

$$k_2 := \frac{1}{8}$$

EUROCOMP:

F - total vertical load

EI - flexural rigidity

A - Shear area of web

Gxy - in-plane shear modulus of web

$$k_{1p10} := \frac{1}{48}$$

$$k_{2p10} := \frac{1}{4}$$

k1

5/384

1/48

k2

1/8

1/4

uniformly distributed load

point load, 10m

$$k_{1p7} := \frac{7 \text{ m}}{48 \cdot L} \cdot \left(3 - \frac{4 \cdot (7 \text{ m})^2}{L^2} \right) = 0.018$$

long term (quasi permanent load combination)

Middle bridge section

$$\delta_{Mfinal} := \delta_M(k_1, q_{qp} \cdot L \cdot 1 \text{ m}, E_{cr.g}, I) = 81.642 \text{ mm}$$

$$\delta_{Vfinal} := \delta_V(k_2, q_{qp} \cdot L \cdot 1 \text{ m}, G_{cr.g}, A_w, L) = 4.84 \text{ mm}$$

$$\delta_{final} := \delta_{Mfinal} + \delta_{Vfinal} - d_{pre} = 26.483 \text{ mm}$$

Edge section

$$\delta_{Mfinal.edge} := \delta_M(k_1, q_{qp.edge} \cdot L \cdot 1 \text{ m}, E_{cr.g}, I_{edge}) = 115.143 \text{ mm}$$

$$\delta_{Vfinal.edge} := \delta_V(k_2, q_{qp.edge} \cdot L \cdot 1 \text{ m}, G_{cr.g}, A_{w.edge}, L) = 5.035 \text{ mm}$$

$$\delta_{final.edge} := \delta_{Mfinal.edge} + \delta_{Vfinal.edge} - d_{pre} = 60.178 \text{ mm}$$

Short term (short term variable load action + long term part of permanent action)

$$q_{creep} := g_k + q_{soil} = 17 \frac{\text{kN}}{\text{m}^2}$$

$$q_{creep.edge} := g_k + q_{soil.edge} = 35 \frac{\text{kN}}{\text{m}^2}$$

$$q_{inst} := q_{char} - g_k - q_{soil} = 3.486 \frac{\text{kN}}{\text{m}^2}$$

$$q_{inst.edge} := q_{char.edge} - g_k - q_{soil.edge} = 5.714 \frac{\text{kN}}{\text{m}^2}$$

$$\delta_{Minst} := \delta_M(k_1, q_{inst} \cdot L \cdot 1 \text{ m}, E_{sls.g}, I) + \delta_M(k_{1p10}, Q_{s.v.1k}, E_{sls.g}, I) + \delta_M(k_{1p7}, Q_{s.v.2k}, E_{sls.g}, I)$$

$$\delta_{Mcreep} := \delta_M(k_1, q_{creep} \cdot L \cdot 1 \text{ m}, E_{cr.g}, I) - \delta_M(k_1, q_{creep} \cdot L \cdot 1 \text{ m}, E_{sls.g}, I) = 42.105 \text{ mm}$$

$$\delta_{Mshort} := \delta_{Minst} + \delta_{Mcreep} = 65.24 \text{ mm}$$

No k2 for point load at 7 m, k2 for point load at 10 m taken insted

$$\delta_{Vinst} := \delta_V(k_2, q_{inst} \cdot L \cdot 1 \text{ m}, G_{sls.g}, A_w, L) + \delta_V(k_{2p10}, Q_{s.v.1k} + Q_{s.v.2k}, G_{sls.g}, A_w, L)$$

$$\delta_{Vcreep} := \delta_V(k_2, q_{creep} \cdot L \cdot 1 \text{ m}, G_{cr.g}, A_w, L) - \delta_V(k_2, q_{creep} \cdot L \cdot 1 \text{ m}, G_{sls.g}, A_w, L)$$

$$\delta_{Vshort} := \delta_{Vinst} + \delta_{Vcreep} = 4.142 \text{ mm}$$

$$\delta_{short} := \delta_{Mshort} + \delta_{Vshort} = 69.383 \text{ mm}$$

Created with PTC Mathcad Express. See www.mathcad.com for more information.

Edge section

$$\delta_{Minst} := \delta_M(k_1, q_{inst.edge} \cdot L \cdot 1 \text{ m}, E_{sls.g}, I_{edge}) = 8.694 \text{ mm}$$

$$\delta_{Mcreep} := \delta_M(k_1, q_{creep.edge} \cdot L \cdot 1 \text{ m}, E_{cr.g}, I_{edge}) - \delta_M(k_1, q_{creep.edge} \cdot L \cdot 1 \text{ m}, E_{sls.g}, I_{edge})$$

$$\delta_{Mshort.edge} := \delta_{Minst} + \delta_{Mcreep} = 68.963 \text{ mm}$$

$$\delta_{Vinst} := \delta_V(k_2, q_{inst.edge} \cdot L \cdot 1 \text{ m}, G_{sls.g}, A_{w.edge}, L) = 0.383 \text{ mm}$$

$$\delta_{Vcreep} := \delta_V(k_2, q_{creep.edge} \cdot L \cdot 1 \text{ m}, G_{cr.g}, A_{w.edge}, L) - \delta_V(k_2, q_{creep.edge} \cdot L \cdot 1 \text{ m}, G_{sls.g}, A_{w.edge}, L)$$

$$\delta_{Vshort.edge} := \delta_{Vinst} + \delta_{Vcreep} = 3.003 \text{ mm}$$

$$\delta_{short.edge} := \delta_{Mshort.edge} + \delta_{Vshort.edge} = 71.965 \text{ mm}$$

Strength in bending

$$M_{Rd} := \frac{I \cdot f_{t.g}}{(a + 2 \cdot t_f)} = 10.316 \text{ MN} \cdot \text{m}$$

$$M_{Rd.edge} := \frac{I_{edge} \cdot f_{t.g}}{(a + 2 \cdot t_f)} = 14.838 \text{ MN} \cdot \text{m}$$

$$\frac{M_{uls}}{M_{Rd}} = 0.203$$

$$\frac{M_{uls.edge}}{M_{Rd.edge}} = 0.185$$

$$\frac{M_{char}}{M_{Rd}} = 0.149$$

$$\frac{M_{char.edge}}{M_{Rd.edge}} = 0.144$$

$$\frac{M_{qp}}{M_{Rd}} = 0.095$$

$$\frac{M_{qp.edge}}{M_{Rd.edge}} = 0.126$$

Precambering

possible amount of precambering

$$\delta_{Mg.creep} := \delta_M(k_1, q_{creep} \cdot L \cdot 1 \text{ m}, E_{cr.g}, I) = 79.31 \text{ mm}$$

$$\delta_{Vg.creep} := \delta_V(k_2, q_{creep} \cdot L \cdot 1 \text{ m}, G_{cr.g}, A_w, L) = 4.702 \text{ mm}$$

$$\delta_{g.creep} := \delta_{Mg.creep} + \delta_{Vg.creep} = 84.012 \text{ mm}$$

Edge section

Created with PTC Mathcad Express. See www.mathcad.com for more information.

$$\delta_{Mg.creep} := \delta_M(k_1, q_{creep.edge} \cdot L \cdot 1 \text{ m}, E_{cr.g}, I_{edge}) = 113.521 \text{ mm}$$

$$\delta_{Vg.creep} := \delta_V(k_2, q_{creep.edge} \cdot L \cdot 1 \text{ m}, G_{cr.g}, A_{w.edge}, L) = 4.964 \text{ mm}$$

$$\delta_{gcreep.edge} := \delta_{Mg.creep} + \delta_{Vg.creep} = 118.485 \text{ mm}$$

Deflection checks and summarization

Deflection for middle and edge beam, long term (quasi permanent load)

Limit:

$$\delta_{final} = 26.483 \text{ mm}$$

$$\delta_{final.edge} = 60.178 \text{ mm}$$

$$\delta_{max} = 80 \text{ mm}$$

Deflection for middle and edge beam, short term defl. of var. load + long term defl. from creep part of deadweight (quasi permanent load)

Limit:

$$\delta_{short} = 69.383 \text{ mm}$$

$$\delta_{short.edge} = 71.965 \text{ mm}$$

$$\delta_2 = 66.667 \text{ mm}$$

$$h = 1.2 \text{ m}$$

Heigth between flange centres

$$b = 180 \text{ mm}$$

$$b_{edge} = 120 \text{ mm}$$

Spacing between webs

$$t_w = 15 \text{ mm}$$

$$t_{w.edge} = 19.5 \text{ mm}$$

Thickness of web

$$L_w = 1.276 \text{ m}$$

$$A_w = 0.106 \text{ m}^2$$

Length for 1 web and area for 1 m wide web section

$$A_{w.edge} = 0.207 \text{ m}^2$$

$$I = 0.027 \text{ m}^4$$

$$I_{edge} = 0.038 \text{ m}^4$$

Total material use (not equivalent):

$$A_{total} := (A_w + 2 \cdot 1 \text{ m} \cdot t_f) \left(\frac{W - 2 \cdot W_{edge}}{1 \text{ m}} \right) = 4.39 \text{ m}^2$$

$$A_{total.edge} := (A_{w.edge} + 2 \cdot 1 \text{ m} \cdot t_{f.edge}) \cdot \frac{2 \cdot W_{edge}}{1 \text{ m}} = 2.474 \text{ m}^2$$

$$A_{g.total.combined} := A_{total} + A_{total.edge} = 6.864 \text{ m}^2$$

Selfweight

$$g_k := g \cdot \frac{A_w + 2 \cdot t_f \cdot 1 \text{ m}}{1 \text{ m}} \cdot \rho_g = 2.902 \frac{\text{kN}}{\text{m}^2}$$

$$g_{k.edge} := g \cdot \frac{A_{w.edge} + 2 \cdot t_{f.edge} \cdot 1 \text{ m}}{1 \text{ m}} \cdot \rho_g = 4.905 \frac{\text{kN}}{\text{m}^2}$$

Created with PTC Mathcad Express. See www.mathcad.com for more information.

Appendix G – Hand calculations, final design

Basic geometry

$L := 20 \text{ m}$	Structural span
$W := 40 \text{ m}$	Structural width
$W_{edge} := 5.3 \text{ m}$	Width of edge section

Load

$q_{fk} := 2 \frac{\text{kN}}{\text{m}^2} + \frac{120 \frac{\text{kN}}{\text{m}}}{2 \cdot L + 30 \text{ m}} = 3.71 \frac{\text{kN}}{\text{m}^2}$	traffic load
$s := 2.5 \frac{\text{kN}}{\text{m}^2}$	Snowload
$Q_{s.v.1k} := 80 \text{ kN} \cdot \frac{1 \text{ m}}{2.7 \text{ m}} = 29.63 \text{ kN}$	Service vehicle distributed on 2.7 m. Since the calculations are for a 1 m wide cross-section the load is calculated for 1 m in transverse direction.
$Q_{s.v.2k} := 40 \text{ kN} \cdot \frac{1 \text{ m}}{2.7 \text{ m}} = 14.81 \text{ kN}$	
$q_{soil} := 12 \frac{\text{kN}}{\text{m}^2}$	Soil load in main part of bridge
$q_{soil.edge} := 30 \frac{\text{kN}}{\text{m}^2}$	Soil load in edge section of bridge
$g_k := 3 \frac{\text{kN}}{\text{m}^2}$	Selfweight

Deflection limits

$$\delta_{max} := \frac{L}{250} = 80 \text{ mm} \quad \delta_2 := \frac{L}{300} = 66.67 \text{ mm}$$

Taken from EUROCOMP Table 4.2, General public flooring.

delta_max: "The sagging in the final state relative to the straight line joining the (supports?)".

delta_2: "The variation of the deflection of the beam due to the variable loading plus any time dependent deformations due to permanent load".

$$d_{pre} := 30 \text{ mm}$$

Load combination

For evaluation of different load combinations see separate appendix about load combinations.

Variable load:	$\psi_{0f} := 0.4$	$\psi_{1f} := 0.4$	$\psi_{2f} := 0$
Service vehicle:	$\psi_{0fw} := 0$	$\psi_{1fw} := 0$	$\psi_{2fw} := 0$
Snow load:	$\psi_{0s} := 0.8$	$\psi_{1s} := 0.6$	$\psi_{2s} := 0.2$
ULS	$\gamma_G := 1.35$	$\gamma_{Qf} := 1.35$	$\gamma_Q := 1.5$

Middle section

ULS load combination

$$q_{uls} := \gamma_G \cdot g_k + \gamma_G \cdot q_{soil} + \gamma_{Qf} \cdot \psi_{0f} \cdot q_{fk} + \gamma_Q \cdot \psi_{0s} \cdot s = 25.26 \frac{kN}{m^2} \quad \text{service vehicle main load}$$

Service vehicle

$$Q_{s.v.1} := \gamma_{Qf} \cdot Q_{s.v.1k} = 40 \text{ kN} \quad \text{Addition to uls load combination}$$

$$Q_{s.v.2} := \gamma_{Qf} \cdot Q_{s.v.2k} = 20 \text{ kN}$$

SLS load combinations

$$q_{char} := g_k + q_{soil} + \psi_{0f} \cdot q_{fk} + \psi_{0s} \cdot s = 18.49 \frac{kN}{m^2} \quad \text{Service vehicle main load, characteristic value}$$

$$q_{qp} := g_k + q_{soil} + \psi_{2f} \cdot q_{fk} + \psi_{2s} \cdot s = 15.5 \frac{kN}{m^2} \quad \text{no service vehicle}$$

Edge section

ULS load combination

$$q_{uls,edge} := \gamma_G \cdot g_k + \gamma_G \cdot q_{soil,edge} + \gamma_{Qf} \cdot \psi_{0f} \cdot q_{fk} + \gamma_Q \cdot \psi_{0s} \cdot s = 49.56 \frac{kN}{m^2}$$

SLS load combination

$$q_{char,edge} := g_k + q_{soil,edge} + q_{fk} + \psi_{0s} \cdot s = 38.71 \frac{kN}{m^2}$$

$$q_{qp,edge} := g_k + q_{soil,edge} + \psi_{2f} \cdot q_{fk} + \psi_{2s} \cdot s = 33.5 \frac{kN}{m^2}$$

Load actions

$$M_{uls} := 2.094 \text{ MN} \cdot \text{m}$$

$$M_{uls,edge} := 2.748 \text{ MN} \cdot \text{m}$$

$$M_{char} := 1.54 \text{ MN} \cdot \text{m}$$

$$M_{char,edge} := 2.136 \text{ MN} \cdot \text{m}$$

$$M_{qp} := 0.975 \text{ MN} \cdot \text{m}$$

$$M_{qp,edge} := 1.875 \text{ MN} \cdot \text{m}$$

$$V_{uls} := 364.072 \text{ kN}$$

$$V_{uls,edge} := 549.557 \text{ kN}$$

$$V_{char} := 280.242 \text{ kN}$$

$$V_{char,edge} := 427.143 \text{ kN}$$

$$V_{qp} := 195 \text{ kN}$$

$$V_{qp,edge} := 375 \text{ kN}$$

Material properties

$$\rho_g := 2022 \frac{kg}{m^3}$$

Density

Elastic modulus (E) in x and y direction and shear modulus (G).
Flange:

$$E_{f,k} := 32.387 \text{ GPa} \quad E_{f,k,y} := 15.472 \text{ GPa}$$

$$G_{f,k} := 5.651 \text{ GPa}$$

Web, middle section:

$$E_{w,k} := 15.219 \text{ GPa} \quad E_{w,y,k} := 16.8822 \text{ GPa}$$

$$G_{w,k} := 10.201 \text{ GPa}$$

Web, edge section

$$E_{w,edge,k} := 21.594 \text{ GPa} \quad E_{w,edge,y,k} := 17.594 \text{ GPa}$$

$$G_{w,edge,k} := 8.401 \text{ GPa}$$

Characteristic capacity,

$$f_{t,k} := 470.664 \text{ MPa} \quad \text{tensile strength}$$

$$\tau_{xy,k} := 70 \text{ MPa} \quad \text{Shear strength}$$

Material safety factors

$$\gamma_{M1} := 2.25 \quad \gamma_{M2} := 1.1 \quad \gamma_{M3} := 2.6$$

$$\gamma_M := \gamma_{M1} \cdot \gamma_{M2} \cdot \gamma_{M3} = 6.44 \quad \text{Eurocomp}$$

$$\gamma_{M1} := 1.35 \quad \gamma_{M2} := 1.35$$

$$\gamma_M := \gamma_{M1} \cdot \gamma_{M2} = 1.82$$

Conversion factors for environmental conditions and creep

$$\eta_c := 0.38 \quad \text{Conversion factor for creep action}$$

$$\eta_{cmd} := 0.81 \quad \text{Conversion factor for momentary loading}$$

Material properties for instant load conditions:

Flange

$$E_f := E_{f,k} \cdot \eta_{cmd} = 26.23 \text{ GPa} \quad E_{f,y} := E_{f,k,y} \cdot \eta_{cmd} = 12.53 \text{ GPa}$$

$$G_f := G_{f,k} \cdot \eta_{cmd} = 4.58 \text{ GPa}$$

Web, middle section

$$E_w := E_{w,k} \cdot \eta_{cmd} = 12.33 \text{ GPa} \quad E_{w,y} := E_{w,y,k} \cdot \eta_{cmd} = 13.67 \text{ GPa}$$

$$G_w := G_{w,k} \cdot \eta_{cmd} = 8.26 \text{ GPa}$$

... ..

Web edge section

$$E_{w,edge} := E_{w,edge,k} \cdot \eta_{cmd} = 17.49 \text{ GPa}$$

$$E_{w,edge,y} := E_{w,edge,y,k} \cdot \eta_{cmd} = 14.25 \text{ GPa}$$

$$G_{w,edge} := G_{w,edge,k} \cdot \eta_{cmd} = 6.8 \text{ GPa}$$

Material properties for long term load conditions:

Flange

$$E_{f,cr} := E_{f,k} \cdot \eta_c = 12.31 \text{ GPa}$$

$$E_{f,y,cr} := E_{f,k,y} \cdot \eta_c = 5.88 \text{ GPa}$$

$$G_{f,cr} := G_{f,k} \cdot \eta_c = 2.15 \text{ GPa}$$

Web, middle section

$$E_{w,cr} := E_{w,k} \cdot \eta_c = 5.78 \text{ GPa}$$

$$E_{w,y,cr} := E_{w,y,k} \cdot \eta_c = 6.42 \text{ GPa}$$

$$G_{w,cr} := G_{w,k} \cdot \eta_c = 3.88 \text{ GPa}$$

Web, edge section

$$E_{w,edge,cr} := E_{w,edge,k} \cdot \eta_c = 8.21 \text{ GPa}$$

$$E_{w,edge,y,cr} := E_{w,edge,y,k} \cdot \eta_c = 6.69 \text{ GPa}$$

$$G_{w,edge,cr} := G_{w,edge,k} \cdot \eta_c = 3.19 \text{ GPa}$$

Material properties, ULS load conditions

Flange

$$E_{f,ULS} := E_{f,k} \cdot \frac{\eta_{cmd}}{\gamma_M} = 14.39 \text{ GPa}$$

$$E_{f,y,ULS} := E_{f,k,y} \cdot \frac{\eta_{cmd}}{\gamma_M} = 6.88 \text{ GPa}$$

$$G_{f,ULS} := G_{f,k} \cdot \frac{\eta_{cmd}}{\gamma_M} = 2.51 \text{ GPa}$$

Web, middle section

$$E_w := E_{w,k} \cdot \frac{\eta_{cmd}}{\gamma_M} = 6.76 \text{ GPa}$$

$$E_{w,y,ULS} := E_{w,y,k} \cdot \frac{\eta_{cmd}}{\gamma_M} = 7.5 \text{ GPa}$$

$$G_{w,ULS} := G_{w,k} \cdot \frac{\eta_{cmd}}{\gamma_M} = 4.53 \text{ GPa}$$

Web, edge section

$$E_{w,edge,ULS} := E_{w,edge,k} \cdot \frac{\eta_{cmd}}{\gamma_M} = 9.6 \text{ GPa}$$

$$E_{w,edge,y,ULS} := E_{w,edge,y,k} \cdot \frac{\eta_{cmd}}{\gamma_M} = 7.82 \text{ GPa}$$

$$G_{w,edge,ULS} := G_{w,edge,k} \cdot \frac{\eta_{cmd}}{\gamma_M} = 3.73 \text{ GPa}$$

Strength in shear

Web area necessary:

Web area necessary according to EUROCOMP for middle respective edge section:

$$A_w := \frac{\gamma_M \cdot V_{uls}}{\tau_{xy,k}} = (9.48 \cdot 10^{-3}) \text{ m}^2 \quad A_{w,edge} := \frac{\gamma_M \cdot V_{uls,edge}}{\tau_{xy,k}} = 0.01 \text{ m}^2$$

Web geometry, middle section

The height of the cross section is given as a function of the thickness and spacing of the webs. The thickness $t(w)$ is the total thickness of each web, that means the thickness of both web plates together.

$$h := 0.8 \text{ m}, 0.85 \text{ m} \dots 2 \text{ m} = \begin{bmatrix} 0.8 \\ \vdots \end{bmatrix} \text{ m}$$

Height of cross section

$$A_w = (9.48 \cdot 10^{-3}) \text{ m}^2$$

Webarea of 1 m wide crosssection

Spacing of webs

Thickness of webs corresponding to specific spacing

$$b_{50} := 50 \text{ mm}$$

$$t_{w,50} := \frac{A_w}{h} \cdot \frac{b_{50}}{1 \text{ m}} = \begin{bmatrix} 0.59 \\ \vdots \end{bmatrix} \text{ mm}$$

$$b_{100} := 100 \text{ mm}$$

$$t_{w,100} := \frac{A_w}{h} \cdot \frac{b_{100}}{1 \text{ m}} = \begin{bmatrix} 1.18 \\ \vdots \end{bmatrix} \text{ mm}$$

$$b_{150} := 150 \text{ mm}$$

$$t_{w,150} := \frac{A_w}{h} \cdot \frac{b_{150}}{1 \text{ m}} = \begin{bmatrix} 1.78 \\ \vdots \end{bmatrix} \text{ mm}$$

$$b_{200} := 200 \text{ mm}$$

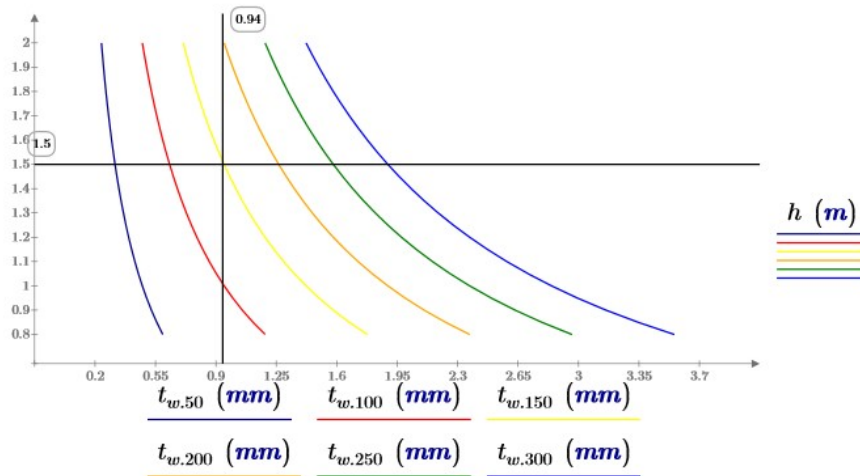
$$t_{w,200} := \frac{A_w}{h} \cdot \frac{b_{200}}{1 \text{ m}} = \begin{bmatrix} 2.37 \\ \vdots \end{bmatrix} \text{ mm}$$

$$b_{250} := 250 \text{ mm}$$

$$t_{w,250} := \frac{A_w}{h} \cdot \frac{b_{250}}{1 \text{ m}} = \begin{bmatrix} 2.96 \\ \vdots \end{bmatrix} \text{ mm}$$

$$b_{300} := 300 \text{ mm}$$

$$t_{w,300} := \frac{A_w}{h} \cdot \frac{b_{300}}{1 \text{ m}} = \begin{bmatrix} 3.55 \\ \vdots \end{bmatrix} \text{ mm}$$



Web thickness as function of crosssectionheight and spacing of web elements.
A thickness between 0,2 - 3,5 mm is not reasonable. The number should range from 1 mm upwards. $A(w) = 6 A(w)$

$$h := 0.8 \text{ m}, 0.85 \text{ m} \dots 2 \text{ m} = \begin{bmatrix} 0.8 \\ \vdots \end{bmatrix} \text{ m}$$

Height of cross section

$$A_w := 6 \cdot A_w = 0.06 \text{ m}^2$$

Webarea of 1 m wide crosssection

Spacing of webs

Web thickness corresponding to specific web spacing

$$b_{50} := 50 \text{ mm}$$

$$t_{w.50} := \frac{A_w}{h} \cdot \frac{b_{50}}{1 \text{ m}} = \begin{bmatrix} 3.55 \\ \vdots \end{bmatrix} \text{ mm}$$

$$b_{100} := 100 \text{ mm}$$

$$t_{w.100} := \frac{A_w}{h} \cdot \frac{b_{100}}{1 \text{ m}} = \begin{bmatrix} 7.11 \\ \vdots \end{bmatrix} \text{ mm}$$

$$b_{150} := 150 \text{ mm}$$

$$t_{w.150} := \frac{A_w}{h} \cdot \frac{b_{150}}{1 \text{ m}} = \begin{bmatrix} 10.66 \\ \vdots \end{bmatrix} \text{ mm}$$

$$b_{200} := 200 \text{ mm}$$

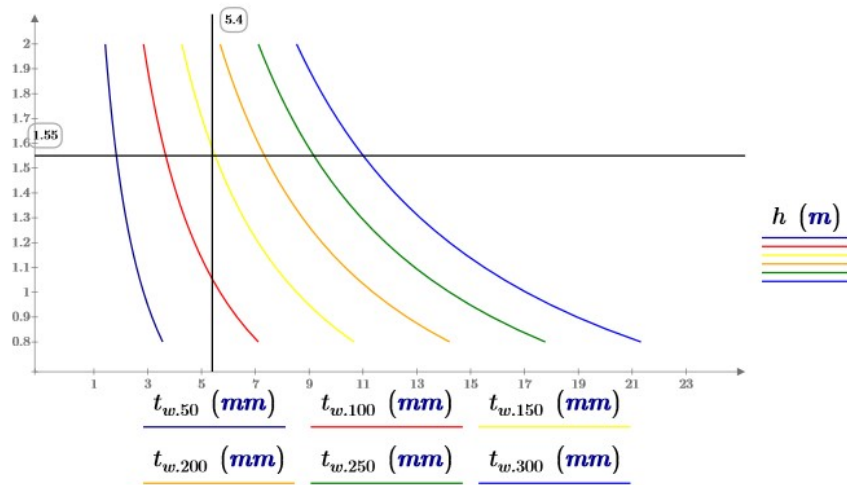
$$t_{w.200} := \frac{A_w}{h} \cdot \frac{b_{200}}{1 \text{ m}} = \begin{bmatrix} 14.22 \\ \vdots \end{bmatrix} \text{ mm}$$

$$b_{250} := 250 \text{ mm}$$

$$t_{w.250} := \frac{A_w}{h} \cdot \frac{b_{250}}{1 \text{ m}} = \begin{bmatrix} 17.77 \\ \vdots \end{bmatrix} \text{ mm}$$

$$b_{300} := 300 \text{ mm}$$

$$t_{w.300} := \frac{A_w}{h} \cdot \frac{b_{300}}{1 \text{ m}} = \begin{bmatrix} 21.33 \\ \vdots \end{bmatrix} \text{ mm}$$



Web thickness as function of cross-section height and width of web elements

Web geometry, edge section

$$h := 0.8 \text{ m}, 0.85 \text{ m} \dots 2 \text{ m} = \begin{bmatrix} 0.8 \\ \vdots \end{bmatrix} \text{ m} \quad \text{Height of cross-section}$$

$$A_{w,edge} := 3 \cdot A_{w,edge}$$

Shear area increased for same reason as in middle section.

Spacing of webs

Thickness of webs corresponding to specific spacing

$$b_{50} := 50 \text{ mm}$$

$$t_{w,50,edge} := \frac{A_{w,edge}}{h} \cdot \frac{b_{50}}{1 \text{ m}} = \begin{bmatrix} 2.68 \\ \vdots \end{bmatrix} \text{ mm}$$

$$b_{100} := 100 \text{ mm}$$

$$t_{w,100,edge} := \frac{A_{w,edge}}{h} \cdot \frac{b_{100}}{1 \text{ m}} = \begin{bmatrix} 5.37 \\ \vdots \end{bmatrix} \text{ mm}$$

$$b_{150} := 150 \text{ mm}$$

$$t_{w,150,edge} := \frac{A_{w,edge}}{h} \cdot \frac{b_{150}}{1 \text{ m}} = \begin{bmatrix} 8.05 \\ \vdots \end{bmatrix} \text{ mm}$$

$$b_{200} := 200 \text{ mm}$$

$$t_{w,200,edge} := \frac{A_{w,edge}}{h} \cdot \frac{b_{200}}{1 \text{ m}} = \begin{bmatrix} 10.73 \\ \vdots \end{bmatrix} \text{ mm}$$

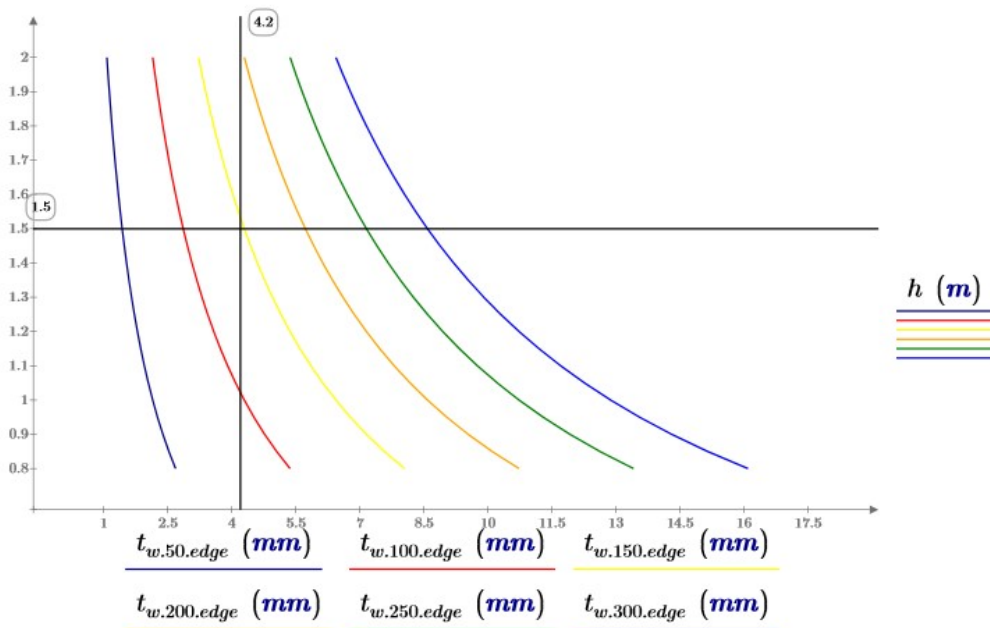
$$b_{250} := 250 \text{ mm}$$

$$t_{w,250,edge} := \frac{A_{w,edge}}{h} \cdot \frac{b_{250}}{1 \text{ m}} = \begin{bmatrix} 13.41 \\ \vdots \end{bmatrix} \text{ mm}$$

$$b_{300} := 300 \text{ mm}$$

$$t_{w,300,edge} := \frac{A_{w,edge}}{h} \cdot \frac{b_{300}}{1 \text{ m}} = \begin{bmatrix} 16.1 \\ \vdots \end{bmatrix} \text{ mm}$$

Created with PTC Mathcad Express. See www.mathcad.com for more information.



Web thickness as function of height of crosssection and width of web elements.

Strength in bending

Nessecary W due to bending in ULS

$$W := \frac{\gamma_M \cdot M_{uls}}{f_{t,k}} = (8.11 \cdot 10^{-3}) \text{ m}^3 \quad W_{edge} := \frac{\gamma_M \cdot M_{uls,edge}}{f_{t,k}} = 0.01 \text{ m}^3$$

Deflection

In this section the necessary moment of inertia I according to bending is calculated

$$I_\delta(k_1, F_V, E, \delta_M) := k_1 \cdot \frac{F_V \cdot L^3}{E \cdot \delta_M}$$

Nessecary moment of inertia as function of deflection due to bending, F total load on beam

$$\delta_V(k_2, F, G_{xy}, A, L) := k_2 \cdot \frac{F \cdot L}{A \cdot G_{xy}}$$

Deflection due to shear, F total load on beam

$$k_1 := \frac{5}{384}$$

$$k_2 := \frac{1}{8}$$

$$k_{1p10} := \frac{1}{48}$$

$$k_{2p10} := \frac{1}{4}$$

EUROCOMP:

F - total vertical load

EI - flexural rigidity

A - Shear area of web

G_{xy} - in-plane shear modulus of web

k1 k2

5/384 1/8

1/48 1/4

uniformly distributed load

point load, 10m

$$k_{1p7} := \frac{7 \text{ m}}{48 \cdot L} \cdot \left(3 - \frac{4 \cdot (7 \text{ m})^2}{L^2} \right) = 0.02$$

long term (quasi permanent load combination)

Middle bridge section

$$\delta_{Vfinal} := \delta_V(k_2, q_{qp} \cdot L \cdot 1 \text{ m}, G_{w.cr}, A_w, L) = 3.52 \text{ mm}$$

$$\delta_M := \delta_{max} - \delta_{Vfinal} + d_{pre} = 106.48 \text{ mm}$$

$$I_{\delta final} := I_{\delta}(k_1, q_{qp} \cdot L \cdot 1 \text{ m}, E_{f.cr}, \delta_M) = 0.02 \text{ m}^4$$

Edge section

$$\delta_{Vfinal.edge} := \delta_V(k_2, q_{qp.edge} \cdot L \cdot 1 \text{ m}, G_{w.edge.cr}, A_{w.edge}, L) = 12.22 \text{ mm}$$

$$\delta_M := \delta_{max} - \delta_{Vfinal.edge} + d_{pre} = 0.1 \text{ m}$$

$$I_{\delta final.edge} := I_{\delta}(k_1, q_{qp.edge} \cdot L \cdot 1 \text{ m}, E_{f.cr}, \delta_M) = 0.06 \text{ m}^4$$

Short term (short term variable load action + long term part of permanent action)

Permanent loads

$$q_{creep} := g_k + q_{soil} = 15 \frac{\text{kN}}{\text{m}^2}$$

$$q_{creep.edge} := g_k + q_{soil.edge} = 33 \frac{\text{kN}}{\text{m}^2}$$

Characteristic load without the permanent loads

$$q_{inst} := q_{char} - g_k - q_{soil} = 3.49 \frac{\text{kN}}{\text{m}^2}$$

$$q_{inst.edge} := q_{char.edge} - g_k - q_{soil.edge} = 5.71 \frac{\text{kN}}{\text{m}^2}$$

Shear deflection

Note: Both point loads from Q1 and Q2 placed in middle of span (10 m) for shear deflection.

$$\delta_{Vinst} := \delta_V(k_2, q_{inst} \cdot L \cdot 1 \text{ m}, G_w, A_w, L) + \delta_V(k_{2p10}, Q_{s.v.1k} + Q_{s.v.2k}, G_w, A_w, L)$$

$$\delta_{Vcreep} := \delta_V(k_2, q_{creep} \cdot L \cdot 1 \text{ m}, G_{w.cr}, A_w, L) - \delta_V(k_2, q_{creep} \cdot L \cdot 1 \text{ m}, G_w, A_w, L)$$

$$\delta_{Vshort} := \delta_{Vinst} + \delta_{Vcreep} = 2.65 \text{ mm}$$

$$\delta_2 = 66.67 \text{ mm} \quad \text{requirements according to EUROCOMP}$$

$$\delta_M := \delta_2 - \delta_{Vshort} = 64.02 \text{ mm} \quad \text{Maximum allowable deflection from bending}$$

$$I_{\delta inst} := I_{\delta}(k_1, q_{inst} \cdot L \cdot 1 \text{ m}, E_f, \delta_M) + I_{\delta}(k_{1p10}, Q_{s.v.1k}, E_f, \delta_M) + I_{\delta}(k_{1p7}, Q_{s.v.2k}, E_f, \delta_M)$$

Created with PTC Mathcad Express. See www.mathcad.com for more information.

$$I_{\delta creep} := I_{\delta}(k_1, q_{creep} \cdot L \cdot 1 \text{ m}, E_{f.cr}, \delta_M) - I_{\delta}(k_1, q_{creep} \cdot L \cdot 1 \text{ m}, E_f, \delta_M)$$

$$I_{\delta short} := I_{\delta inst} + I_{\delta creep} = 0.03 \text{ m}^4$$

Necessary Moment of inertia
for requirement delta 2

Edge section

$$\delta_{V inst} := \delta_V(k_2, q_{inst.edge} \cdot L \cdot 1 \text{ m}, G_{w.edge}, A_{w.edge}, L) = 0.98 \text{ mm}$$

$$\delta_{V creep} := \delta_V(k_2, q_{creep.edge} \cdot L \cdot 1 \text{ m}, G_{w.edge.cr}, A_{w.edge}, L) - \delta_V(k_2, q_{creep.edge} \cdot L \cdot 1 \text{ m}, G_{w.edge}, A_{w.edge}, L)$$

$$\delta_{V short.edge} := \delta_{V inst} + \delta_{V creep} = 7.37 \text{ mm}$$

$$\delta_2 = 66.67 \text{ mm}$$

requirements according to EUROCOMP

$$\delta_M := \delta_2 - \delta_{V short.edge} = 59.3 \text{ mm}$$

Maximum allowable deflection from bending

$$I_{\delta inst} := I_{\delta}(k_1, q_{inst.edge} \cdot L \cdot 1 \text{ m}, E_f, \delta_M)$$

$$I_{\delta creep} := I_{\delta}(k_1, q_{creep.edge} \cdot L \cdot 1 \text{ m}, E_{f.cr}, \delta_M) - I_{\delta}(k_1, q_{creep.edge} \cdot L \cdot 1 \text{ m}, E_f, \delta_M)$$

$$I_{\delta short.edge} := I_{\delta inst} + I_{\delta creep} = 0.06 \text{ m}^4$$

Necessary Moment of inertia
for requirement delta 2

Summarization

Minimum requirements on geometry for different requirements:

Shear (ULS):	$A_w = 0.06 \text{ m}^2$	$A_{w.edge} = 0.04 \text{ m}^2$
Bending (ULS):	$W = (8.11 \cdot 10^{-3}) \text{ m}^3$	$W_{edge} = 0.01 \text{ m}^3$
Deflection (q.p.):	$I_{\delta final} = 0.02 \text{ m}^4$	$I_{\delta final.edge} = 0.06 \text{ m}^4$
Deflection (char. + q.p.):	$I_{\delta short} = 0.03 \text{ m}^4$	$I_{\delta short.edge} = 0.06 \text{ m}^4$
	$I_{\delta} := \max(I_{\delta final}, I_{\delta short})$	$I_{\delta.edge} := \max(I_{\delta final.edge}, I_{\delta short.edge})$

Middle section

Flange geometry

From bending

$$I_{bending} := W \cdot \frac{h}{2} = \begin{bmatrix} 3.24 \cdot 10^{-3} \\ \vdots \end{bmatrix} \text{ m}^4$$

Minimum moment of inertia from bending
requirements.

Created with PTC Mathcad Express. See www.mathcad.com for more information.

$$I_{\delta} = 0.03 \text{ m}^4$$

Minimum moment of inertia from deflection requirements.

The moment of inertia from the deflection criteria is dimensioning.

$$I_y(b, h) := \frac{\overrightarrow{b \cdot h^3}}{12}$$

$$I_r(b, h, r) := \overrightarrow{b \cdot h \cdot r^2}$$

Formula for moment of inertia

Width of calculated crossection

$$b_f := 1 \text{ m}$$

$$t_w := \frac{A_w}{h} = \begin{bmatrix} 0.07 \\ \vdots \end{bmatrix} \text{ m}$$

Total thickness of web /m

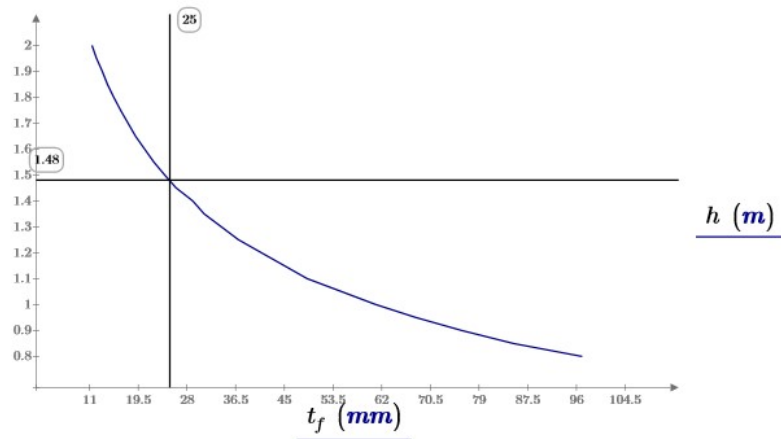
Moment of inertia from web

$$I_w := I_y \left(t_w \cdot \frac{E_w}{E_f}, h \right) = \begin{bmatrix} 7.82 \cdot 10^{-4} \\ \vdots \end{bmatrix} \text{ m}^4$$

thickness of flange to reach the required moment of inertia as function of high

$$h = \begin{bmatrix} 0.8 \\ 0.85 \\ 0.9 \\ 0.95 \\ 1 \\ 1.05 \\ 1.1 \\ 1.15 \\ 1.2 \\ 1.25 \\ 1.3 \\ 1.35 \\ 1.4 \\ 1.45 \\ 1.5 \\ 1.55 \\ 1.6 \\ 1.65 \\ 1.7 \\ 1.75 \\ 1.8 \\ 1.85 \\ 1.9 \\ 1.95 \\ 2 \end{bmatrix} \text{ m} \quad t_f := \begin{bmatrix} 97 \\ 85 \\ 76 \\ 68 \\ 61 \\ 55 \\ 49 \\ 45 \\ 41 \\ 37 \\ 34 \\ 31 \\ 29 \\ 26.1 \\ 24.1 \\ 22.2 \\ 20.6 \\ 19 \\ 17.7 \\ 16.4 \\ 15.2 \\ 14.1 \\ 13.2 \\ 12.2 \\ 11.4 \end{bmatrix} \text{ mm} \quad 2 \cdot I_y(b_f, t_f) + 2 \cdot I_r \left(b_f, t_f, \frac{h}{2} \right) + I_w - I_{\delta} = \begin{bmatrix} 2.36 \cdot 10^{-3} \\ 2.08 \cdot 10^{-3} \\ 2.23 \cdot 10^{-3} \\ 2.23 \cdot 10^{-3} \\ 2.15 \cdot 10^{-3} \\ 2.08 \cdot 10^{-3} \\ 1.53 \cdot 10^{-3} \\ 1.77 \cdot 10^{-3} \\ 1.68 \cdot 10^{-3} \\ 1.21 \cdot 10^{-3} \\ 1.19 \cdot 10^{-3} \\ 8.68 \cdot 10^{-4} \\ 1.21 \cdot 10^{-3} \\ 3.97 \cdot 10^{-4} \\ 2.52 \cdot 10^{-4} \\ -7.24 \cdot 10^{-6} \\ -1.15 \cdot 10^{-4} \\ -4.21 \cdot 10^{-4} \\ -5.04 \cdot 10^{-4} \\ -7.57 \cdot 10^{-4} \\ -1.03 \cdot 10^{-3} \\ -1.3 \cdot 10^{-3} \\ -1.37 \cdot 10^{-3} \\ -1.77 \cdot 10^{-3} \\ -1.92 \cdot 10^{-3} \end{bmatrix} \text{ m}^4$$

Created with PTC Mathcad Express. See www.mathcad.com for more information.



Flange thickness as function of height of cross-section.

Edge section section

Flange geometry

$$I_{bending,edge} := W_{edge} \cdot \frac{h}{2} = \begin{bmatrix} 4.26 \cdot 10^{-3} \\ \vdots \end{bmatrix} m^4$$

Minimum moment of inertia from bending requirements.

$$I_{\delta,edge} = 0.06 m^4$$

Minimum moment of inertia from deflection requirements.

The moment of inertia from the deflection criteria is dimensioning.

$$b_f := 1 m$$

Width of calculated cross-section

$$t_{w,edge} := \frac{A_{w,edge}}{h} = \begin{bmatrix} 0.05 \\ \vdots \end{bmatrix} m$$

Total thickness of web / m

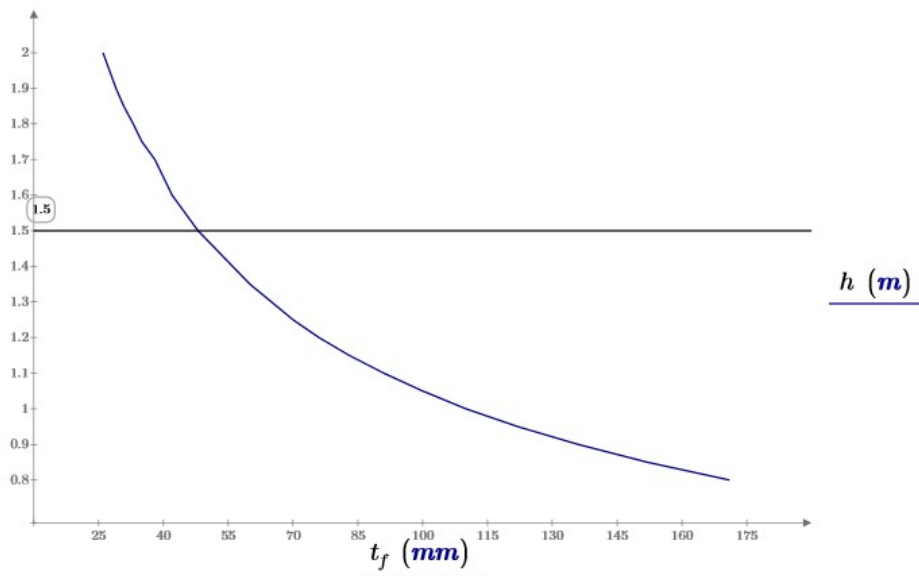
$$I_{w,edge} := I_y \left(t_{w,edge} \cdot \frac{E_w}{E_f}, h \right) = \begin{bmatrix} 5.9 \cdot 10^{-4} \\ \vdots \end{bmatrix} m^4$$

Moment of inertia from web

Created with PTC Mathcad Express. See www.mathcad.com for more information.

Thickness of flange to reach required moment of inertia as function of height

$h =$	m	$t_f :=$	mm	$2 \cdot I_y(b_f, t_f) + 2 \cdot I_r\left(b_f, t_f, \frac{h}{2}\right) + I_w - I_{\delta.edge} =$	m^4
0.8		171		$-1.66 \cdot 10^{-3}$	
0.85		152		$-1.62 \cdot 10^{-3}$	
0.9		136		$-1.51 \cdot 10^{-3}$	
0.95		122		$-1.54 \cdot 10^{-3}$	
1		110		$-1.55 \cdot 10^{-3}$	
1.05		100		$-1.36 \cdot 10^{-3}$	
1.1		91		$-1.34 \cdot 10^{-3}$	
1.15		83		$-1.4 \cdot 10^{-3}$	
1.2		76		$-1.45 \cdot 10^{-3}$	
1.25		70		$-1.34 \cdot 10^{-3}$	
1.3		65		$-9.62 \cdot 10^{-4}$	
1.35		60		$-1.06 \cdot 10^{-3}$	
1.4		56		$-6.94 \cdot 10^{-4}$	
1.45		52		$-7.41 \cdot 10^{-4}$	
1.5		48		$-1.23 \cdot 10^{-3}$	
1.55		45		$-9.91 \cdot 10^{-4}$	
1.6		42		$-1.1 \cdot 10^{-3}$	
1.65		40		$-2.11 \cdot 10^{-4}$	
1.7		38		$4.53 \cdot 10^{-4}$	
1.75		35		$-6.55 \cdot 10^{-4}$	
1.8		33		$-5.73 \cdot 10^{-4}$	
1.85		30.8		$-1.1 \cdot 10^{-3}$	
1.9		29.0		$-1.24 \cdot 10^{-3}$	
1.95		27.5		$-1.06 \cdot 10^{-3}$	
2		26.0		$-1.11 \cdot 10^{-3}$	



Created with PTC Mathcad Express. See www.mathcad.com for more information.

Flange thickness as function of crossection height.

If the maximum possible flange thickness is set to 25 mm there is no feasible solution. If the web area must be increased.

The same assumption ($t_f = 25 \text{ mm}$) gives $h = 1,55 \text{ m}$ in the midle section of the bridge.

$$t_{f,edge} := 25 \text{ mm}$$

$$h := 1.5 \text{ m}$$

Flange thickness and hight are assumed

$$I_{f,edge} := 2 \cdot I_y(b_f, t_{f,edge}) + 2 \cdot I_r\left(b_f, t_{f,edge}, \frac{h}{2}\right) = 0.03 \text{ m}^4$$

Moment of inertia from flanges

$$I_{\delta,edge} = 0.06 \text{ m}^4$$

Required moment of inertia

$$I_{w,edge} := I_{\delta,edge} - I_{f,edge} = 0.03 \text{ m}^4$$

Required moment of inertia from webs

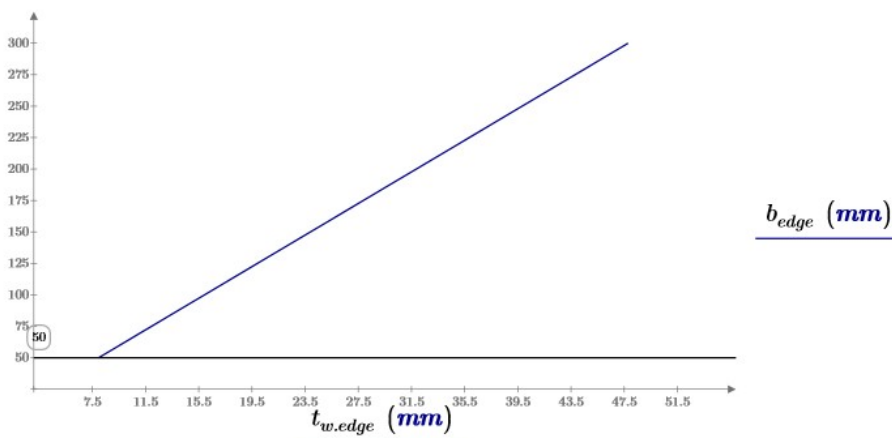
$$t_{w,edge} := \frac{12 \cdot I_{w,edge}}{h^3} \cdot \frac{E_f}{E_{w,edge}} = 159.29 \text{ mm}$$

Required total thickness of webs on 1 m wide crossection

$$b_{edge} := 50 \text{ mm}, 55 \text{ mm}..300 \text{ mm} = \begin{bmatrix} 50 \\ 55 \\ \vdots \end{bmatrix} \text{ mm}$$

$$t_{w,edge} := t_{w,edge} \cdot \frac{b_{edge}}{1 \text{ m}} = \begin{bmatrix} 7.96 \cdot 10^{-3} \\ \vdots \end{bmatrix} \text{ m}$$

Thickness of webs as function of thickness



Web thickness in edge section as function of width of web elements.

Middle section

$h := 1.5 \text{ m}$	$b := 150 \text{ mm}$	Hight and spacing of webs
$t_f := 25 \text{ mm}$		Thickness of flanges
$t_w := \frac{A_w}{h} \cdot \frac{b}{1 \text{ m}} = 5.69 \text{ mm}$		Thickness of individual web plate
$t_W := \frac{A_w}{h} = 0.04 \text{ m}$		Total thickness of web / m

$$I_w := I_y \left(t_W \cdot \frac{E_w}{E_f}, h \right) = (2.75 \cdot 10^{-3}) \text{ m}^4$$

$$I_f := 2 \cdot I_y \left(b_f, t_f \right) + 2 \cdot I_r \left(b_f, t_f, \frac{h}{2} \right) = 0.03 \text{ m}^4$$

$I := I_w + I_f = 0.0309 \text{ m}^4$	Moment of inertia for cross section
---------------------------------------	-------------------------------------

$I_\delta = 0.0296 \text{ m}^4$	Minimum moment of inertia
---------------------------------	---------------------------

Edge section

$b_{f.edge} := 50 \text{ mm}$	Spacing of webs
$t_{f.edge} := t_f = 25 \text{ mm}$	
$t_{w.edge} := 8 \text{ mm}$	Thickness of individual web plate

$t_{W.edge} := \frac{1 \text{ m}}{b_{f.edge}} \cdot t_{w.edge} = 160 \text{ mm}$	Total thickness of web / m
--	----------------------------

$$I_{w.edge} := I_y \left(t_{W.edge} \cdot \frac{E_{w.edge}}{E_f}, h \right) = 0.03 \text{ m}^4$$

$$I_{f.edge} := 2 \cdot I_y \left(b_f, t_{f.edge} \right) + 2 \cdot I_r \left(b_f, t_{f.edge}, \frac{h}{2} \right) = 0.03 \text{ m}^4$$

$I_{edge} := I_{w.edge} + I_{f.edge} = 0.0581 \text{ m}^4$	Moment of inertia for cross section
--	-------------------------------------

$I_{\delta.edge} = 0.058 \text{ m}^4$	Minimum moment of inertia for cross section
---------------------------------------	--

Deflection

Formulas for bending

$$\delta_M(k_1, F_V, E, I) := k_1 \cdot \frac{F_V \cdot L^3}{E \cdot I}$$

Deflection due to bending, F total load on beam

$$\delta_V(k_2, F, G_{xy}, A, L) := k_2 \cdot \frac{F \cdot L}{A \cdot G_{xy}}$$

Deflection due to shear, F total load on beam

$$k_1 := \frac{5}{384}$$

$$k_2 := \frac{1}{8}$$

$$k_{1p10} := \frac{1}{48}$$

$$k_{2p10} := \frac{1}{4}$$

EUROCOMP:

F - total vertical load

EI - flexural rigidity

A - Shear area of web

Gxy - in-plane shear modulus of web

k1

k2

5/384

1/8

uniformly distributed load

1/48

1/4

point load, 10m

$$k_{1p7} := \frac{7 \text{ m}}{48 \cdot L} \cdot \left(3 - \frac{4 \cdot (7 \text{ m})^2}{L^2} \right) = 0.02$$

long term (quasi permanent load combination)

Middle bridge section

$$\delta_{Mfinal} := \delta_M(k_1, q_{qp} \cdot L \cdot 1 \text{ m}, E_{f.cr}, I) = 84.98 \text{ mm}$$

$$\delta_{Vfinal} := \delta_V(k_2, q_{qp} \cdot L \cdot 1 \text{ m}, G_{w.cr}, A_w, L) = 3.52 \text{ mm}$$

$$\delta_{final} := \delta_{Mfinal} + \delta_{Vfinal} - d_{pre} = 58.49 \text{ mm}$$

Edge section

$$\delta_{Mfinal.edge} := \delta_M(k_1, q_{qp.edge} \cdot L \cdot 1 \text{ m}, E_{f.cr}, I_{edge}) = 97.55 \text{ mm}$$

$$\delta_{Vfinal.edge} := \delta_V(k_2, q_{qp.edge} \cdot L \cdot 1 \text{ m}, G_{w.edge.cr}, A_{w.edge}, L) = 12.22 \text{ mm}$$

$$\delta_{final.edge} := \delta_{Mfinal.edge} + \delta_{Vfinal.edge} - d_{pre} = 79.78 \text{ mm}$$

Short term (short term variable load action + long term part of permanent action)

$$q_{creep} := g_k + q_{soil} = 15 \frac{\text{kN}}{\text{m}^2}$$

$$q_{creep.edge} := g_k + q_{soil.edge} = 33 \frac{\text{kN}}{\text{m}^2}$$

$$q_{inst} := q_{char} - g_k - q_{soil} = 3.49 \frac{\text{kN}}{\text{m}^2}$$

$$q_{inst.edge} := q_{char.edge} - g_k - q_{soil.edge} = 5.71 \frac{\text{kN}}{\text{m}^2}$$

$$\delta_{Minst} := \delta_M(k_1, q_{inst} \cdot L \cdot 1 \text{ m}, E_f, I) + \delta_M(k_{1p10}, Q_{s.v.1k}, E_f, I) + \delta_M(k_{1p7}, Q_{s.v.2k}, E_f, I)$$

$$\delta_{Mcreep} := \delta_M(k_1, q_{creep} \cdot L \cdot 1 \text{ m}, E_{f.cr}, I) - \delta_M(k_1, q_{creep} \cdot L \cdot 1 \text{ m}, E_f, I) = 43.66 \text{ mm}$$

Created with PTC Mathcad Express. See www.mathcad.com for more information.

Note: Both point loads from Q1 and Q2 placed in middle of span (10 m) for shear deflection.

$$\delta_{Vinst} := \delta_V(k_2, q_{inst} \cdot L \cdot 1 \text{ m}, G_w, A_w, L) + \delta_V(k_{2p10}, Q_{s.v.1k} + Q_{s.v.2k}, G_w, A_w, L)$$

$$\delta_{Vcreep} := \delta_V(k_2, q_{creep} \cdot L \cdot 1 \text{ m}, G_{w.cr}, A_w, L) - \delta_V(k_2, q_{creep} \cdot L \cdot 1 \text{ m}, G_w, A_w, L)$$

$$\delta_{Vshort} := \delta_{Vinst} + \delta_{Vcreep} = 2.65 \text{ mm}$$

$$\delta_{short} := \delta_{Mshort} + \delta_{Vshort} = 64.05 \text{ mm}$$

Edge section

$$\delta_{Minst} := \delta_M(k_1, q_{inst.edge} \cdot L \cdot 1 \text{ m}, E_f, I_{edge}) = 7.81 \text{ mm}$$

$$\delta_{Mcreep} := \delta_M(k_1, q_{creep.edge} \cdot L \cdot 1 \text{ m}, E_{f.cr}, I_{edge}) - \delta_M(k_1, q_{creep.edge} \cdot L \cdot 1 \text{ m}, E_f, I_{edge})$$

$$\delta_{Mshort.edge} := \delta_{Minst} + \delta_{Mcreep} = 58.82 \text{ mm}$$

$$\delta_{Vinst} := \delta_V(k_2, q_{inst.edge} \cdot L \cdot 1 \text{ m}, G_w, A_{w.edge}, L) = 0.81 \text{ mm}$$

$$\delta_{Vcreep} := \delta_V(k_2, q_{creep.edge} \cdot L \cdot 1 \text{ m}, G_{w.cr}, A_{w.edge}, L) - \delta_V(k_2, q_{creep.edge} \cdot L \cdot 1 \text{ m}, G_w, A_{w.edge}, L)$$

$$\delta_{Vshort.edge} := \delta_{Vinst} + \delta_{Vcreep} = 6.07 \text{ mm}$$

$$\delta_{short.edge} := \delta_{Mshort.edge} + \delta_{Vshort.edge} = 64.89 \text{ mm}$$

$$\delta_{Minst} + \delta_{Vinst} = 8.61 \text{ mm}$$

$$\delta_{Mcreep} + \delta_{Vcreep} = 56.28 \text{ mm}$$

Deflection checks and summarization

Deflection for middle and edge beam, long term (quasi permanent load)

Limit:

$$\delta_{final} = 58.49 \text{ mm}$$

$$\delta_{final.edge} = 79.78 \text{ mm}$$

$$\delta_{max} = 80 \text{ mm}$$

Deflection for middle and edge beam, short term defl. of var. load + long term defl. from creep part of deadweight (quasi permanent load)

Limit:

$$\delta_{short} = 64.05 \text{ mm}$$

$$\delta_{short.edge} = 64.89 \text{ mm}$$

$$\delta_2 = 66.67 \text{ mm}$$

Check abaqus deflections

Middle bridge section

$$\delta_{Mfinal} := \delta_M(k_1, q_{uls} \cdot L \cdot 1 \text{ m}, E_{f.ULS}, I) + \delta_M(k_{1p10}, Q_{s.v.1}, E_{f.ULS}, I) + \delta_M(k_{1p7}, Q_{s.v.2}, E_{f.ULS}, I)$$

$$\delta_{Vfinal} := \delta_V(k_2, q_{uls} \cdot L \cdot 1 \text{ m}, G_{w.ULS}, A_w, L) + \delta_V(k_{2p10}, Q_{s.v.1} + Q_{s.v.2}, G_{w.ULS}, A_w, L)$$

$$\delta_{final} := \delta_{Mfinal} + \delta_{Vfinal} = 146.03 \text{ mm}$$

Edge section

$$\delta_{Mfinal.edge} := \delta_M(k_1, q_{uls.edge} \cdot L \cdot 1 \text{ m}, E_{f.ULS}, I_{edge}) = 123.38 \text{ mm}$$

$$\delta_{Vfinal.edge} := \delta_V(k_2, q_{uls.edge} \cdot L \cdot 1 \text{ m}, G_{w.edge.ULS}, A_{w.edge}, L) = 15.46 \text{ mm}$$

$$\delta_{final.edge} := \delta_{Mfinal.edge} + \delta_{Vfinal.edge} = 138.84 \text{ mm}$$

Created with PTC Mathcad Express. See www.mathcad.com for more information.